

SUBCELLULAR LOCALIZATION OF TOBACCO MAPKS

by

Alana Clegg

B.Sc., Carleton University, 2001

A THESIS SUBMITTED IN PARTIAL FULFILLMENT OF THE REQUIREMENTS
FOR THE DEGREE OF MASTER OF SCIENCE

in

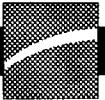
THE FACULTY OF GRADUATE STUDIES
Agricultural Science

We accept this thesis as conforming
to the required standard

THE UNIVERSITY OF BRITISH COLUMBIA

Oct 2004

©Alana Marie Clegg



Library Authorization

In presenting this thesis in partial fulfillment of the requirements for an advanced degree at the University of British Columbia, I agree that the Library shall make it freely available for reference and study. I further agree that permission for extensive copying of this thesis for scholarly purposes may be granted by the head of my department or by his or her representatives. It is understood that copying or publication of this thesis for financial gain shall not be allowed without my written permission.

ALANA CLEGG

Name of Author (please print)

06/10/2004

Date (dd/mm/yyyy)

Title of Thesis:

Subcellular Localization of Tobacco MAPKs

Degree:

MSc

Year:

2004

Department of

Agricultural Sciences

The University of British Columbia
Vancouver, BC Canada

ABSTRACT:

Plants effect intracellular changes in response to a variety of external stimuli. Harpin, a bacterial elicitor from the bean halo-blight pathogen *Pseudomonas syringae pv phaseolicola*, and megaspermin, an oocyte elicitor secreted by *Phytophthora megasperma* H20, are both known to elicit a hypersensitive response (HR) in tobacco. These elicitors also induce phosphorylation of a 48 kDa protein and a 46 kDa protein that have been identified as the Salicylic Acid Induced Protein Kinase (SIPK), and Wound Induced Protein Kinase (WIPK) mitogen activated protein kinases (MAPKs) respectively.

Previous work has shown that transient over-expression of SIPK causes lesion formation in tobacco leaves, suggesting a possible role for SIPK in regulating tobacco HR signaling. Extracellular Regulated Kinase (ERK), a mammalian homologue to SIPK and WIPK, has been shown to localize to different parts of the cell in response to a variety of stresses. The objective of this study was to determine the subcellular localization of the tobacco MAPKs, SIPK and WIPK, in response to challenge by harpin and megaspermin.

Using both SIPK-GFP proteins and *in situ* immunolabeling of SIPK and WIPK, it was determined that the tobacco MAPKs were localized predominantly in the cytoplasm, with some nuclear localization. Upon challenge with harpin and/or megaspermin the phosphorylated forms of the probed MAPKs showed strong nuclear localization. In elicitor induced tobacco cultures, immunolabeling results showed strong nucleolar localization within the nucleus. These results are consistent with the model that activation of ERK-homologues by intracellular effectors leads to translocation of the

activated MAPK from the cytoplasm to the nucleus, most likely to effect transcriptional regulation of stress-related genes.

Table of Contents:

Title.....	i
Abstract.....	ii
Table of Contents.....	iv
List of Tables and Figures.....	vii
Abbreviations.....	ix
Acknowledgements.....	xi
CHAPTER 1: General Introduction.....	1
1.1: Studying Signal Transduction	
1.1.1: Signal Transduction and MAPK cascades.....	1
1.1.2: MAPK Structure and Function.. ..	3
1.1.3: Eukaryotic MAPK Families.....	6
1.1.4: Plant MAPK Families.....	7
1.1.5: Approaches to Analysis of MAPK Pathways.....	10
1.1.6: Hypersensitive Response.....	11
1.1.7: MAPK Elicitors.....	12
1.2: Studying Subcellular Localization of MAPKK and MAPK	
1.2.1: Subcellular Localization.....	15
1.2.2: Subcellular Localization of ERK	15
1.2.3: Methods for Determining Subcellular Localization.....	18
CHAPTER 2: SIPK:GFP Fusion Protein.....	20
2.1: Introduction to GFP	
2.1.1: GFP.....	20
2.1.2: GFP Fusion Proteins.....	20
2.1.3: GFP Expression <i>In Planta</i>	21
2.2: Materials and Methods.....	23
2.2.1: Plant Growth Conditions.....	23
2.2.2: Bacterial Growth Conditions.....	23
2.2.3: Restriction Digestions.....	23
2.2.4: Strategy for Fusion Protein Construction.....	24
2.2.5: Cloning of SIPK.....	24
2.2.6: Cloning of GFP.....	27
2.2.7: Construction of the Fusion Protein.....	28
2.2.8: Construction of the Fusion Protein Linker.....	31

2.2.9: Yeast Vector Construction.....	32
2.2.10: Yeast Transformation.....	33
2.2.11: Expression in Yeast.....	34
2.2.12: Binary Vector Construction.....	34
2.2.13: Cloning of SIPK:GFP with Linker into pCAMBIA 1300 + MCS.....	36
2.2.14: Plant Transformation using Agroinfiltration.....	36
2.2.15: Infiltration of Agrobacterium for Transient Expression <i>In</i> <i>Planta</i>	37
2.3: Results.....	39
2.3.1: Cloning of SIPK.....	39
2.3.2: Cloning of GFP.....	39
2.3.3: Construction of the Fusion Protein.....	41
2.3.4: Fusion Protein Linker.....	42
2.3.5: Yeast Vector Construction.....	43
2.3.6: Expression in Yeast.....	43
2.3.7: Binary Vector Construction.....	46
2.3.8: Cloning Construct into Binary Vector.....	47
2.3.9: Plant Transformation using Agroinfiltration.....	47
2.4: Discussion.....	50
CHAPTER 3: Immunolabelling of Tobacco MAPKs.....	56
3.1: General Introduction to Immunolabelling	
3.1.1: Immunolabelling.....	56
3.1.2: Fluorochromes and Fluorescence.....	56
3.1.3: Fixation.....	56
3.1.4: Digestion/Removal of Cell Wall.....	57
3.1.5: Immunolabelling of SIPK and WIPK.....	58
3.2: Materials and Methods	
3.2.1: Tobacco Seedling Growth and Treatment with Harpin and Megaspermin.....	59
3.2.2: Cell Culture Growth and Treatment with Harpin and Megaspermin.....	59
3.2.3: Fixation of Samples in Paraformaldehyde.....	59
3.2.4: Digestion/Removal of Cell Wall.....	60
3.2.5: Immunolabelling	
3.2.5.1: Primary Antibodies.....	60
3.2.5.2: Secondary Antibodies.....	60
3.2.5.3: Controls.....	61
3.2.5.4: Immunolabelling Protocol.....	61
3.2.7: Quantification	63

3.3: Results.....	63
3.4: Discussion.....	79
Immunolabelling Troubleshooting.....	91
CHAPTER 4: General Discussion.....	94
APPENDICES.....	99
BIBLIOGRAPHY.....	104

LIST OF TABLES AND FIGURES

Chapter 1

Figure 1.1: Atomic structure of the MAPK kinase ERK2 at 2.3 Å resolution.....	4
Figure 1.2: 'Group A' plant MAPKs, showing common domains.....	9
Table 1.1: Plant MAPK Activation.....	14
Table 1.2: Subcellular Localization of ERK and ERK homologues.....	17

Chapter 2

Figure 2.1: Schematic of Amplification of SIPK and mGFP5 into TOPO TA 2.1 Vector.....	29
Figure 2.2: Strategy of SIPK-GFP Fusion Construction and Use	30
Figure 2.3: Transfer of 35S Driven MCS from pRT 101 to pCAMBIA 1300.....	35
Figure 2.4: TOPO TA 2.1 Vector Containing SIPK, and mGFP5 Fragments for Ligation.....	40
Figure 2.5: Colony PCR of the Fusion of SIPK:GFP into the TOPO TA 2.1 Cloning Vector.....	41
Figure 2.6: PCR Confirmation of Insertion of Linker between SIPK and GFP in the TOPO TA 2.1 Cloning Vector.....	42
Figure 2.7: Insertion of SIPK:GFP Fusion Sequence into the pYES TOPO TA 2.1 Yeast Expression Vector.....	43
Figure 2.8: Expression of SIPK-GFP Protein with Inserted Linker in Yeast Induced with Galactose.....	45
Figure 2.9: Digest Profile for the Insertion of the 35S Driven MCS from pRT 101 to pCAMBIA 1300.....	46
Figure 2.10: Insertion of SIPK:GFP with Linker into the Binary Vector pCAMBIA+MCS.....	47
Figure 2.11: Agrobacterium Colony PCR of Putative SIPK:GFP Fusion Protein Construct Insertion.....	48
Figure 2.12 a,b: Transient Expression by Agro-Infiltration of the SIPK:GFP with Linker Fusion Protein in Tobacco Leaves.....	49
Table 2.1: Primer Sequences.....	38
Table 2.2: Vectors.....	38

Chapter 3

Figure 3.1: Immunolabeling Control Samples of Fixed Suspension Culture Wild Type Tobacco Cells.....	65
Figure 3.2: Anti-ERK Immunolabeled Untreated and 30 min Harpin-Treated WT Tobacco Cells.....	72
Figure 3.3: Anti-ERK Comparison of Harpin and Megaspermin-Treated Cell Culture.....	73
Figure 3.4: Anti-ERK Immunolabeled Untreated and 30 min Harpin-Treated OX Tobacco Cells	74

Figure 3.5: Anti-pERK Immunolabeled Untreated and 30 min Harpin-Treated WT Tobacco Cells.....	75
Figure 3.6: Anti-pERK Immunolabeled Comparison of Harpin and Megaspermin- Treated Cultured cells.....	76
Figure 3.7: Anti-pERK Immunolabeled Untreated and 30 min Harpin-Treated OX:SIPK Tobacco Cells.....	77
Figure 3.8: Anti-FLAG Immunolabeled WT, OX-SIPK, and 30 min Harpin- Treated OX-SIPK Tobacco Cells.....	78

ABBREVIATIONS:

2-4 D = 2-4 dichlorophenoxyacetic acid
AtMPK3 = Arabidopsis MAPK 3
AtMPK6 = Arabidopsis MAPK 6
bp = base pair
BSA = bovine serum albumin
CaMV = cauliflower mosaic virus
CD domain = common docking domain
dATP = deoxyadenosine triphosphate
dCTP = deoxycytidine triphosphate
ddH₂O = distilled de-ionized water
DNA = deoxyribonucleic acid
dNTPs = deoxynucleotide triphosphate
DMSO = dimethyl sulfoxide
DTT = dithiothreitol
dTTP = deoxythymidine triphosphate
ED domain = ERK docking domain
EDTA = ethylenediaminetetraacetic acid
EGTA = ethylene glycol bis(2-aminoethyl ether)-N,N,N',N'-tetraacetic acid
EM = electron microscopy
ERK = Extracellular Regulated Kinase
ERMK = Elicitor-Responsive MAPK (also PcMPK3)
EV = empty vector
FITC = fluorescein-5-isothiocyanate
FLAG = bacterial flagellin-derived epitope
g = gravitational force
GFP = green fluorescent protein
GUS = beta-glucuronidase
HA = Heme Agglutinin
HEPES = N-(2-hydroxyethyl) piperazine-N'-(2-ethanesulfonic) acid
HPF = high pressure freezing
HR = hypersensitive response
h = hours
JNK = c-Jun N-terminal protein kinase
kb = kilobase
kDa = kiloDalton
LB = Luria-Bertani
LM = light microscopy
LUC = luciferase
MAPK = Mitogen-Activated Protein Kinase (also MPK)
MAPKK = Mitogen-Activated Protein Kinase Kinase (also MKK)
MAPKKK = Mitogen-Activated Protein Kinase Kinase Kinase
MCS = multiple-cloning site
min = minutes
MKK = see MAPKK

MPK = see MAPK
MS = Murashige and Skoog tissue culture medium
mRNA = messenger ribonucleic Acid
NES = nuclear export signal
NLS = nuclear localization site
Nm = nanometers
NtMEK2 = tobacco MEK 2
O.D.₆₀₀ = optical density at 600 nm
ORF = open reading frame
OX = SIPK-overexpressing line
PAMP = pathogen-associated molecular pattern
PcMPK3 = Parsley MAPK 3 (also ERMK)
PcMPK6 = Parsley MAPK 6
PCR = polymerase-chain reaction
pERK = phospho-ERK
PKA = Protein Kinase A
PR = pathogenesis related
PRKK = pathogen-responsive MAPKK (alfalfa)
PVPP = polyvinylpyrrolidone
PVDF = polyvinylidene fluoride
RFP = red fluorescent protein
RNA = ribonucleic acid
rpm = revolutions per minute
RT = room temperature
SAPK = Stress-Activated Protein Kinase
SC medium = synthetic complete medium
SDS = sodium dodecyl sulfate
SIMK = Stress-Induced Protein Kinase
SIMKK = Stress-Induced Protein Kinase Kinase
SIPK = Salicylic acid-Induced Protein Kinase
SIPKK = Salicylic acid-Induced Protein Kinase
TAE = tris-acetate EDTA
Taq = *Thermus aquaticus*
TBST = tris-buffered saline tween
TEY = threonine, glutamate, tyrosine
TDY = threonine, aspartic acid, tyrosine
TXY motif = threonine, "X" (any amino acid), tyrosine motif
TMV = tobacco mosaic virus
U = units
UV = ultra violet
YFP = yellow fluorescent protein
WIPK = Wound Induced Protein Kinase
WRKY = tryptophan, arginine, lysine, tyrosine
X-Gal = 5-bromo-4-chloro-3-indolyl-Beta-D-galactoside

ACKNOWLEDGEMENTS:

Some of the values in Table 1.0 were taken from correspondence with Dr. Marcus Samuel. Also thanks to Dr. Marcus Samuel for use of the GST-SIPK vector, and for help with cell culture maintenance and western analysis.

Western blot of harpin activation of cultured cells was borrowed from the work of Hardy Hall.

The pCAMBIA 1300-MCS construct was obtained from Greg Lampard

Thank-you to the UBC Bioimaging facility for training and use of the confocal microscope.

Thank-you to my masters thesis committee; Dr. Brian Ellis, Dr. Lacey Samuels and Dr. Jim Kronstad for their focused advice.

Thank-you to Dr. Lacey Samuels and her lab for help with immunolabeling techniques, use of the fluorescent microscope, and for advice. Also thanks to Geoff Wasteneys and his lab members for help with whole cell immunolabelling protocol manipulation.

A special thank-you to Dr. Brian Ellis for his continual patience, guidance, and support.

CHAPTER ONE: GENERAL INTRODUCTION

1.1: Studying Signal Transduction

1.1.1: Signal Transduction and MAPK cascades

Life is modulated by signal cascades that relay information about environmental changes to affect intracellular responses which allow organisms to cope successfully with changing conditions. The necessary information is often relayed by signal transduction pathways that in eukaryotic cells can include protein kinases, phosphoprotein phosphatases, lipases, nucleotide exchange factors, ion channels, G proteins, lipid kinases and transcription factors (Braun and Walker, 1996). Among the protein kinases, mitogen-activated protein kinases (MAPKs) are versatile signal transducing enzymes that are involved in multiple pathways. Their rapid and transient activation by various stresses strongly influence homeostasis, making MAPKs important proteins for study (Zhang and Klessig, 2001).

MAPKs are only one part of signaling pathways linking upstream receptors to downstream targets through upstream mitogen activated protein kinase kinase kinases (MAPKKKs) and mitogen activated protein kinase kinase (MAPKKs) (Jonak et al., 2002). MAPK signals are a phospho-transfer event between cognate upstream kinases and downstream targets (Tanoue et al., 2001). MAPKs are low abundance serine-threonine protein kinases that can mediate, transmit, and amplify cellular signals resulting in biochemical and physiological responses (Mitogen-activated protein kinase cascades in plants: a new nomenclature, 2002).

MAPK/MAPKK/MAPKKK gene families are highly conserved in eukaryotes. MAPK sequences have been found to be highly conserved from primitive protozoans such as

Plasmodium to the more highly evolved metazoans (Kultz, 1998). Plants have more MAPK family members than animals. Genome analysis has revealed 14 family members in yeast, 25 in *C. elegans*, 47 in *Drosophila*, 47 in humans, and over 90 in *Arabidopsis thaliana* (Manning et al., 2002). Of the 90 or more identified arabidopsis MAPK signaling family members there are 20 MAPKs, 10 MAPKKS, and over 60 MAPKKKs (Jonak et al., 2002). This wide array of MAPKs supports recognition of a wide variety of stimuli, a versatility that is especially important for stationary organisms such as plants, which depend for their survival on efficiently sensing and responding to environmental change. In effecting appropriate responses, the plant's resources are wisely spent allowing the plant to compete for survival. The higher number of plant MAPKs might suggest plant MAPKs may play additional roles within the plant (Mizoguchi et al., 1997) or might reflect MAPK redundancy within plant species. Perhaps the MAPK number differences reveal fundamental differences in MAPK signaling mechanisms between plant and animal kingdoms. It is important to keep in mind that the record of genes revealed in genome analysis does not reveal the full diversity of the family, however, since alternative splicing of RNA transcripts from a single gene can yield different protein variants. Alternative splicing can generate dozens or even hundreds of different mRNA isoforms from a single transcript (Breitbart et al., 1987). It has been estimated that 42% of human genes may display alternative splicing (Kan et al., 2001). A notable example of experimentally identified MAPK family splice variants is associated with the eukaryotic MAPK c-Jun N-terminal protein kinase (JNK). JNKs have been shown to be involved in mammalian embryonic development but also play a role in regulating programmed cell death. Alternative splicing of JNK transcripts creates at least ten

different JNK MAPK isoforms of 46-55 kDa that differ in their substrate affinities (Barr and Bogoyevitch, 2001). Alternative splicing might give more MAPK options in animal systems, explaining the lower number of identified animal MAPKs. Whether plant MAPKs routinely undergo alternative splicing has yet to be investigated, although the alternative splicing process does appear to operate in plant cells (Lazar and Goodman, 2000; Eckardt, 2002).

1.1.2: MAPK Structure and Function

All MAPKs have 11 common subdomains characteristic of serine/threonine protein kinases (Hanks et al., 1988). Crystallographic analyses indicate that the active site of MAPKs is in an activation loop found between two of the lobes of the protein (Zhang et al., 1995). This activation loop contains a TXY motif typical of phosphorylation activation (Gartner et al., 1992). Full activation of MAPK has been shown to require the phosphorylation of both the threonine and tyrosine residues in this TXY motif between kinase domains VII and VIII, inducing conformational change that increases the accessibility of the substrate binding pocket (Mitogen-activated protein kinase cascades in plants: a new nomenclature, 2002) (Canagarajah et al., 1997). MAPKs are deactivated by the dephosphorylation of either one or both of the residues in the activation loop (Volmat and Pouyssegur, 2001). Figure 1.1 shows the atomic structure of the MAPK extracellular regulated kinase (ERK) 2.

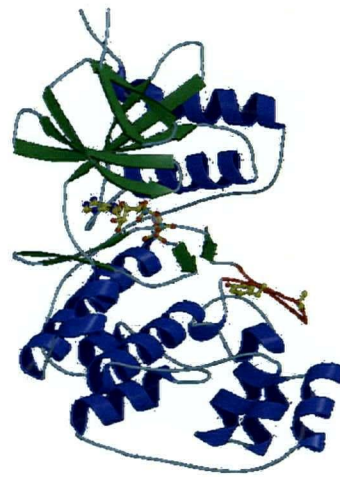


Figure 1.1: Atomic structure of the MAP kinase ERK2 at 2.3Å resolution.
Faming Zhang, Arne Strand, David Robbins, Melanie H Cobb and Elizabeth J. Goldsmith.
Nature, 367:704-711(1994)

Once activated, MAPKs have the ability to activate other proteins. The substrates of MAPKs are phosphorylated on serine or threonine residues that are immediately followed by a proline (Gonzalez et al., 1991) and the phosphorylation event must be efficient and specific enough to avoid unwanted cross-talk within MAPK cascades or with other signaling pathways (Tanoue et al., 2001). Cellular MAPK specificity is regulated by the presence of docking domains of MAPK modules, and through scaffold proteins (Tanoue et al., 2001). The C-terminus of a MAPK has the ability to bind to MAPKKs, MAPK-activated protein kinases, and phosphatases (Tanoue et al., 2001) through an interaction domain called the common docking (CD) domain. The ERK docking (ED) site located on the opposite side from the active center, forms a groove with the CD domain, and site directed mutagenesis of either of the two domains caused a shift in MAPK substrate binding efficiency (Tanoue et al., 2001). Co-immunoprecipitation assays indicate that both the CD and ED contribute to protein interaction efficiency and specificity, but the CD and ED domains are not the only MAPK domains important for docking (Tanoue et al., 2001). It has been reported that multiple regions of the MAPK ERK2 are important for determining the enzymatic specificity of upstream kinases (MAPKKs) (Wilsbacher et al., 1999).

Scaffold proteins are also thought to play a role in controlling MAPK specificity. Scaffold proteins are proteins that function to bring other proteins together for interaction. These proteins usually have multiple protein binding domains such as WD40 repeats.

Scaffold protein interactions with MAPKs have been well characterized in yeast (Jonak et al., 2002), and function as docking proteins that can concentrate and localize MAPK components to designated subcellular locations (van Drogen and Peter, 2001).

Scaffold proteins have been identified in plants; however, no MAPK/scaffold protein interactions have yet been reported.

The yeast scaffold protein Ste5 was shown to interact in a conserved MAPK cascade required for mating in *Sacharomyces cerevisiae*. Ste5 is a zinc-finger-like protein that can form a multikinase complex with the MAPKKK Ste11, the MAPKK Ste7, and the MAPK Fus3. Two-hybrid analysis indicates that Ste11, Ste7, and Fus3 associate with different domains of Ste5, while Kss1 associates with the same domain as Fus3, implying that Ste5 is capable of simultaneously binding a MAPKKK, MAPKK, and MAPK (Choi et al., 1994).

1.1.3: Eukaryotic MAPK Families

Mammalian MAPKs can be divided into at least three main subfamilies; Jun kinases/stress-activated protein kinases (JNK/SAPKs), p38 MAPKs, and extracellular signal-regulated kinases (ERKs). The plant homologues of ERK 1 and 2 are the target proteins of this study, although JNKs and p38 MAPKs show similar patterns of signal transduction.

Stress-activated protein kinases (SAPK)/Jun N-terminal kinases (JNK) are mammalian MAPKs that are activated by a variety of environmental stresses, inflammatory cytokines, growth factors and GPCR agonists. Activated SAPK/JNK has been shown to translocate to the nucleus, where it regulates the activity of several transcription factors such as c-Jun, ATF-2 and p53 (Davis, 1999; Leppa and Bohmann, 1999).

p38 MAPKs are mammalian MAPKs that are also activated by a variety of environmental stresses and inflammatory cytokines. p38 MAPK downstream targets

include HSP27 and MAPKAP-2 as well as several transcription factors including ATF-2, Stat1, the Max/Myc complex, MEF-2, Elk-1 and (indirectly) CREB via activation of MSK1 (Tibbles and Woodgett, 1999).

Mammalian cells contain two ERK-type MAPKs, ERK1 and ERK2, which are also commonly called MAPK 42 and MAPK 44, respectively, based on their molecular weight. Mammalian ERKs are most notably involved in regulating gene transcription and cell cycle progression (Pearson *et al.*, 2001). Some of the identified ERK regulated targets are receptor tyrosine kinases (Porter and Vaillancourt, 1998), integrins (Giancotti and Ruoslahti, 1999), and ion channels (Rane, 1999).

Although the specific components of the signaling cascade vary with different stimuli, the basic architecture of the ERK activation pathway usually includes a set of adaptors (e.g. Shc, GRB2, Crk) that link the receptor to a guanine nucleotide exchange factor (e.g. Sos, C3G) that help to transduce the signal to small GTP binding proteins (Ras, Rap1). These, in turn, activate the core unit of the MAPK cascade composed of a MAPKKK (Raf), a MAPKK (MEK1/2) and MAPK (ERK) (Lewis *et al.*, 1998).

In plant systems there is no evidence of p38 or JNK-MAPK homologues. Instead plants appear to have evolved a divergent and specialized set of ERK homologues. These plant ERKs have been found to play roles in the transduction of a wide variety of stimuli, effecting physiological, hormonal and developmental responses that will be discussed in greater detail below.

1.1.4: Plant MAPK Families

The *A. thaliana* genome sequence contains 20 putative MAPK annotations. These MAPKs are divided into 4 groups (A-D) based on overall phylogenetic clustering.

Groups A,B, and C encompass MAPKs with a TEY subtype of the TXY motif and those with TDY fall into group D (Mitogen-activated protein kinase cascades in plants: a new nomenclature, 2002).

The ERK 1 and 2 plant homologues are members of Group A MAPKs, which are involved with environmental and hormonal response signaling. Figure 1.2 shows some of the group A members, and their common domains.

Arabidopsis is used as a template for annotation of other plant genomes, although the homology and synteny are not perfect. Nevertheless, the high degree of sequence conservation within the MAPK family has allowed MAPK homologues in other species to be annotated by sequence similarity to arabidopsis. Plant MAPK homologues not only show considerable sequence similarity, but there is also strong evidence that they display similar signaling patterns. For example the arabidopsis and the tobacco ERK 1 and 2 homologues have both been shown to be activated by fungal elicitors (Desikan et al., 2001); (Asai et al., 2002); (Zhang et al., 2000); (Lee et al., 2001). Table 1.1 lists specific elicitors and the respective activated ERK homologues in several plant species and humans. Many of the elicitors induce similar MAPK activation profiles in different species, indicating similar plant signaling patterns.

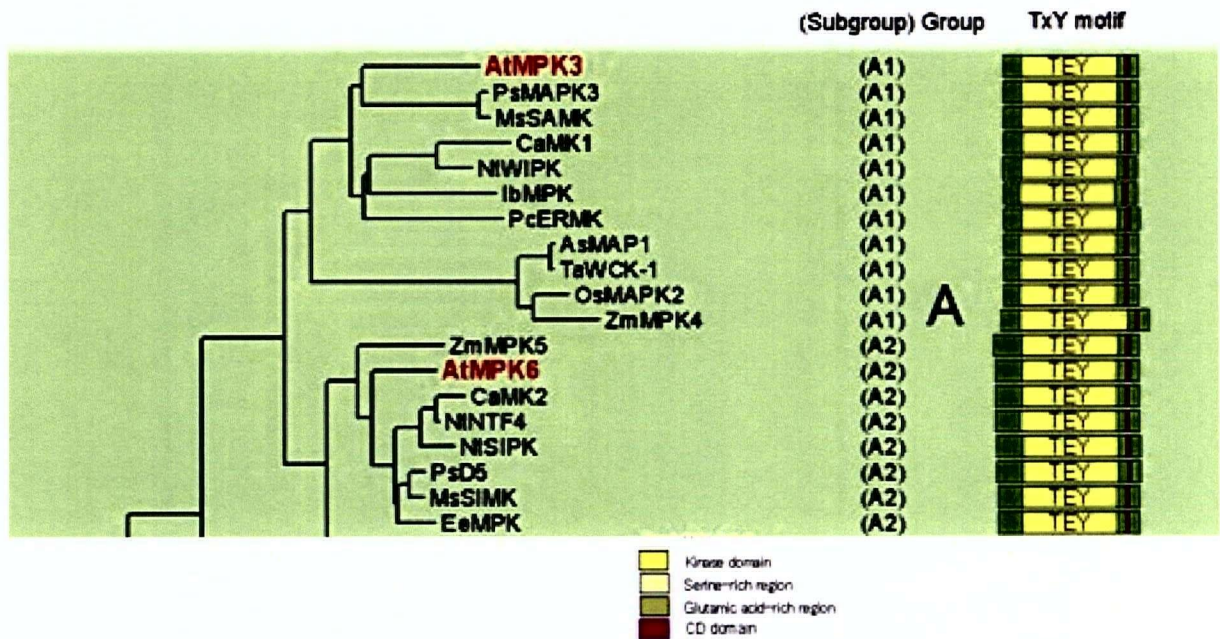


Figure 1.2: 'Group A' plant MAPKs, showing common domains
 Mitogen-activated protein kinase cascades in plants: a new nomenclature (2002) *Trends in Plant Science* 7: 301-308

The known homologues of ERK 1 and 2 include AtMPK6 and AtMPK3 in arabidopsis, salicylic-induced protein kinase (SIPK) and wound-induced protein kinase (WIPK) in tobacco, stress-induced MAPK (SIMK) and stress-activated MAPK (SAMK) in alfalfa (Jonak et al., 2002), and PcMPK6 and PcMPK3 (Lee et al., 2004) (also called elicitor-responsive MAPK (ERMK)) in parsley (Jonak et al., 2002).

In non-plant studies, MAPKKs have been found to typically exhibit specificity for one MAPK, but some plant MAPKKs are able to activate multiple MAPKs (Jonak et al., 2002). For example, in tobacco, NtMEK2 was found to activate both SIPK and WIPK (Yang et al., 2001), while the arabidopsis MKK4 and MKK5 can activate both MPK3 and MPK6 (Asai et al., 2002).

Mammalian and plant MAPKKs may have different regulating roles and capabilities within their respective kinase signaling cascade. Yeast-two hybrid studies showed that SIMK interacted with SIMKK, a close homologue of AtMKK4/AtMKK5 and NtMEK2 (Kiegerl et al., 2000), but biochemical analysis showed that SIMKK activates both SIMK and MMK3 in cells treated with an elicitor, while it activates only SIMK when the cells were challenged with salt stress (Jonak et al., 2002). In general, plant MAPK signaling cascades regulate input signals by means of cross-talking proteins to effect multiple output signals.

1.1.5: Approaches to Analysis of MAPK Pathways

MAPK signaling cascades are complex networks with multiple stages of regulation. Dissection of these cascades can be achieved by *in vitro* methods such as protein purification, immunodetection, kinetic analysis, and biochemical assays, or *in vivo* techniques such as genetic disruption/mutagenesis, transcomplementation, two-hybrid

assays, and immunodetection and transgenic analysis (Tena et al., 2001). The most commonly used strategies are yeast two-hybrid studies, *in vitro* protein-protein interaction studies, and the use of transient expression of various combinations of MAPK pathway components in protoplasts (Jonak et al., 2002). *In vivo* study of MAPK activation and interactions is particularly difficult due to the low abundance of phosphorylated proteins at physiological levels.

In a yeast two-hybrid system, using the tobacco MAPK SIPK as bait, Liu *et al* (2001) recovered MAPKK (SIPKK) as the only interactor. Although SIPKK showed both interaction and co-precipitation with SIPK, it was unable to phosphorylate SIPK *in vitro* (Liu et al., 2000). Studies in alfalfa showed similar precipitation and *in vitro* phosphorylation results between PRKK and the SIPK homologue, SIMK (Cardinale et al., 2002). These results indicate that although modular interactions can be detected, they are not good predictors of *in vivo* activity, and they are not necessarily the determinants of MAPK specificity. While upstream activators of both SIPK and SIMK have been identified, no downstream interactors are known. Possible reasons for this situation include a requirement for other protein partners, such as chaperone proteins and scaffold proteins as seen in yeast, or differing upstream signaling partners recognized by MAPKs or by other signaling molecules. Quick, transient activation of the substrate, or weak interaction between SIPK/SIMK and its substrate could also explain the failure to identify downstream targets.

1.1.6: Hypersensitive Response

The hypersensitive response (HR) is a plant defense mechanism associated with resistance (Dangl et al., 1996). The mechanisms are not clearly understood but it is

known that after exposure to some plant stresses such as UV light, fungal or bacterial infection there is an accumulation of specific pathogen resistance (PR) gene transcripts along with the formation of lesions at infection sites in the plant tissue. The lesions are somewhat isolated, or restricted from the surrounding healthy tissue (Hammond-Kosack and Jones, 1996). Along with lesion formation, a plant displaying a hypersensitive response typically develops immunity to subsequent attacks from a broad range of pathogens (Ryals et al., 1994). This broad-range pathogenic immunity is associated with disease resistance and serves to protect the plants' survival against ever-evolving pathogens.

1.1.7: MAPKs Elicitors

MAPK cascades are transiently activated by a variety of input signals, including pathogen infection, elicitors, wounding, low temperature, drought, hyper and hypo osmolarity, high salinity, touch, and reactive oxygen species (Mitogen-activated protein kinase cascades in plants: a new nomenclature, 2002). An elicitor is any applied biological agent which brings forth a response from the plant.

One well studied pattern of MAPK induction is the pathogen-associated molecular pattern (PAMP) in *Drosophila*. PAMPs are triggers of signal transduction pathways responsible for transcriptional activation of pathogen defense genes. Conservation of the MAPK signal cascade in plants results in a native immune protection system similar to that of *Drosophila* against non-host disease. (Lee et al., 2004). Two PAMP-like elicitors in tobacco and are Harpin and Megaspermin.

Harpin is a protein from the bean halo-blight pathogen *Pseudomonas syringae* pv *phaseolicola* (harpin^{psph}), which is known to elicit a HR and an accumulation of pathogen-related (PR)-gene transcripts in the non-host tobacco (Lee et al., 2001).

Megaspermin is a glycoprotein (“elicitin”) secreted by *Phytophthora megasperma* H20. There are three different forms (α , β , γ) that are known to induce the HR response in tobacco (Baillieul et al., 2003). When applied to tobacco cultured cells, elicitors induce rapid protein phosphorylation, Ca^{2+} influx, extracellular and transient H_2O_2 production (Baillieul et al., 2003).

Many studies have examined MAPK signaling in plants in response to stimuli, such as challenge by bacterial or fungal attack, cold, drought, wounding, and osmotic stress. Table 1.1 lists specific treatments reported to activate ERK homologues in several species.

Although all of the same stresses have not yet been tested in all the aforementioned species, it is clear that similar elicitors show similar MAPK activation patterns across species.

Arabidopsis AtMPK6 has been shown to be elicited by bacterial flagellin peptide (flg22) (Asai et al., 2002). The Sheen group also showed that AtMKK4/AtMKK5 and AtMPK3/AtMPK6 were all activated by flagellin peptide (Asai et al., 2002), showing multiple MAPK activations from one elicitor.

Table 1.1: Plant MAPK Activation

MAPK	Organism	Treatment	Reference
AtMPK6	<i>Arabidopsis thaliana</i>	-microbial elicitors -xylanase (fungal) -H ₂ O ₂ -KO ₂ -harpin (fungal) -bacterial flagellin	- (Nuhse et al., 2000) - (Nuhse et al., 2000) - (Yuasa et al., 2001) - (Yuasa et al., 2001) - (Desikan et al., 2001) - (Asai et al., 2002)
AtMPK3	<i>Arabidopsis thaliana</i>	- H ₂ O ₂ - flagellin (bacterial)	- (Kovtun et al., 2000) - (Asai et al., 2002)
SIPK	<i>Nicotiana tabacum</i>	-salicylic acid -TMV -wounding -fungal elicitors -harpin -osmotic stress -hyperosmotic stress -UV -NO	- (Zhang and Klessig, 1997) - (Zhang and Klessig, 1998)a - (Zhang and Klessig, 1998)b - (Zhang and Klessig, 2000) - (Lee et al., 2001) - (Hoyos and Zhang, 2000) - (Cazale et al., 1999) - (Miles, 2002) - (Klessig et al., 2000)
WIPK	<i>Nicotiana tabacum</i>	-wounding -osmotic stress -TMV	- (Seo et al., 1995) - (Droillard et al., 2000) - (Zhang and Klessig, 1998)a
SIMK	<i>Medicago truncatula</i> (Alfalfa)	-osmotic stress -salt stress -fungal elicitors	- (Munnik et al., 1999) - (Kiegerl et al., 2000) - (Cardinale et al., 2002)
SAMK	<i>Medicago truncatula</i> (Alfalfa)	-wounding -cold -drought	- (Bogre et al., 1997) - (Jonak et al., 1996) - (Jonak et al., 1996)

Although there are many similarities among these elicitation patterns, there are also differences. In tobacco suspension cell culture, SIPK and WIPK showed phosphorylation activity in response to hypo-osmotic stress by in-gel kinase assays, and were identified by immunoblotting (Droillard et al., 2000). However, the same group also showed that SIPK, but not WIPK, was activated by hyperosmotic stress (Cazale et al., 1999). Thus, many plant stresses affect the same downstream kinases but within different physiological contexts, how the activated kinases regulate specific cellular responses in each context is unknown. Likely regulatory factors include the duration of the MAPK

activation, the kinase subcellular localization, kinase accumulation and stimulus thresholds, and variability in protein-kinase/substrate interaction.

1.2: Studying Subcellular localization of MAPKK and MAPK

1.2.1: Subcellular Localization

Subcellular localization refers to the location, or distribution of a given molecule within a cell. A given protein's subcellular localization can be dictated by information encoded within its sequence such as nuclear, chloroplast, mitochondrial, or ER-localizing domains. MAPKK localization is determined by its nuclear export signal (NES) in the near N-terminal region (Fukuda et al., 1997), which renders it functionally a cytoplasmically localized protein. The 3D structural features of a protein, such as trans-membrane domains, can direct proteins into membranes. The distribution of charged residues can render the protein more hydrophobic or hydrophilic and thus help dictate its placement within the cell. Although many proteins have fixed positions within the cell, some proteins, upon activation, move from one part of the cell to another.

1.2.2: Subcellular Localization of ERK

The mechanisms controlling the localization of MAPKs are not based on localization sequences. It is believed that MAPK is localized to the cytoplasm by specific interactions with its upstream MAPKK(s), from which it dissociates upon activation of that MAPK pathway (Fukuda et al., 1997). MAPKK is thus a cytoplasmic anchoring protein for MAPK. Upon MAPK release from its cognate MAPKK in yeast, the MAPK activates a number of protein effectors located in different regions of the cell including the cytosol, cell periphery and the nucleus (Horgan and Stork, 2003). The subcellular localization of activated ERKs is important to cellular responses. ERK-mediated

activation occurs throughout the cell, but nuclear localization appears to be associated with longer term effects, such as involvement in cell growth and division (Marshall, 1995). It has been shown that under strong mitogens, ERKs move rapidly and persistently to the nucleus (Lenormand et al., 1993). It has also been suggested that protein kinase A (PKA) is required as well to import the phosphorylated form of ERK into the nucleus (Impey et al., 1998). When ERK is localized to the nucleus, it regulates gene expression by phosphorylating various transcription factors directly, such as p62^{TCF}/elk-1 (Seth et al., 1991) or indirectly, such as CREB (Xing et al., 1998).

Various analytical techniques have been used to study ERK and its homologues in many different systems, using different MAPK stimuli, so it is difficult to derive a single model explaining ERK activation, localization, and use of effectors. There are, however, many activation, localization and effector similarities across these various studies.

In humans, ERK 1 moves to the nucleus when stimulated by strong mitogens, and is associated with various nuclear targets, such as spindle poles and chromosome ends during mitosis (Table 1.2). However, ERKs have also been shown to localize to the mitochondria, and to autophagosomes.

Plant ERK homologue studies have also revealed multiple areas for ERK subcellular localization, such as the actin cytoskeleton in growing root hair tips of alfalfa (Samaj et al., 2002). Treatment with a fungal elicitor in cultured parsley cells sent the ERK 1 homologue from the cytoplasm to the nucleus (Ligterink et al., 1997).

Table 1.2: Subcellular Localization of ERK and ERK homologues

Homologue Name	Species/Genus	Subcellular localization	Inducer	Reference
ERK 1	<i>Homo sapiens</i>	-cytoplasm to nucleus -mitochondria and autophagosomes -spindle poles -midbody -chromosome periphery	-strong mitogens -Lewy Body disease -prophase, anaphase -cytokinesis -metaphase	(Lenormand et al., 1993) - (Zhu et al., 2002) -(Shapiro et al., 1998) -(Shapiro et al., 1998) - (Shapiro et al., 1998)
AtMPK6	<i>Arabidopsis thaliana</i>	?		
SIPK	<i>Nicotiana tabacum</i>	?		
SIMK	<i>Medicago truncatula</i> (alfalfa)	-nucleus to root tip -cytoplasm to actin cytoskeleton (maybe vesicular)	-root hair formation -treatment with jasplakinolide	- (Samaj et al., 2002)
PcMPK6	<i>Petroselinium hortense</i> (parsley)	-cytoplasm to nucleus	-Pep 13 -fungal elicitor	- (Lee et al., 2004) - (Ligterink et al., 1997)
ERK 2	<i>Homo sapiens</i>	-cytoplasm to nucleus	-growth factor stimulation	- (Horgan and Stork, 2003)
AtMPK3	<i>Arabidopsis thaliana</i>	?		
WIPK	<i>Nicotiana tabacum</i>	?		
SAMK	<i>Medicago truncatula</i> (alfalfa)	?		
PcPMK3 (ERMK)	<i>Petroselinium hortense</i> (parsley)	-cytoplasm to nucleus	Pep13	- (Lee et al., 2004)
SIPK/WIPK (undifferentiated)	<i>Nicotiana tabacum</i>	-cytoplasm and nucleus	Seed germination	- (Coronado et al., 2002)

Compared to yeast and mammals, there has not been extensive research done in plants on subcellular localization of MAPKs, in part due to a lack of efficient tools for analysis *in planta*.

1.2.3: Methods of Determining Subcellular Localization

There are many different methods to determine subcellular localization of proteins. Two of the most common methods include the use of reporter proteins and immunolabeling.

Reporter proteins are proteins that one can detect easily, but are not normally present within the research organism. They can therefore allow one to monitor cellular events that would otherwise be difficult to observe. Some of the more commonly used reporter proteins in plant systems are beta-glucuronidase (GUS), luciferase (LUC) and green fluorescent protein (GFP). GFP based detection allows the imaging of live cells and permits one to view dynamic changes within the cell. This is not achieved by indirect immunofluorescence. Immunofluorescence provides higher spatial resolution than fusion proteins (Arnim, 1998), but requires specific antibodies and cellular fixation.

Immunolabeling employs tagged antibodies (either primary or secondary) which can be visualized within the labeled tissue through microscopy. Immunolabeling allows the researcher to study native protein content, and localization, and yields better resolution of subcellular structures than live cell imaging. Immunolabelling is often used when fusion constructs to a given protein are either too difficult to construct, or feasibly not possible, or when there is an antibody available that is specific for their protein of interest. Some common antibody tags include covalently coupled fluorescent chemicals, gold particles (for EM), or enzymatic reporters such as hydrogen peroxidase.

The intent of this experiment was to examine the subcellular localization of the tobacco MAPKs, SIPK and WIPK, under normal and stressed conditions. Through the construction of a SIPK:GFP fusion construct for use in live cell image reporting, and immunolabelling of fixed cultured tobacco cells with anti-MAPK antibodies, I will examine the subcellular localization patterns of SIPK/WIPK. Subcellular localization of the MAPKs after elicitation with harpin and megaspermin will be examined, and compared to untreated cells.

CHAPTER TWO: SIPK-GFP Fusion Protein

2.1: Introduction to GFP

2.1.1: GFP

Green fluorescent protein (GFP) is a commonly used reporter for biological systems because it allows live, *in vivo* image reporting of one's protein of interest without destruction of the biological sample. This 27 kDa protein, originally isolated from *Aequorea victoria*, contains a chromophore that becomes excited through the absorption of photons in the 396-475 nm range, and emits green fluorescence at approximately 508 nm (Cubit, 1995; Heim et al., 1994). The chromophore originates from a self-catalyzed covalent modification of the amino acid sequence Ser-Tyr-Gly at positions 65-67, which catalyze to form a *p*-hydroxybenzylidene-imidazolidinone species. GFP is superior to many chromophores as it does not photobleach, a process where fluorochromes can get irreversibly damaged due to repeated excitation with an intensive light source. (van Drogen and Peter, 2004). Its small size (~27 kDa), stability and bright fluorescence make it an ideal reporter for biological systems. In addition to the native green version of GFP, site-directed mutagenesis has since been used to develop many effective GFP variants, including different chromophores. The spectral shifts of these chromophores yield different fluorescent colours, notably the red shift mutant (RFP) and yellow shift mutant (YFP) (Brandizzi et al., 2004). Use of different shift mutants of GFP permits multiple labeling within the cell, and provides an opportunity to optimize fluorescence results.

2.1.2: GFP Fusion Proteins

By use of recombinant DNA manipulations, GFP can be fused to specific proteins making it possible to study subcellular localization of the chimeric protein *in vivo*. Both

C-terminal and N-terminal fusions have been used, and such flexibility is important since both the C and/or N-terminus of a given protein can possess essential binding sites or other important functions that could be affected by fusion to another protein. Similarly, attachment to GFP can potentially cause problems with proper folding or domain conformation. A recent study demonstrated that internal insertion of GFP within a chimeric protein could be used effectively in high throughput screening of plant proteins for subcellular location.

2.1.3: GFP Expression in *Planta*

Expression of native GFP in arabidopsis was originally found to be unstable (Davis and Vierstra, 1998). Incorrect splicing was responsible for the protein instability, and optimization of the codon usage in the unstable region yielded a stable exogenous GFP, but with a weak fluorescent signal (Davis and Vierstra, 1998). mGFP5 is a specific version of the green GFP variant which has been shown to give good results in plant systems (Brandizzi et al., 2002; Kim et al., 2003; Sheahan et al., 2004). Strong expression of the green chromophore is important in plants because it is often necessary for the GFP signal to compete with the background autofluorescent signal from chlorophyll, xylem, lignin and other autofluorescent bodies present within the tissue under study.

Expression of GFP in plant systems can be designed to be transient, or stable. For proteins whose over-expression may be lethal to the cell or for proteins that are rapidly degraded, transient expression is preferred. Transient expression allows fast and easy visualization of results and is therefore often used as an indicator of gene transfer and

expression efficiency. Stable transgenics, on the other hand, allow for easily repeatable and long time-course experiments (Weld et al., 2001).

Both transient and stable ectopically expressed GFP has been shown to be localized throughout the plant cell, with some stronger nuclear and vascular tissue fluorescence (von Arnim et al., 1998). These patterns might reflect GFP's small size (27 kDa) and the associated ease of diffusion into the nucleus, although it has also been suggested that GFP may contain a cryptic nuclear localization site (NLS) (von Arnim et al., 1998). Because of diffusibility, GFP-protein fusions must have a larger overall size than the size exclusion limit for the nucleus if the construct is expected to report nuclear versus cytosolic localization (von Arnim et al., 1998). Large proteins cannot passively diffuse through the nuclear pore and must be actively transported in if they are to carry out a function within the nucleus.

GFP fusion proteins are used often when specific antibodies towards their protein are not available, or when cellular fixation processes disrupt the antibody's capability to recognize the protein. GFP is ideal for live cell imaging of the dynamics of intracellular movement, localization, and potential destruction of the protein. New constructs introduced to host species can, however, show variable expression levels of the fusion protein, which vary from native form expression levels. These different levels of expression can change the normal cellular dynamics of a cell, and give misleading imaging results. Other effects such as co-suppression can also cause undesired effects upon the existing signaling pathway which would give misleading results. Co-suppression of a gene can occur when a related gene is expressed, or by the introduction of a related transgene (Pal-Bhadra et al., 1997). Homology-dependent gene silencing is a co-

suppression phenomenon in plants. Exogenously expressed genes introduced into a plant containing a homologous gene can cause not only the suppression of the transgene, but also suppression of the native gene (Meyer and Saedler, 1996). To monitor false localization results, GFP-fusion protein localization can be confirmed by immunolabeling, or by construct regulation by the protein's native promoters.

2.2: Materials and Methods

2.2.1: Plant Growth Conditions

Nicotiana tabacum Xanthi nc seeds were sterilized using 50% JAVEX[®] bleach for 10 min, followed by 5 consecutive 10-min washes in sterile ddH₂O. Seeds were plated on ½ strength MS plates and grown under controlled conditions (25/20 °C, 16-h-light/8-h-dark cycle). After 2 weeks, the seedlings were transferred to Magenta tubs containing ½ MS with no added sugar and grown under the same controlled environment conditions.

2.2.2: Bacterial Growth Conditions

Bacterial cells were routinely cultured on Luria-Bertani (LB) medium solidified with 1.5% (w/v) bactoagar (Difco). Where required, media were supplemented with kanamycin (50 µg/mL) and 5-bromo-4-chloro-3-indolyl-Beta-D-galactoside (X-Gal) (40 mg/mL). Plates were incubated at 37 °C for 16-24 h. Liquid cultures of LB medium supplemented with the appropriate concentration of antibiotics were incubated aerobically with agitation for 12-18 h at 37°C.

2.2.3: Restriction Digestions

DNA (1 µg) was added to 1 µL restriction enzyme, 5 µL 10X restriction buffer, and ddH₂O to make 50 µL total volume, and mixed by pipetting. The digestion mix was

incubated at 37 °C for 1-3 h., depending on enzyme efficiency. Digestion was arrested by incubation at 50 °C for 5 min, and samples were stored on ice or at -20°C until further use.

2.2.4: Strategy for Fusion Protein Construction

To construct a SIPK:GFP fusion protein that could be expressed in both yeast and plant systems, a strategy was devised using plasmids available in the lab. Both SIPK and GFP ORFs were available on plasmids (Figure 2.1). For cloning purposes the TOPO TA 2.1 cloning vector was a good candidate to house the SIPK and GFP amplicons (Figure 2.1). To aid cloning, restriction enzyme target sequences were added to the SIPK and GFP primers. SIPK primers contained a *XhoI* site on the forward primer and *NotI* site on the reverse primer. Similarly, a *NotI* site was added to the GFP forward primer and an *XbaI* site added to the GFP reverse primer (Figure 2.1). The *NotI* site on both fragments would link SIPK and GFP together. To keep GFP in frame when fused to SIPK, and extra base pair was added to the GFP forward primer.

TOPO TA 2.1 cloning vector containing SIPK in the orientation that placed the 3' end of SIPK next to the *XbaI* site in the TOPO TA 2.1 cloning vector multiple cloning site (MCS) (Figure 2.2) could be digested with *NotI* and *XbaI* to accept the GFP digested fragment with *NotI* and *XbaI* sticky ends. Once the two fragments were fused in the TOPO TA 2.1 cloning vector, the fragment could be digested out, or amplified with SIPK forward and GFP reverse primers to be integrated either in a yeast expression vector, or a binary vector for expression *in planta* (Figure 2.2).

2.2.5: Cloning of SIPK

Cloning of the SIPK ORF into the TOPO TA 2.1 cloning vector strategy is outlined in Figure 2.1. SIPK was amplified by PCR from a GST-fusion expression plasmid

(provided by Marcus Samuel) using the SIPK primers listed in Table 2.1. The PCR amplification of SIPK was performed using HiFi Platinum Taq (Invitrogen) and *XhoI* SIPK forward and *NotI* reverse primers (Table 2.1). A 50 μ L PCR reaction mixture included 5 μ L 10X PCR amplification buffer, 2.0 μ L $MgSO_4$, 2.5 μ L 10 mM dNTPs, 2 μ L of 10mM each of the forward and reverse primer, 1 μ L Platinum HiFi Taq, and ddH₂O to make 50 μ L.

The PCR amplification program performed on a Biometra T-gradient thermocycler was set at 95 °C for 5 min, followed by 32 cycles of 95 °C for 30 sec., 55 °C for 30 sec., and 68 °C for 1 min, with a final elongation cycle at 68 °C for 10 min.

The SIPK amplicon was ligated into the TOPO TA 2.1 vector as directed by the manufacturer. PCR product (2 μ L) was mixed with 1 μ L salt solution, 1 μ L TOPO TA 2.1 vector and ddH₂O in a total volume to 5 μ L. The reaction was mixed gently, incubated at room temperature (RT) for 5 min, and 2 μ L of the ligation product was used to transform 100 μ L CaCl₂-competent DH5 α *E. coli* cells. The transformation mixture was cooled on ice for 20 min, followed by heat shock treatment at 42 °C for 45 sec, then immediately placed on ice for 2 min LB medium (500 μ L) was added to the transformation mix which was allowed to recover for 1 h with aerobic agitation at 120 rpm. 50 μ L of the transformation mix was then plated on LB medium plates solidified with 1.5% agar (Difco) containing 50 μ g/mL ampicillin, and 40mg/mL X-gal and incubated at 37 °C overnight. Putative transformants were initially identified by blue/white LacZ screening followed by colony PCR analysis. Candidate colonies were inoculated by sterile toothpick transfer into the PCR amplification reaction consisting of 5 μ L 10X PCR amplification buffer, 2 μ L 50 mM $MgCl_2$, 2 μ L 10 mM dNTPs, 1 μ L each

of forward and reverse 10 mM SIPK primers, 1 μ L Taq DNA polymerase, and ddH₂O to make 50 μ L. The amplification program was performed on a Biometra T-gradient thermocycler as detailed above, and the products were examined by gel electrophoresis (0.8% agarose, 1X TAE buffer).

Plasmids were isolated from positive transformants using Wizard Prep Purification Kit (Promega). Transformant cells were incubated aerobically overnight in 5mL LB medium supplemented with 50 μ g/ μ L ampicillin, harvested by centrifugation at 10,000 g for 2 min, and re-suspended in 300 μ L 'Cell Resuspension Solution'. 'Cell Lysis Solution' (300 μ L) was added, and the solution inverted 4 times, followed by addition of 10 μ L 'Alkaline solution', and 10 min incubation at RT. 'Neutralization Solution' (300 μ L) was added, mixed by inversion, then centrifuged at 10,000 g for 10 min to pellet cell debris and chromosomal DNA. The supernatant was then transferred to a Wizard kit column in a 2 mL collection tube, and spun at 10,000 g for 1 min. The eluate was discarded, 750 μ L 'Wash Solution' was applied to the column, and the column was spun at 10,000 g for 2 min. The eluate was discarded, and a second wash with 250 μ L 'Wash Solution' was applied to the column as described above. The column was spun at 10,000 g for 2 min and the column was then transferred to a fresh microfuge tube. The plasmid DNA was eluted from the column by the addition of 50 μ L ddH₂O followed by centrifugation at 10,000 g for 2 min. The eluate containing the plasmid DNA was stored on ice, or at -20 °C until further use. Plasmid concentration and quality was determined by comparison to a DNA mass ladder on a 0.8% agarose gel.

Plasmid DNA from putative transformants was then analyzed by restriction digestion with *NotI* and *XbaI*. The digestion mix consisted of 5 μ L 10X React[®]3 buffer, 1.5 μ L

NotI restriction enzyme (Invitrogen), 1 μ L *XbaI* restriction enzyme (Invitrogen), 1 μ g plasmid DNA, and ddH₂O to make 50 μ L. The mix was incubated 4 h at 37 °C with occasional mixing, followed by centrifugation.

One of the *NotI* sites was located on the insert, and a second *NotI* site, followed by an *XbaI* site, was located on the host TOPO TA 2.1 vector. Proper orientation of the insert was expected to show a digestion profile of ~5.0 kb vector plus the insert fragment and a small (~100bp) fragment of the MCS. Improper orientation of the insert would give an ~3.9 kb vector product, and a ~1.2 kb insert fragment.

2.2.6: Cloning of GFP

The strategy for cloning of GFP into the TOPO TA 2.1 cloning vector strategy is shown in Figure 2.1. The DNA coding sequence for GFP was PCR-amplified from the plasmid pCAMBIA 1302, which contains the mGFP5 version of GFP. PCR amplification of GFP was performed using HiFi Platinum Taq (Invitrogen). A 50 μ L PCR reaction consisting of 5 μ L 10X buffer, 2.0 μ L MgSO₄, 2.5 μ L 10 mM dNTPs, 2 μ L of 10mM each of the forward *NotI* GFP and reverse *XbaI* GFP primers (Table 2.1), 1 μ L Platinum HiFi Taq, and ddH₂O to 50 μ L. The PCR amplification program on a Biometra T-gradient thermocycler consisted of 95 °C for 5 min, followed by 32 cycles of 95 °C for 30 sec., 55 °C for 30 sec., and 68 °C for 1 min, with final elongation cycle of 68 °C for 10 min. The GFP amplicon was digested with *XbaI* and *NotI*, and purified using a QIAquick[®] Spin Kit (QIAGEN). Buffer PB was combined with the digested PCR amplicon in a 5:1 ratio, mixed gently, and applied to a QIAquick spin column in a 2 mL collection tube. The column was centrifuged at 10,000 g for 1 min. The flow-through was discarded, and 0.75 mL buffer PE was added to the column. The column was

centrifuged at 10,000 g for 1 min. The flow-through was discarded and the column centrifuged an additional min at 10,000 g. The column was transferred to a new microfuge tube, 50 μ L ddH₂O was applied to the column, and the column was held for 3 min at RT before centrifugation for 1 min at 10,000 g. The eluate was stored on ice or at -20°C until further use.

2.2.7: Construction of the Fusion Protein

The TOPO TA 2.1 vectors containing GFP and SIPK were both digested with *NotI* and *XbaI* to produce a linearized SIPK-TOPO TA 2.1 vector and a GFP fragment. Both fragments were excised from a 0.8% agarose gel in 1X TAE buffer using a QIAquick gel purification Kit. Gel fragments were weighed in microfuge tubes, and 3 volumes buffer QG was added to each gel fragment. The mixtures were incubated at 50°C for 10 min (or until the gel dissolved), and 1 gel-volume 100% isopropanol was added to the sample. The solutions were gently mixed before transfer to QIAquick columns in 2 mL collection tubes and centrifuged at 10,000 g for 1 min. The flow-through was discarded and 750 μ L buffer PE was added to the column. The column was centrifuged at 10,000 g for 1 min. The flow through was discarded and the column centrifuged an additional min. at 10,000 g. The column was placed in a new microfuge tube, 50 μ L ddH₂O was applied to the column, and the column was incubated for 3 min at RT before centrifugation for 1 min at 10,000 g. The eluate was stored on ice or at -20 °C until further use.

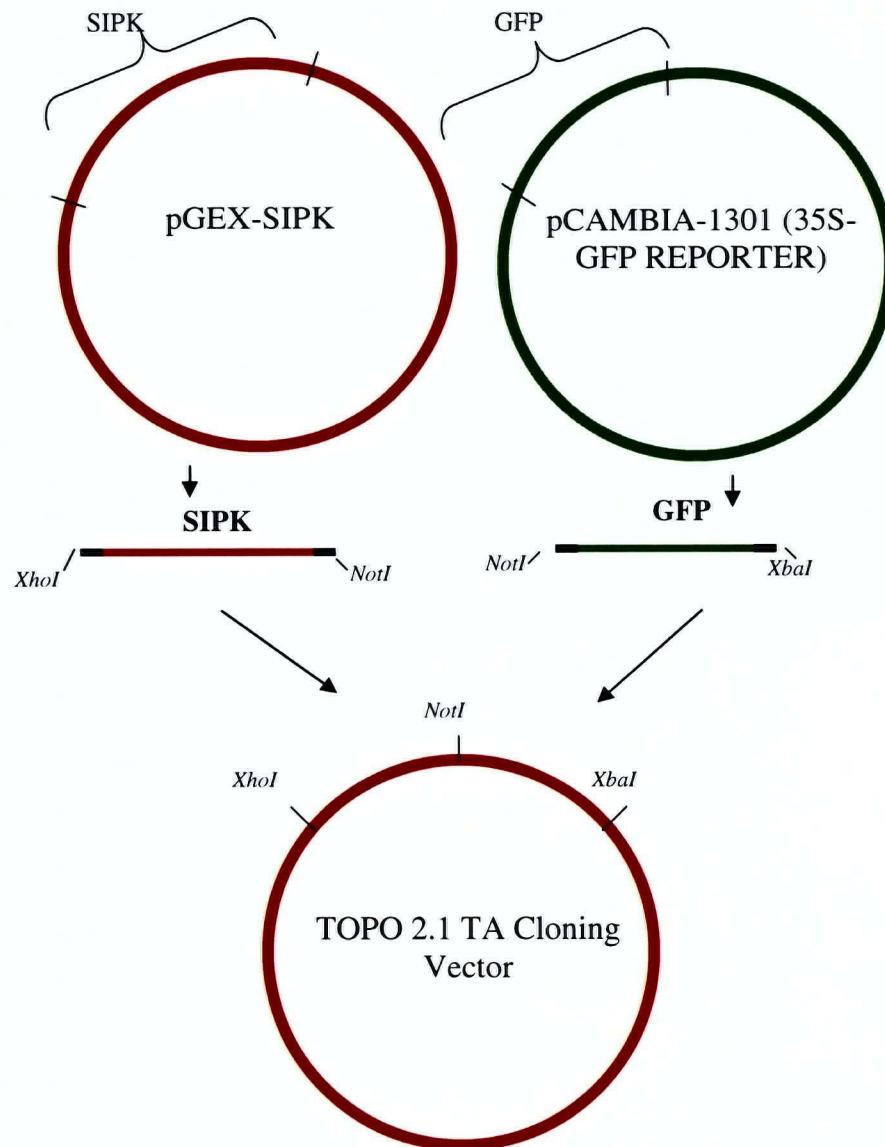


Figure 2.1: Schematic of Amplification of SIPK and mGFP5 into TOPO TA 2.1 Vector

Figure 2.1 depicts the amplification of SIPK and mGFP5 ORFs, and their insertion into the TOPO TA 2.1 vector.

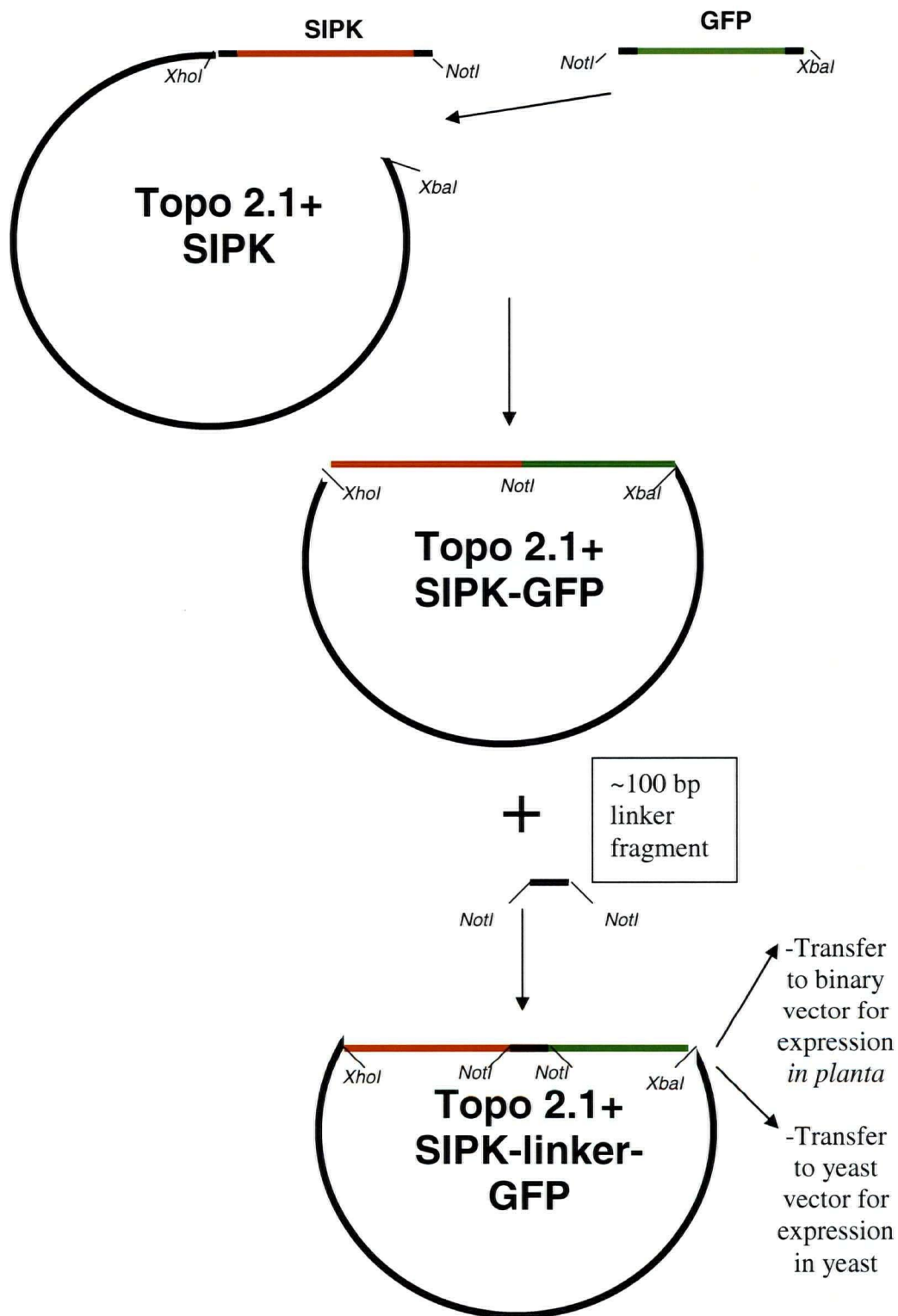


Figure 2.2: Strategy of SIPK-GFP Fusion Construction and Use

Figure 2.2 shows the fusion of SIPK and GFP, as well as the addition of a linker fragment in the fusion zone. The SIPK:GFP fusion with linker can then be transferred to a yeast or plant binary vector for expression.

The concentration and quality of the fragments were determined by comparison to a DNA mass ladder on a 0.8% agarose gel in preparation of ligation. A total of 1 µg total DNA (vector and insert) in a 3:1 insert to vector ratio was added to a 15 µL total volume reaction consisting of 3 µL 5X ligase buffer, 1 µL ligase, 0.5µL 5mM ATP, and ddH₂O to 15 L. The reaction was incubated overnight at 4 °C. The ligation product was transformed into CaCl₂-competent DH5α, plated on ampicillin supplemented LB agar as described in section 2.2.2. Putative transformants were analyzed by colony PCR using SIPKF and GFPR primers, and colonies showing the expected ~2kb fragment were sent for sequencing to ensure the fusion protein sequence was contained and that there were no mismatches or frameshifts.

2.2.8: Construction of the Fusion Protein Linker

After the SIPK:GFP fusion construct was completed and transferred into a binary vector, it was discovered that expression was not detectable by western analysis or by RT-PCR (data not shown), and it was postulated that the fusion protein was not folding properly. A linker fragment between the two proteins was constructed to widen the space between the two proteins to allow both to fold properly.

An~100bp linker fragment was constructed by amplification of a 3X HA tag from pKS/3S HA (Table 2.2) using the linker F and R primers with added *NotI* sites (Table 2.1) and PCR amplification conditions as previously described in section 2.2.5. Both the 3X HA tag fragment and the TOPO TA 2.1 SIPK:GFP fusion vector were digested with *NotI*. 1000U (1µL) CIP (New England Biolabs) was added to 30 µL linearized fusion protein vector and incubated at 37 °C for 1 h to dephosphorylate the vector ends. DMSO was added to the linker fragment (to make 10% DMSO final concentration) to allow for better

agarose gel separation of the small linker fragment from primer dimers and undigested fragments of amplified 3X HA tag linker sequence. The linker fragment was gel-purified on a 2% agarose gel in 1X T.A.E buffer. The digested fusion protein vector was gel-purified on a 0.8% agarose gel as described in section 2.2.5. Concentration and quality of the linker and vector were determined by comparison to a mass ladder on a 0.8% agarose gel in preparation for ligation.

The linker was ligated into the linearized, dephosphorylated fusion protein vector at a 3:1 insert to vector ratio. The ligation product was transformed into CaCl₂-competent DH5 α , and plated on LB plates supplemented with ampicillin as previously described in section 2.2.2. Putative transformants were analyzed by colony PCR using SIPK F and GFP R primers (Table 2.1) and run on a 0.8% agarose gel as previously described in section 2.2.5. The fusion protein containing the linker fragment amplicon was run next to control SIPK:GFP fusion amplicons which did not contain the added linker. Amplicons exhibiting a fragment 100 bp larger than those without the linker were sent for sequencing.

2.2.9: Yeast Vector Construction

The vector pYES 2.1 was used for the cloning and expression of the fusion construct in yeast. PCR amplification of the TOPO TA 2.1 cloning vector containing the SIPK-linker-GFP was performed using HiFi Platinum Taq (Invitrogen) using 10 mM *XhoI* SIPK forward and 10 mM *XbaI* GFP reverse primers (Table 2.1) as previously described in section 2.2.5.

The amplification product was ligated into the pYES 2.1 vector as directed by the manufacturer, and as previously described for cloning into TOPO 2.1 TA cloning vector

(section 2.2.5). Candidate transformant plasmids were isolated using Wizard Prep Purification Kit and analyzed by colony PCR as previously described in 2.2.5 with the GAL1F and GFPR primers (Table 2.1) to confirm orientation of the insert. The desired orientation would read 5' to 3' of the 3X HA tag.

2.2.10: Yeast Transformation

Yeast Extract/Peptone/Dextrose (YPD) medium (10 mL) was inoculated with a colony of INVSc1 yeast cells and grown overnight at 30 °C with shaking at 150 rpm. Overnight cultures were diluted to an OD₆₀₀ of 0.4, pelleted at 250 rpm for 10 min, and re-suspended in 40 mL 1X TE. Cells were pelleted at 2500 rpm for 10 min, and suspended once more in 2 mL 1X LiAc/0.5X TE and incubated at RT for 10 min. Yeast suspension (100 µL) was mixed with 1 µg plasmid DNA, 100 µg sheared herring sperm DNA, 700 µL 1X LiAc/ 40% PEG-3350/ 1X TE and incubated at 30 °C for 30 min. DMSO (88 µL) was added to the suspension, heat shocked at 42 °C for 7 min, then centrifuged for 10 sec. at 18,000 rpm. The supernatant was removed, and the pellet was re-suspended in 1 mL 1X TE and then re-pelleted as above. The washed pellet was re-suspended in 50 µL 1XTE and plated on selective media containing no uracil (selected for by uracil phototrophy).

The construct was isolated using a plasmid isolation kit (QIAGEN) as directed by the manufacturer with the exception of an added glass bead step in the lysis step. Approximately 300 µL glass beads were added to 1 mL re-suspended yeast cells. Cells were shaken on at max speed for 3 intervals of 10 min at 4 °C. Colony PCR was used to confirm the presence of the fusion protein construct in pYES 2.1 as previously described in section 2.2.5 with SIPKF and GFPR primers (Table 2.1).

2.2.11: Expression in Yeast

For construct expression, overnight cultures of positive transformants were grown in SC medium without uracil. The pYES TOPO 2.1 TA vector has a *URA3* gene, which produces uracil, acting as a selective marker in uracil-deficient media. Cultures were appropriately diluted to obtain 50 mL of O.D₆₀₀ = 4, and culture dilutions were centrifuged at 8,000 g for 10 min. The supernatant was discarded, and cells were re-suspended in 50 mL induction medium containing 2% galactose. Cells were harvested for time course expression samples at 0, 3, 8 and 16 h., and viewed on a Leica DMR fluorescence microscope equipped with an FITC filter set (excitation 465-495 nm). The fluorescence microscope was equipped with a QICAM along with the program Openlab 3.0[®] for the viewing and interpretation of captured images.

2.2.12: Binary Vector construction

The binary vector pCAMBIA 1300 vector did not have a 35S-driven promoter for the MCS. The 35S promoter and MCS from pRT101 were therefore transferred to pCAMBIA 1300 as shown in Figure 2.3

The vector pCAMBIA 1300-MCS contained the restriction sites *PstI*, *SphI*, and *HindIII*. pCAMBIA 1300-MCS, and pRT101 (Table 2.2) were digested separately with *HindIII* as previously described in section 2.2.3. Both digestion mixtures were run separately on a 0.8% agarose gel, and the *HindIII* liberated 35S-MCS fragment from the pRT101 vector and the linearized pCAMBIA 1300-MCS were gel-purified as previously described in section 2.2.5. The concentrations of the fragments were determined by comparison to a mass ladder on a 0.8% gel in preparation for ligation. The fragments were ligated in a 3:1 insert to vector ratio, and used to transform CaCl₂-competent DH5 α .

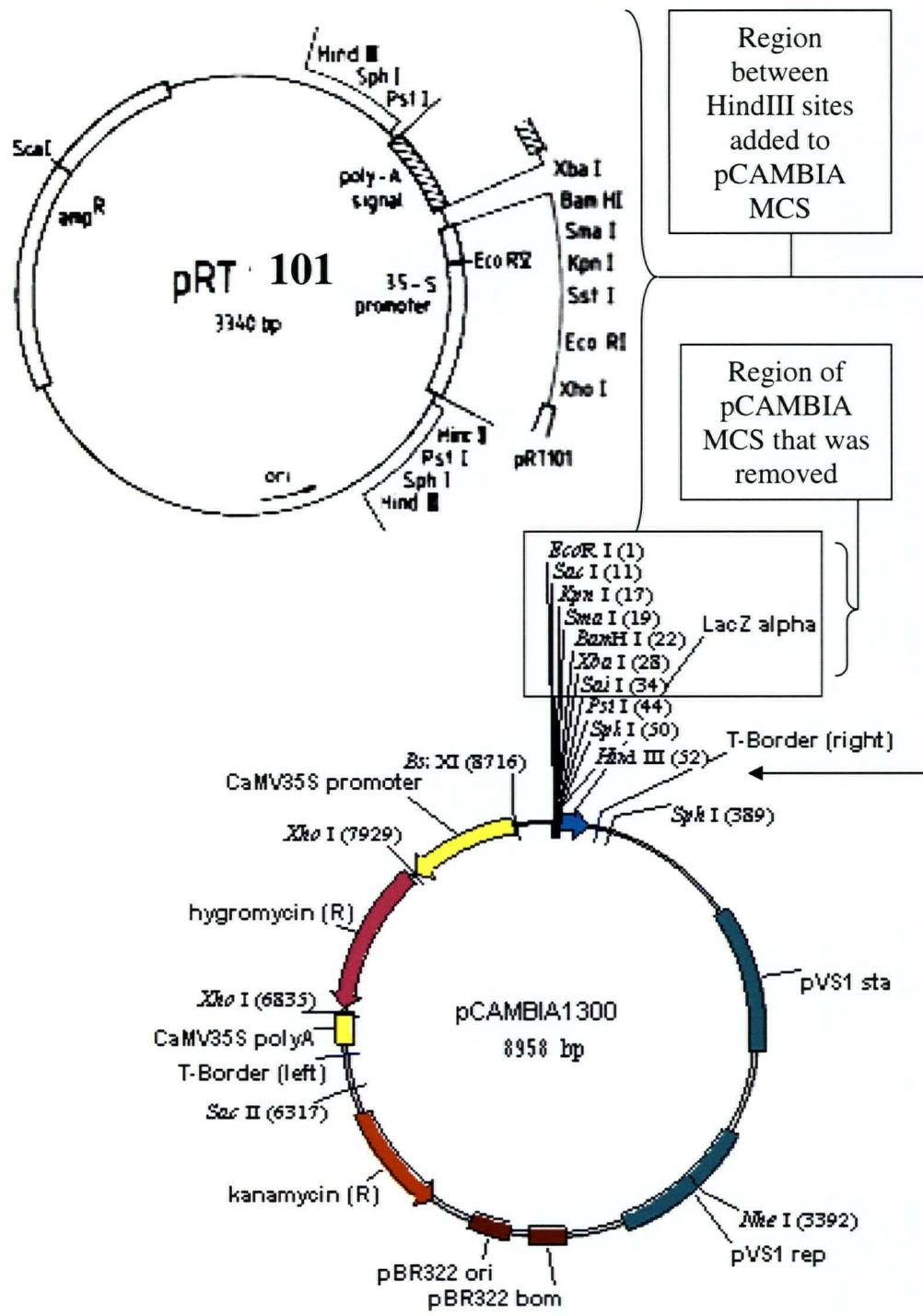


Figure 2.3: Transfer of 35S Driven MCS from pRT 101 to pCAMBIA 1300

Figure 2.3 depicts the MCS portion between *HindIII* sites in the vector pRT101 that will be digested and inserted into a pCAMBIA 1300 vector which has had a large portion of its MCS removed. The new construct is entitled pCAMBIA + MCS

as previously described in section 2.2.5. Putative transformants were analyzed by restriction endonuclease digestion using *HindIII*, *XhoI*, *XbaI*, *BamHI*, *Sall*, and *PstI* to identify the orientation of the 35-S driven MCS, and any residual restriction sites that may have been present in pCAMBIA –MCS. The new construct was named pCAMBIA 1300 + MCS.

2.2.13: Cloning SIPK:GFP with Linker into pCAMBIA 1300 + MCS

The SIPK:GFP fusion with 100 bp linker and pCAMBIA 1300 + MCS were digested separately with *XbaI* and *XhoI* as previously described in section 2.2.3. The linearized pCAMBIA 1300 + MCS vector and 2 kb SIPK:GFP with linker fragment were gel-purified and their concentrations determined in comparison to a mass ladder on a 0.8% gel in preparation for ligation as previously described in section 2.2.5. The two fragments were ligated in a 3:1 insert to vector ratio, transformed into DH5 α cells, and plated on LB media containing 50 μ g/mL kanamycin. Putative transformants were analyzed by colony PCR as previously described in section 2.2.5 using 35S forward, and GFP reverse primers (Table 2.1).

2.2.14: Plant Transformation using Agroinfiltration

SIPK:GFP with 100 bp linker in pCAMBIA 1300+MCS, along with the controls of a 35S driven GFP in pCAMBIA (pCAMBIA 1302), and an empty vector (pCAMBIA 1300 + MCS) were transformed into either *Agrobacterium tumefaciens* strain GV 3101, or strain EHA 101. Vector DNA (1 μ g) was placed on 200 μ L CaCl₂ competent *Agrobacterium*. The tubes were immediately placed in liquid nitrogen, followed by incubation at 37 °C for 5 min. LB (1 mL) was added to the transformation mixture, and the tubes were incubated at 28 °C with shaking at 180 rpm for 3 to 4 h. Cells were

pelleted at 12,000 g for 2 min, and re-suspended in 200 μ L LB. Samples were plated on selective LB plates as previously described in section 2.2.2 for DH5 α .

Four-week-old Xanthi tobacco plants grown in a sterile environment on $\frac{1}{2}$ strength MS medium were routinely used as infiltration hosts. Leaf discs cut from leaves of infiltration hosts with sterile scalpels were dipped for 1 min into *Agrobacterium* cultures grown to an OD₆₀₀ of 0.8. Leaf discs were then rinsed with fresh MS medium, placed on parafilm-sealed plates of shoot induction medium (see Appendix 1) with no antibiotics, and incubated at RT in the dark for 2 days. Leaf discs were then transferred to shoot induction medium supplemented with antibiotics (Appendix 1) and grown at 25/20 $^{\circ}$ C, 16-h-light/8-h-dark cycle. New shoots were transferred to fresh medium and grown under the same conditions. When shoots were 2-3 leaves in size, they were transferred to root induction medium (Appendix 1).

2.2.15: Infiltration of *Agrobacterium* for Transient Expression *in planta*

Agrobacterium strains containing the constructs SIPK:GFP with linker in pCAMBIA 1300+MCS, pCAMBIA 1302, and the empty vector control pCAMBIA 1300 + MCS were grown to an OD₆₀₀ = 0.8. The cultures were transferred to $\frac{1}{2}$ MS medium, and infiltrated into host tobacco leaves. Tissue for protein and RT-PCR analysis was harvested and frozen in liquid nitrogen after 2 days, and plants were monitored for lesion formation for 3-5 days.

Table 2.1: Primer Sequences

<u>Primer Name</u>	<u>Primer Sequence</u>
<i>XhoI</i> SIPKF (forward)	5'- CAC TCG AGA TGG ATG GTT CTG GTC AGC AGA CGG ACA-3'
<i>NotI</i> SIPKR (reverse)	5'- CAG CGG CCG CCC ATA TGC TGG TAT TCA GGA TTA AAT-3'
<i>NotI</i> GFPF (forward)	5'- CAG CGG CCG CAT GGT AGA TCT GAC TAG TAA AGG AGA-3'
<i>XbaI</i> GFPR (reverse)	5'- CAT CTA GAT CAC ACG TGG TGG TGG TGG TGG TGG CTA-3'
<i>NotI</i> LinkerF (forward)	5'- GGC GGC GGC CGC GGA TCC ACT AGT TAC CCA TAC GAT GTT CCT GAC TAT G-3'
<i>NotI</i> LinkerR (reverse)	5'- AAG CGG CCA GCG TAA TCT GGA ACG TC-3'
35S Forward (forward)	5'- ATG ACG CAC AAT CCC ACT-3'
GAL 1 (forward)	(Invitrogen, provided with pYES 2.1 kit)

Table 2.2: Vectors

<u>Plasmid Name</u>	<u>Source</u>
pGEX-SIPK	Marcus Samuel
TOPO TA 2.1 Cloning Vector	Invitrogen
TOPO 2.1 + SIPK:GFP	New intermediate construct
pKS/3X HA	Oncogene 17:1097
TOPO 2.1 + SIPK-linker-GFP	New intermediate construct
pCAMBIA 1300-MCS	Greg Lampard: pCAMBIA 1300 with deleted MCS
pCAMBIA 1302 (35S GFP)	CAMBIA vectors
pRT 101	Nucleic Acids Res. 15 (14), 5890 (1987)
pCAMBIA + MCS	New construct from pCAMBIA-MCS and pRT101 MCS between <i>HindIII</i> sites
SIPK:GFP Fusion Vector with Linker	New construct in pCAMBIA + MCS
pYES 2.1 TA Cloning Vector	Invitrogen
pYES 2.1 + SIPK-linker-GFP	New construct from insertion of fusion protein into pYES 2.1
pYES 2.1 + GFP	Greg Lampard: GFP from pCAMBIA 1302 inserted into pYES 2.1

2.3: RESULTS

2.3.1: Cloning of SIPK

SIPK was successfully cloned as confirmed both by digestion of the TOPO TA 2.1 vector with *XbaI* and *NotI* producing ~ 1.2kb fragment, and also by sequencing showing no mismatched base pairs to the genbank database sequence of SIPK (gi:27374989).

2.3.2: Cloning of GFP

GFP was successfully cloned as confirmed by digestion of the TOPO TA 2.1 vector with *NotI* and *XhoI* producing ~750 bp fragment, and also by sequencing, which showed no mismatched base pairs to the genbank sequence (gi:7638073). Figure 2.4 shows the purified SIPK-TOPO vector digested with *XbaI* and *NotI* in anticipation of the mGFP5 fragment, and the mGFP5 fragment, also digested with *NotI* and *XbaI*. The clean bands show the expected sizes for the fragments, and no indication of degradation.

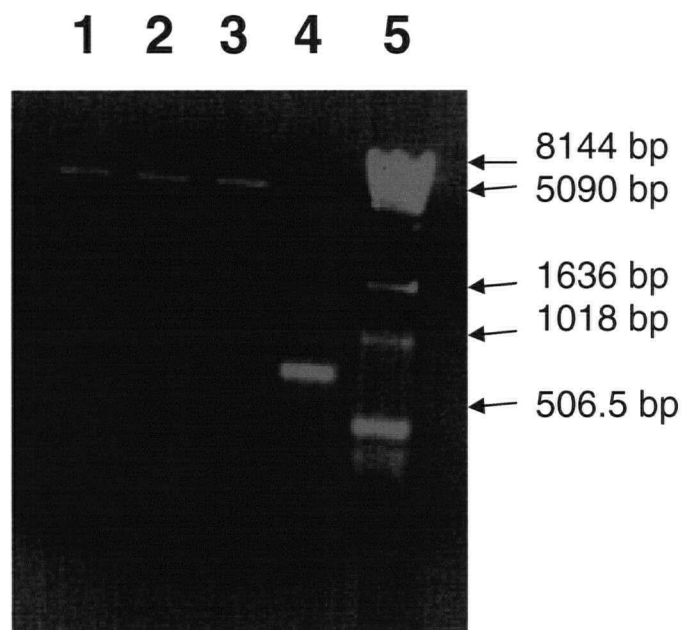


Figure 2.4: TOPO TA 2.1 vector containing SIPK, and mGFP5 Fragments for ligation

Figure 2.4 shows the results of the SIPK containing TOPO TA 2.1 vector digested with *NotI* and *XbaI* endonucleases (lanes 1-3). The approximately 5000 bp single band shown indicates a linearized SIPK-TOPO vector. Lane 4 shows a ~ 750 bp mGFP5 fragment digested from an mGFP5 containing TOPO vector digested with the endonucleases *NotI* and *XbaI*. Lane 5 shows the 1kbp vector from Invitrogen. Fragments were run on a 0.8% agarose gel in 1 X T.A.E buffer at 80V for 45 min.

2.3.3: Construction of Fusion Protein

The fusion protein construct was shown to be correct by digestion with appropriate restriction enzymes producing the proper ~2 kb fragment (figure 2.5), and by sequencing over the fusion site.

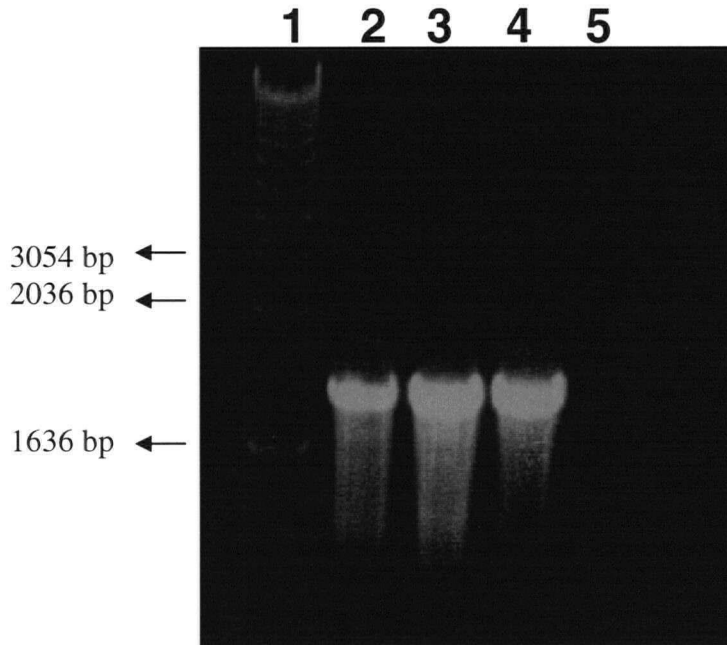


Figure 2.5: Colony PCR of the Fusion of SIPK:GFP into the TOPO TA 2.1 Cloning Vector

Figure 2.5 shows positive insertion of mGFP5 into the TOPO-SIPK vector as determined by colony PCR. Lane 1 shows the Invitrogen 1kb ladder, and lanes 2-5 show separate colony PCR amplicons approximately 2000 bp in length indicative of SIPK fused to mGFP5. Fragments were run on a 0.8% agarose gel in 1 X T.A.E buffer at 80V for 45 min.

2.3.4: Fusion Protein Linker

Insertion of the linker was successful as shown by colony PCR over the entire fusion protein in comparison to the fusion protein without the linker insertion (figure 2.6). There was a noticeable 100 bp difference between colonies containing the linker, and colonies without the linker. The insertion of the linker was further analyzed by sequence analysis. It was noticed by sequencing of 6 separate ligation events that all linkers were inserted in the opposite orientation to that originally desired. Due to time constraints and an inability to explain these events, the construct with the opposite orientation of the linker sequence was chosen for further work. The protein translation of the sequence is as follows: AAASVLYNAIYIGSSIVRDVIGIARIVRNIVWVTSGSAAA

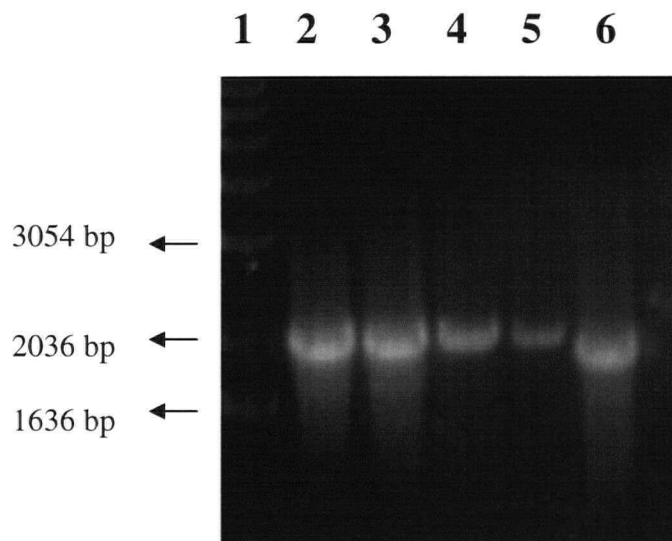


Figure 2.6: PCR Confirmation of Insertion of Linker between SIPK and GFP in the TOPO 2.1 cloning vector

Figure 2.6 shows the results of the insertion of the linker fragment between the SIPK and the mGFP5 fragments. Amplicons showing positive insertion of the ~ 100 bp fragment between the SIPK:GFP fusion would run at approximately 2100 bp (Lanes 2-5) when compared the control SIPK-mGFP5 fusion without the linker at ~2000 bp (lane 6) amplified with SIPK F and GFP R primers and run on a 0.8% agarose gel in 1X T.A.E buffer at 80V for 45 min. Lane 1 shows the 1 kbp ladder (Invitrogen).

2.3.5: Yeast Vector Construction

Insertion of the SIPK:GFP with linker fusion sequence into the pYES vector was confirmed by growth on SC-uracil medium, and by colony PCR using the GAL1 forward and GFP reverse primers to confirm orientation of the insert (Figure 2.7). Three positive insertion colonies were chosen to transform from DH5 α into the yeast strain INVSc1.

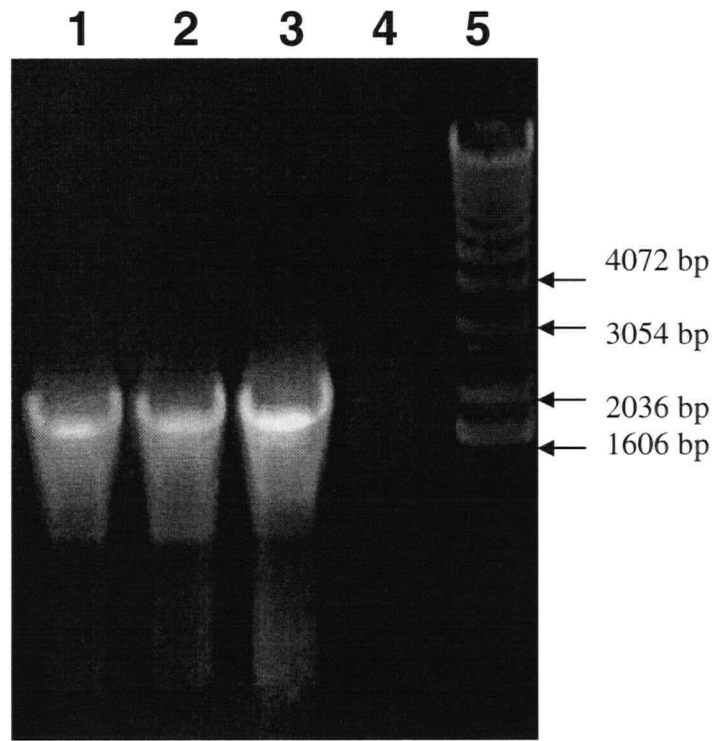


Figure 2.7: Insertion of SIPK:GFP Fusion Sequence into the pYES TOPO TA 2.1 Yeast Expression Vector

Figure 2.7 shows the results of the insertion of the SIPK-mGFP5 fusion into pYES TOPO vector. Lanes 1-4 show separate putative transformants of the fusion protein as determined by colony PCR using pGAL forward and GFP reverse primers used to amplify the ~2kbp fragment. Improper orientation of the insert would yield no amplicon with the same reaction conditions (as in lane 4). Fragments were run on a 0.8% agarose gel in 1 X T.A.E buffer at 80V for 45 min.

2.3.6: Expression in Yeast

Expression of the construct was confirmed by fluorescence microscopy (Figure 2.8).

Of the intervals tested, overnight expression produced the highest expression of the

fusion protein, whereas the control vector containing GFP was shown to express strongly after 3 h of induction. The fusion protein does not appear to be expressed in every cell within the culture, whereas the GFP construct appears to express strongly seemingly in all of cells observed.

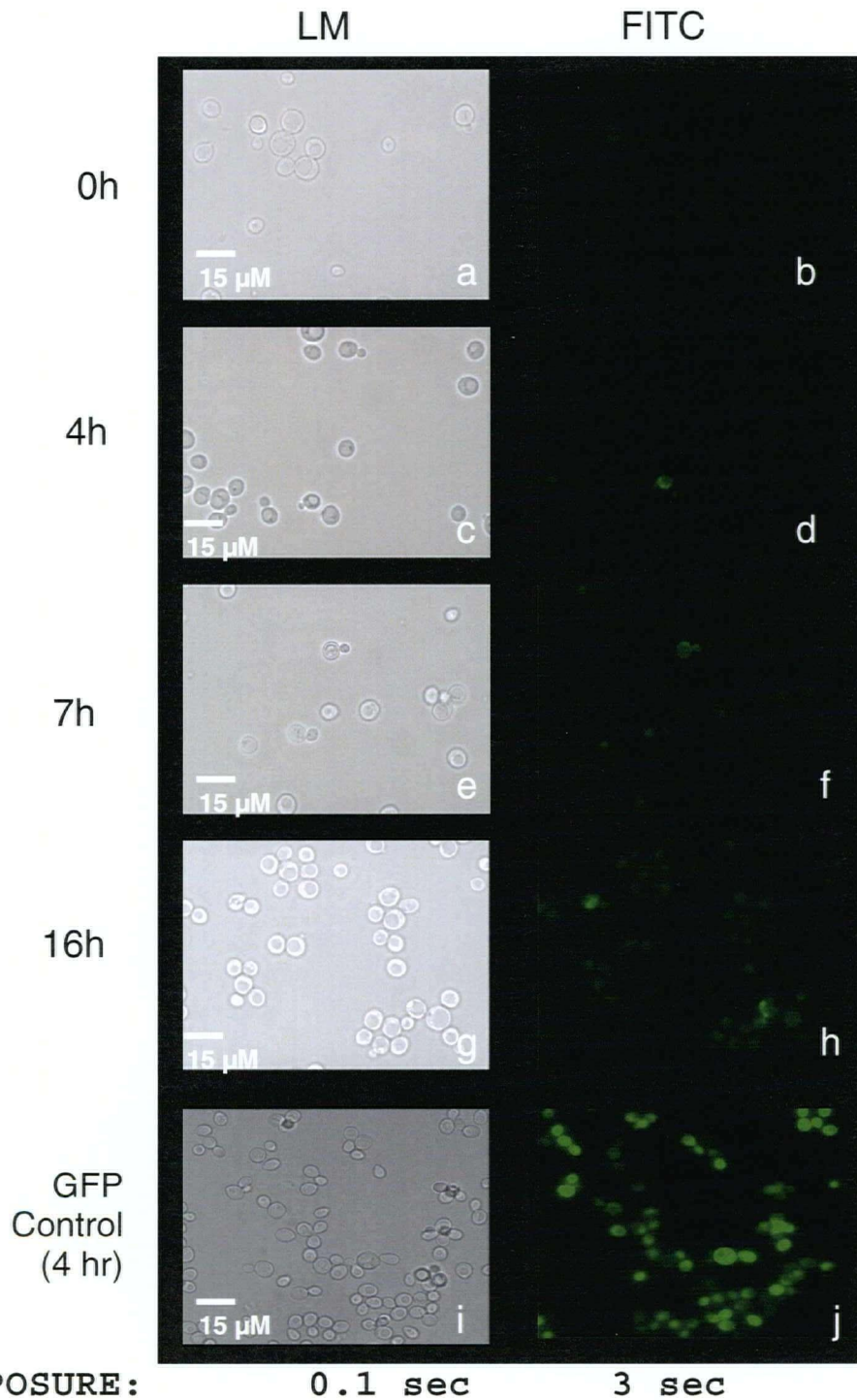


Figure 2.8: Expression of SIPK-GFP Protein with Inserted Linker in Yeast Induced with Galactose

Figure 2.8 shows the expression of the SIPK:GFP construct in yeast under the GAL1 promoter over a period of 16 hours. The GFP control was expressed under the same conditions.

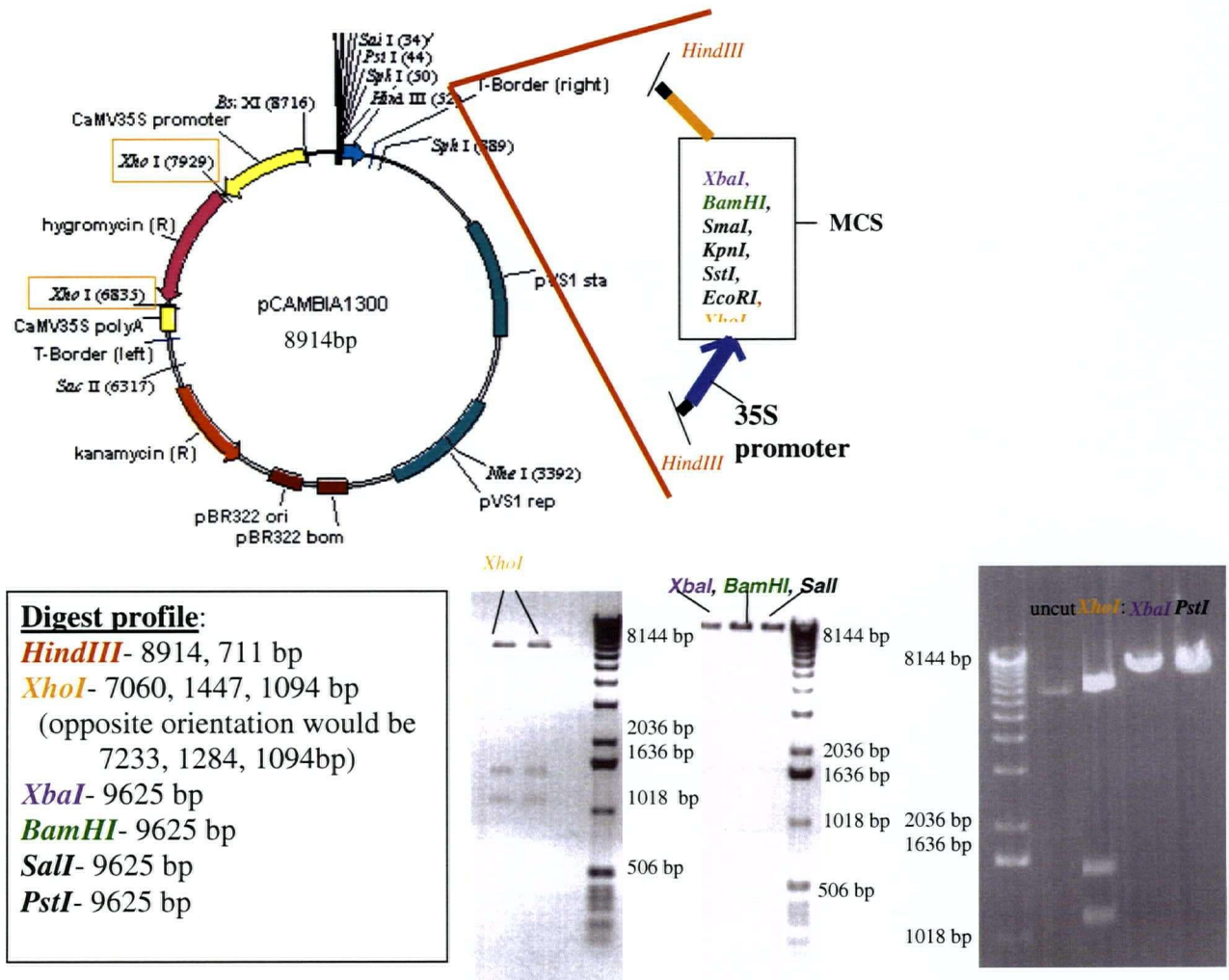


Figure 2.9: Digest Profile for the Insertion of the 35S Driven MCS from pRT 101 to pCAMBIA 1300

Figure 2.9 shows digestion profiles of the of the new pCAMBIA 1300 + MCS vector with various restriction enzymes, and the resultant fragments of those digests as seen on a 0.8% agarose gel in 1X TAE buffer at 80V for 45 min. Digestion with the endonucleases *XhoI*, *XbaI*, *PstI*, *BamHI*, *Sall* and *XhoI* all give the appropriate sized fragments.

2.3.7: Binary Vector Construction

The insertion of the 35S driven MCS from pRT101 between *HindIII* sites into pCAMBIA 1300's *HindIII* site was successful as seen by the fragments produced with digestion using the restriction enzymes *HindIII*, *XhoI*, *XbaI*, *BamHI*, *Sall*, and *PstI*. All

digestions gave the expected sized fragments (figure 2.9), indicating that the fragment was inserted in the desired orientation, that only one copy of the fragment was inserted into the vector, and that the tested restriction sites housed within the MCS digested predictably to give the desired fragment sizes.

2.3.8: Cloning Construct into Binary Vector:

The insertion of the approximately 2 kb sized SIPK-linker-mGFP5 fusion was successful as confirmed by amplification of the fusion construct by colony PCR using SIPK forward and GFP reverse primers, and by sequencing of the construct.

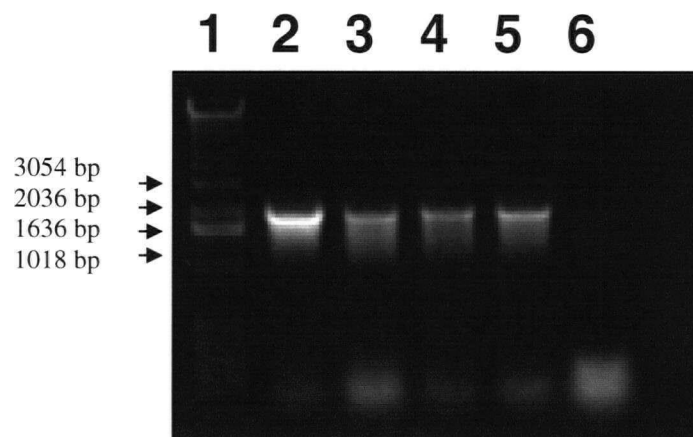


Figure 2.10: Insertion of SIPK:GFP with linker into the Binary vector pCAMBIA+MCS

Figure 2.10 shows the expected amplicon from colony PCR of putative SIPK:GFP with linker containing transformants. Lane 1 shows the Invitrogen 1kb ladder. Lanes 2-6 show colonies A-E, with A-D being positive transformants showing an approximate 2kbp fragment amplified with SIPKF and GFPR primers. Fragments were run on a 0.8% agarose gel in 1 X T.A.E buffer at 80V for 45 min.

2.3.9: Plant Transformation using Agro-infiltration

The construct was successfully inserted into *Agrobacterium* as shown by figure 2.11.

Infiltration of the *Agrobacterium* into the plant tissue was observed visually (Figure 2.12).

Lesions were seen from infiltration of the over-expressing SIPK control construct OX-SIPK. No lesion formation was seen, as expected, from the 35S driven GFP pCAMBIA vector (1302) or the empty vector construct pCAMBIA 1300+MCS in GV3101. The fusion construct, SIPK:GFP with inserted linker, did not show significant lesion formation GV3101 (Figure 2.12A). When the fusion construct was transferred to the Agrobacterium strain EHA 101, and transfected into tobacco leaves, significant lesion formation was apparent (Figure 2.12B), signifying that SIPK is active and functional despite the addition.

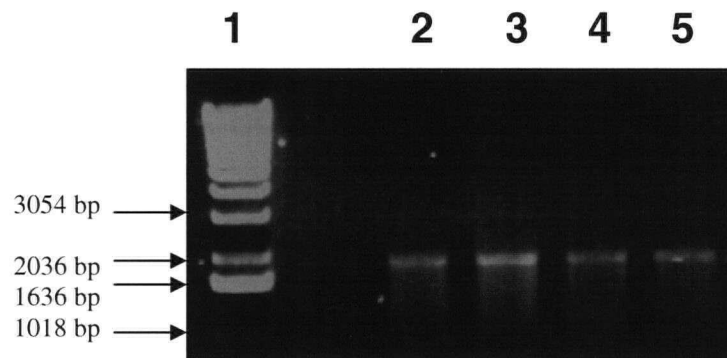


Figure 2.11: Agrobacterium Colony PCR of Putative SIPK:GFP Fusion Protein Construct Insertion

Figure 2.11 shows colony PCR results of putative Agrobacterium colonies. PCR products were amplified with SIPKF and GFP R primers. Lane 1 shows the Invitrogen 1kb ladder. Lanes 2-5 show putative vector containing colonies showing a ~2 kbp amplicon. Fragments were run on a 0.8% agarose gel in 1 X T.A.E buffer at 80V for 45 min.

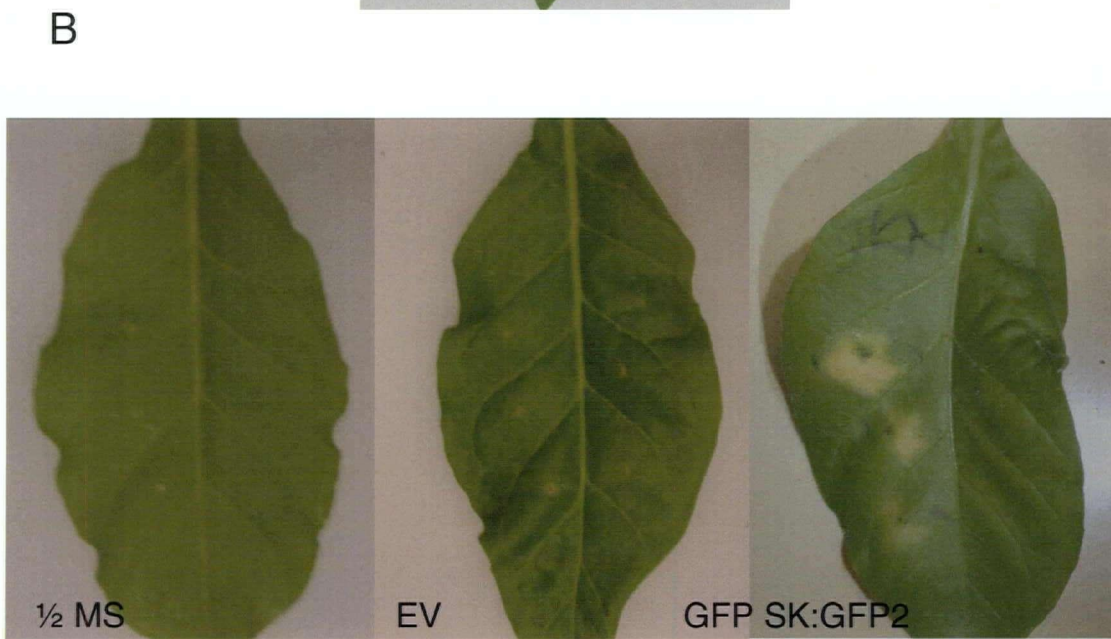
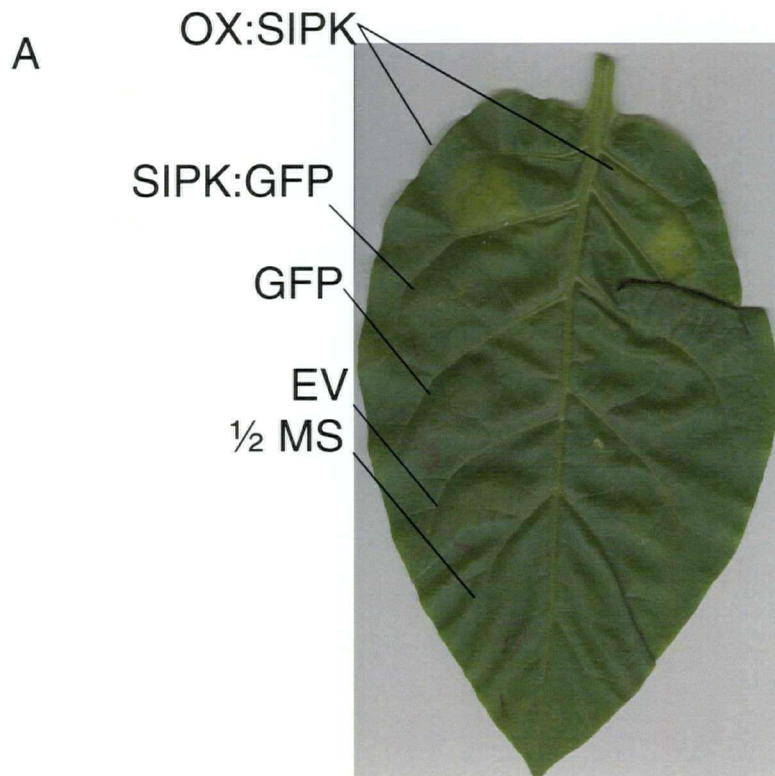


Figure 2.12A,B: Transient Expression by Agro-Infiltration of the SIPK:GFP with Linker fusion protein in Tobacco Leaves

Figure 2.12 shows the results of agroinfiltration of GV3101 (A) and EHA101(B) Agrobacterium cultures containing the SIPK:GFP construct, as well as control cultures containing the empty vector pCAMBIA 1300 +MCS, and a 35S driven GFP in pCAMBIA 1300 + MCS. Lesion formation is indicative of a hypersensitive response.

2.4: DISCUSSION:

Although MAPK-GFP fusions have been reported in yeast and animal systems, there have not yet been any reported in plants. Perhaps MAPK:GFP fusions are difficult to express successfully due to post-translational problems. Improper folding in multiple portions of the protein could compromise cellular recognition of the protein, causing it to be targeted for degradation. Aside from many areas of the protein being important for proper folding, multiple portions of the protein are important for activation/inactivation of the protein of interest. These regions have a function in the protein's ability to activate other proteins. Compromising essential binding or recognition regions of proteins can alter cellular expression levels, activation/deactivation processes, and subcellular localization of the proteins. Both the C- and N- termini are known to often contain important functional regions including signal peptides. The C- and N- termini are also the regions most often used to fuse to reporter proteins. Many fusion constructs are not functional due to compromised C- or N- termini functions. Some N-terminal fusion complications can include obscuring of the endoplasmic reticulum, mitochondrial or chloroplast targeting sequences located therein, thus generating localization artifacts (Tian et al., 2004). In the same regard, some C-terminal fusions have been shown to give misleading results for a variety of proteins, including Cesa1 or Pin1 when compared to other fusions of the same protein (Tian et al., 2004).

A second reason for the lack of reported MAPK:GFP fusions *in planta* might be the low expression levels of endogenous MAPKs, resulting in too few expressed GFP molecules to visualize effectively. Plant systems have a specific hindrance to the visualization of GFP from the natural autofluorescence given off mainly by chloroplasts,

as well as from other light refracting complexes. Special filter sets that block out, or cancel out, unwanted background information are used for fluorescence microscopy to research GFP localization in plants. If expression of GFP is low, it would be difficult to detect the GFP signal from background noise without special filters and a sufficiently sensitive detection system.

Tagged proteins are most often expressed under a strong constitutive rather than the native promoter, which can cause the protein to be expressed under conditions in which it would not normally be expressed, or in cells which it would not normally be expressed (Tian et al., 2004). In this experiment, the plant 35S promoter was used instead of using the native SIPK promoter. The choice of promoter was based primarily on time constraints to find, test, and use the native promoter, and the availability of the 35S promoter for experimental use.

Although this project was not completed to the stage of visualization of the fusion construct *in planta*, there has been valuable information gained about the fusion construct. Primarily, it has been determined that the two portions of the fusion protein, SIPK and GFP, retain activity when fused together in a C-terminal fusion with a linker inserted between them. By sequencing the construct it was determined that the fusion kept GFP in frame for proper translation. It was also determined that there were no mismatched base pairs within the fusion construct sequence. From expression of the construct in yeast, it was determined that the GFP portion of the fusion protein was expressing, as seen by visualization of the fluorochrome under a fluorescence microscope. From agro-infiltration of tobacco leaves it was determined that SIPK is expressed, and that it has retained its ability to cause lesion formation in agro-infiltrated tobacco leaves.

The fusion protein's expression in yeast was found to be optimal after overnight induction with galactose. Due to the low expression of the fusion protein within the culture, even after an overnight incubation, it is possible to hypothesize that in yeast, high expression of the SIPK might only be permitted to be expressed within certain time frames, such as during cell division, or perhaps under induction with a certain stress. ERK 1 has already been determined to be active in regulation of growth and differentiation (Porter and Vaillancourt, 1998).

The localization pattern of the fusion protein SIPK:GFP seen in yeast cells expressing higher levels showed bright spots within the cell, with large bright central spots. The actual subcellular localization of the fusion construct was unclear in yeast cells, due to their small size, and the continual motion present in live yeast cells. Further study could have been done on the expression and subcellular localization of the fusion construct in yeast, but the subcellular localization focus was on SIPK/WIPK's expression in tobacco cells, not yeast. Expression of the construct in yeast was a quick and easy tool to confirm GFP expression when fused to SIPK.

Both the control GFP and the fusion construct showed expression of GFP in yeast. Despite being driven by the same GAL 1 promoter, the expression of GFP was observed to be much higher and stronger than the expression of the GFP:SIPK fusion protein. High expression of GFP is a good indicator that the expressed protein is not targeted for degradation, and also indicates that most likely the expression of the foreign construct does not have any easily observable effects on cellular processes.

The GFP portion of the fusion protein, despite low expression compared to the control GFP construct, was expressed in yeast cells under the GAL 1 promoter. The activity of

SIPK when fused to GFP was tested using agro infiltration. Transient expression of active SIPK from agro-infiltration is known to cause lesions in young leaves (Zhang and Klessig, 2001). Lesion formation from agro-infiltrated SIPK might be attributed to SIPK becoming activated once infiltrated from the wounding stress caused by agro-infiltration. High levels of activated SIPK might trigger cell death, and lesion formation. From my agro-infiltration results, lesion formation was observed in both the control OX:SIPK-infiltrated construct, and the fusion construct. The 35S-driven GFP and empty vector controls did not induce lesion formation (Figure 2.12b).

Of the *Agrobacterium* strains available in the lab, quite a bit of difficulty was had working with the GV3101. Although good results have been obtained with this strain in *arabidopsis*, it did not work well in these experiments using Xanthi tobacco. The expression from the binary vector pCAMBIA 1300 + MCS in GV3101 was either too low to be detected, or transfer of the T-DNA was not successful. Both of these hypotheses would be supported from the lack of lesion formation in transient expression of the fusion protein, and from the lack of a strong signal in both RT-PCR and western analysis (data not shown).

With the information that both the *SIPK* and GFP portions of the construct are functional, some preliminary conclusions can be drawn about the fusion construct as a whole. The linker insertion appears to have kept enough distance between the two proteins to allow for proper folding of both SIPK and GFP. Activity of SIPK from agro-infiltration results indicates essential activation regions of SIPK have not been compromised by its fusion to GFP.

To observe this fusion construct *in planta*, both transient and transgenic expression of the construct could be observed. Transient expression of the construct was examined by both cross-sectioning of agro-infiltrated tissue, and by particle bombardment of leaf tissue (data not shown). No obvious expression of the construct was observed *in planta*, due to high background autofluorescence within the tissue, although with appropriate filters different results may have been found. If expression of the fusion construct *in planta* is similar to its expression in yeast, low expression levels would be expected. Tissue autofluorescence coupled with low expression levels demonstrated transient expression analysis to be an insufficient method for observing subcellular localization of the SIPK:GFP fusion protein in tobacco.

Transgenic analysis of the SIPK:GFP construct was attempted, but was not completed within the time parameters of this experiment. It would be expected that either transgenic callus/cell culture or the roots of tobacco seedlings would allow clear visualization of the construct without interference from strong background autofluorescence. By use of epi-fluorescence microscopy and confocal/fluorescence microscopy, the subcellular locations of the fusion protein could be tracked. Information about the subcellular location of 35S driven SIPK under various conditions could be observed. Changes in subcellular localization could be observed live, allowing translocation times to be determined, as well as the duration of location upon activation. Stable transgenics bearing the SIPK:GFP fusion could also be used to study upstream and downstream SIPK interactors through crosses with transgenics of suspected interactors, for example crossing with a WIPK RNAi or WIPK:YFP stable lines. Phosphatase:YFP stable lines could be used to investigate Bogre's hypothesis that *denovo* synthesis of phosphatases

are involved in MAPK inactivation in plants following MAPK induction by wounding or treatment with elicitors (Bogre et al., 1997); (Suzuki and Shinshi, 1995), though

YFP/GFP

interactions are not as efficient of a pair as CFP and YFP using FRET analysis. Knock out and overexpression lines of upstream double kinases could be used to examine Lee's hypothesis that MAPKK activity is required for sustained MAPK activity (Lee et al., 2004).

In conclusion, the SIPK:GFP fusion construct has been shown to give observable expression in yeast and tobacco leaves, indicating that the fusion construct design and assembly were successful. There are many possible experiments in which SIPK:GFP stably transformed tobacco lines could be employed. This construct thus has the potential to be a valuable tool for future studies.

CHAPTER 3: Immunolabeling of Tobacco MAPKs

3.1: General Introduction to Immunolabeling

3.1.1: Immunolabeling

Immunolabeling is the use of labeled antibody to show the localization of specific macromolecules in fixed tissue sections and cells. Both tissue section and whole cell immunolabeling provides higher spatial resolution than *in vivo* reporter proteins such as GFP. This technique is therefore frequently used in both plant and animal systems. Commonly used antibody labels include covalently-coupled fluorescent molecules, gold particles, and enzymatic reporters such as peroxidase. Macromolecules decorated by immunolabeling can be visualized using electron microscopy (EM), light microscopy (LM) or fluorescence microscopy, depending on the choice of label.

3.1.2: Fluorochromes and Fluorescence

The basic principle of fluorescence is that a compound will absorb light energy at one wavelength and emit part of the absorbed energy as light of a longer wavelength. Fluorescent compounds (fluorochromes) can be detected in very low concentrations. Common fluorochromes that can be covalently bound to antibodies are fluorescein, rhodamine, Texas Red, the Alexa series of fluors, Cy3, and Cy5. Excitation and emission wavelengths, along with fluorochrome stability, are the major factors that determine which fluorochrome is appropriate for a given experiment.

3.1.3: Fixation

The aim of fixation is to put into stasis the subcellular activities and dynamic internal movements of the cell while retaining a physical state that resembles, as closely as possible, the living state of the cell. Some frequently used reagents for this purpose are

formaldehyde, osmium tetroxide and glutaraldehyde (O'Brian, 1981 pp 4.17). Different fixatives have specific strengths and weaknesses in terms of preserving certain cellular structures, and the choice of a fixative is dependent on the goal of the study.

Aldehyde fixatives act by reacting with amino side-chains on proteins. The proteins are thereby immobilized, and are resistant to further deterioration. Di-aldehydes, such as glutaraldehyde, create a very strong cross-linked protein matrix since they have two aldehyde groups available for cross-linking. Strong matrices are critical for detailed ultrastructure analysis of the sample. Mono-aldehydes, such as paraformaldehyde, create a weaker matrix, which can be useful in immunolabeling since a too strongly cross-linked matrix can hinder antibody recognition of the protein (O'Brien, 1981).

Since chemical fixation always modifies cellular structures to a greater or lesser degree, alternative approaches have been actively sought. High Pressure Freezing (HPF) is a method that results in excellent preservation of structure. HPF involves instantaneous freezing of the sample at high pressure to prevent ice crystal formation. Frozen cell water is then slowly substituted with a solvent such as acetone at freezing temperatures (O'Brien, 1981 pp 4.29). While high pressure freezing is a very effective method for preserving cellular and subcellular structures, the requirement for extremely rapid freezing means that only small quantities can be processed at a time. The sample size is therefore small, which can make it difficult to locate a cell displaying the desired traits.

3.1.4: Digestion/Removal of Cell Wall

Plant cell walls can cause immunolabeling problems by reducing permeability of the cell to reagents, as well as by emitting autofluorescence in fluorescence microscopy. Cell

wall autofluorescence predominantly stems from lignin, an aromatic polymer that forms the most prominent non-saccharide component of the cell wall. Because of the problems associated with cell walls, it can sometimes be desirable to digest or remove the cell wall. Digestion or removal of the cell wall can be obtained by gentle digestion with a mixture of hydrolytic enzymes such as cellulase and pectolyase (O'Brien, 1981 pp3.12). Cell wall digestion can be performed on either live or fixed cells, but live cells become extremely fragile in the process.

Fluorescence of lignified cell walls, cuticles, and suberized walls can also be reduced by fixation in osmium (O'Brien, 1981 pp 2.28), but osmium disrupts antigenicity. The removal, or weakening of the cell wall by digestion not only reduces autofluorescence, but also improves cellular permeability.

3.1.5: Immunolabeling of SIPK and WIPK

Previous investigation of harpin and megaspermin-treated tobacco cultured cells in our laboratory revealed that both the 44 and the 48 kDa phosphorylated proteins, SIPK and WIPK, were activated within 30 min of treatment with 40 µg/mL harpin or 40 µg/mL megaspermin (Appendix 2). These results were used as the basis for designing my protocol. Those previous investigations also revealed that the anti-pERK antibody gave little or no non-specific binding to other tobacco proteins on western blots when the antibodies are used at appropriate concentrations. A recent immunolabeling study of maturing tobacco pollen used anti-pERK to detect phosphorylated SIPK and/or WIPK in fixed cells (Coronado et al., 2002). Both fluorescent chemical-tagged antibodies (fluorescence microscopy) and gold-tagged antibodies (TEM) showed that these low abundance kinases are located in both the cytoplasm and nucleus within developing

pollen grains (Coronado et al., 2002). These reports indicate that the anti-*p*ERK antibodies should be capable of reporting the distribution of *p*SIPK/*p*WIPK in tobacco cells.

3.2: Materials and Methods

3.2.1.: Tobacco Seedling Growth and Treatment with Elicitor

Tobacco (*Nicotiana tabacum* cv Xanthi nc.) plants (WT and OX:SIPK) were grown for 2 weeks on agar-solidified half-strength Murashige and Skoog (MS) medium (1962) containing 50 mg/L kanamycin (to select for transgenic plants) under controlled conditions (25/20C, 16-h-light/8-h-dark cycle). Plantlets were floated in 40 µg/mL harpin or 40 µg/mL megaspermin for 30 min. Root tips were immediately excised and fixed in fresh 4% paraformaldehyde in half-strength MS medium.

3.2.2: Cell Culture Growth Conditions and Treatment with Elicitor

N. tabacum cv Xanthi nc. suspension cell cultures were established and maintained in Murashige and Skoog medium (see Appendix 1) supplemented with 1mg/L 2,4-D and 0.1 mg/L kinetin (50mL volume in 250 mL Erlenmeyer flasks), and sub-cultured weekly. The cultures were shaken at 120 rpm (gyratory shaker) in the dark at 25 °C. Cultures (3 days after sub-culture) were treated with 40 µg/mL harpin or with 40 µg/mL megaspermin for 30 min. After exposure, the cells were permitted to settle by gravity, washed with fresh MS medium and fixed in fresh 4% paraformaldehyde in half-strength MS medium.

3.2.3: Fixation of Samples in Paraformaldehyde

Paraformaldehyde (0.4g) was added to 50 mL ½ MS pH 5.5. In the fumehood, the covered mixture was heated to around 60 °C, but not permitted to boil. A few drops of

concentrated NaOH were added to help dissolve the paraformaldehyde. Once dissolved, the mixture was cooled to RT, and the pH adjusted to 5.5. Approximately 1 mL of settled tobacco suspension cells or 12 root tips were added to the paraformaldehyde solution, which was then rotated slowly for 1 hour. The tissue sample was then permitted to settle, the supernatant removed, and the samples were re-suspended in fresh ½ MS buffer.

3.2.4: Digestion/ Removal of Cell Wall

Both root and cell culture samples were digested in 0.1% cellulase (Yakult Honsha Co. Ltd), 0.5% maceroenzyme (Yakult Honsha Co. Ltd), and 0.25% pectinylase (Yakult Honsha Co. Ltd) in 1X TBST containing 0.1% saponin from quillaja bark (Sigma) with rotation at 100 oscillations/min for 20 min. Saponin was used to permeabilize cell membranes to aid immunolabelling solutions to pass through cellular membranes.

3.2.5: Immunolabeling

3.2.5.1: Primary Antibodies

The primary antibodies used in this experiment were anti phospho-ERK (anti-pERK) (1:200 dilution, Cell Signalling), anti-ERK (1:200 dilution, Santa Cruz), anti-FLAG (1:500 dilution)(Sigma) , a negative control rabbit pre-immune serum (1:200 dilution), and a positive control anti-histone antibody (1:500 dilution)(Chemicon). All antibodies were made up in 4%BSA in TBST containing 0.1% saponin.

3.2.5.2: Secondary Antibodies

The primary antibodies used in these experiments were detected with anti-rabbit IgG:Alexa⁵⁹⁴-conjugated secondary antibody (Molecular Probes). Alexa⁵⁹⁴ is a Texas Red-equivalent fluorochrome with emission at 594 nm. The secondary was used at a 1:300 dilution in 4%BSA in TBST.

Stored conjugates sometimes develop precipitates, and were therefore routinely centrifuged (8,000g for 15 sec) before use to remove any particulate matter.

3.2.5.3: Controls

Anti-histone antibody was used as a positive control because histone is an abundant protein in tobacco cells, and is restricted to the nucleus. Use of this nuclear-localized antibody gives a good indication of what a nuclear localization signal pattern should look like. The positive control also confirmed whether a given protocol was working.

Several negative controls were used in these experiments. Samples treated with no primary or secondary antibody gave information about natural background autofluorescence in the sample. These samples were treated with blocking solution instead of either the primary or secondary antibody at the appropriate steps. Samples treated with secondary antibody, but no primary antibody, revealed the extent of non-specific binding of the secondary antibody. Use of pre-immune serum as the primary antibody reveals any non-specific binding associated with rabbit anti-serum.

3.2.5.4: Immunolabeling Protocol

Fixed tissue samples were treated with 50mM EGTA for one hour to chelate any interfering metal ions. Samples were treated with 1% Triton-X 100 with shaking at 100 oscillations/min for 20 min, followed by treatment with ice cold methanol with shaking at 100 oscillations/min for 10 min. Samples were incubated in blocking solution (bovine serum albumin (BSA) (4% w/v) in 1X TBST containing 0.1% saponin and 1mM glycine prepared fresh and filtered) overnight, rinsed with 1X TBST + 0.1% saponin, and blotted dry with Whatman #2 filter paper.

Samples were applied to individual wells of poly-L-lysine-coated 8 mm well slides. Each slide contained 8 individual wells. For observation of cells, a 20 μ L droplet of culture was permitted to settle in each well for 20 min, and excess culture medium was removed by pipetting. Roots were attached by gently squashing the root onto the slide by pressing with the thumb directly on the coverslip over the root. The coverslip was then removed by sliding it to the side, taking care not to mangle the root tip.

Care was taken to keep specimens as moist as possible for immunolabeling, since air drying can produce structural artifacts within a given tissue, mainly on the cell surface, as well as negative effects from oxidation (O'Brien, 1981. pp3.21).

Moist chambers were created for the slides by putting two 1X TBST-soaked filter paper wedges inside a Petri dish. Primary antibody (5 μ L/well) was applied to the individual wells (or blocking solution to appropriate controls) and the slides were then incubated 1 h in the covered chambers at RT.

Following incubation with the primary antibody, slides were rinsed with 1X TBST containing 0.1% saponin, and then let sit in four consecutive baths of fresh 1X TBST containing 0.1% saponin for 10 min each before being blotted dry with filter paper, and placed back in the moist chambers. Secondary antibody (5 μ L/well) was then applied to the individual wells (or blocking solution for appropriate controls), which were incubated for one hour in the covered chambers at RT. Slides were then rinsed with 1X TBST followed by four consecutive 10 min washes in fresh 1X TBST containing 0.1% saponin.

Following treatment with secondary antibody, samples were treated with 5 μ L/well 30 nM DAPI in TBST containing 0.1% saponin for 30 min. The slides were then rinsed with 1X TBST, followed by four consecutive 10-min washes in fresh 1X TBST

containing 0.1% saponin, briefly rinsed in fresh distilled water to remove any excess salts from buffers that might crystallize over time under the coverslip. Samples were blotted dry with filter paper. Mounting medium consisting of 33% aqueous glycerol was added and cover slips were applied. The mounted slides were sealed with clear nail polish, and left in the dark at 4 °C until use.

3.2.5.5: Quantification

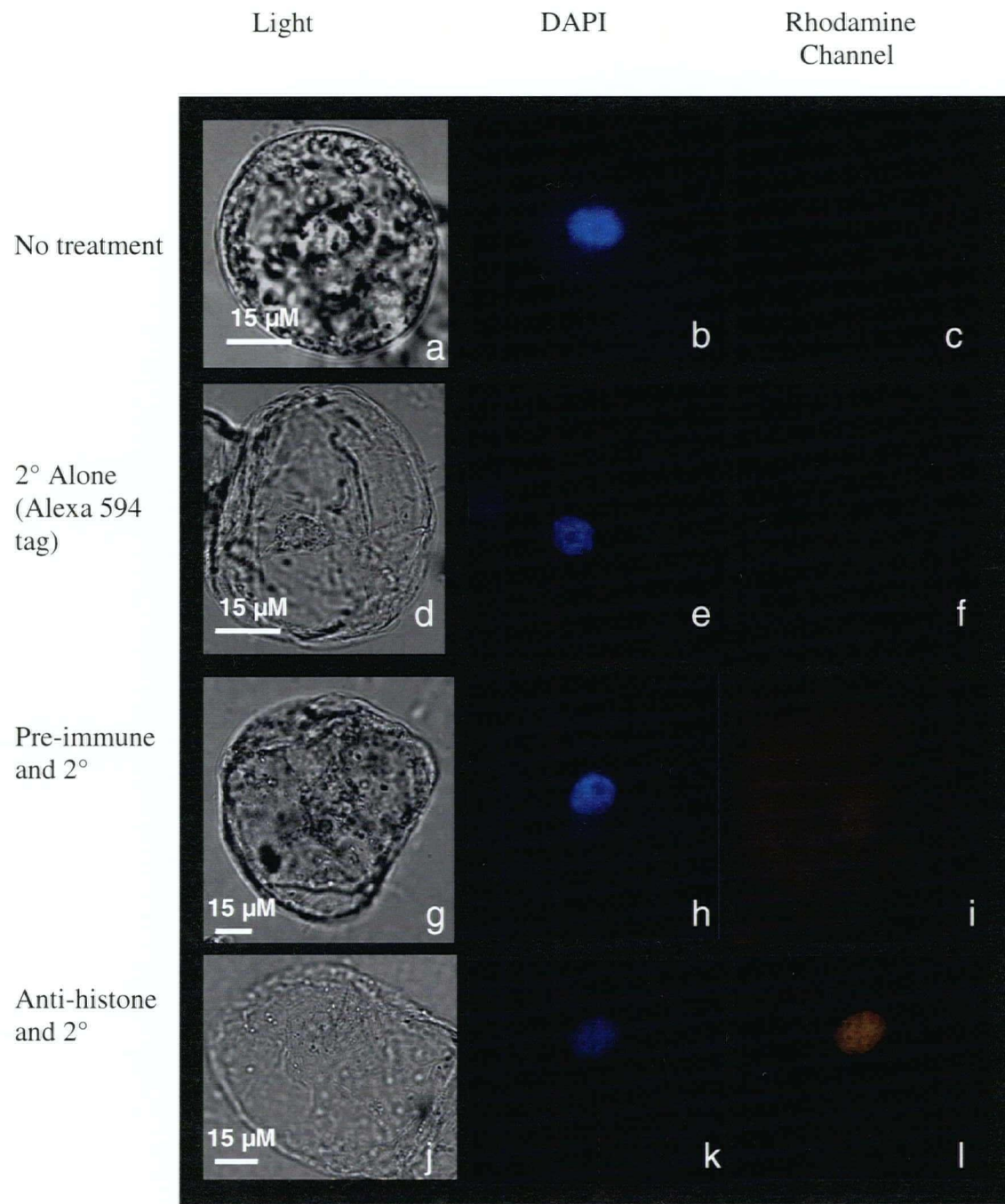
A Leica DMR fluorescence microscope equipped with a Texas Red #2 (rhodamine) filter (emission 645-75 nm) was used to visualize fluorescence. The microscope was equipped with a digital Q-imaging QICAM image capture system running under Openlab 3.0 software for viewing and recording of immunolabeling results. Exposure times were set at 3 sec (unless otherwise noted) so comparisons could be drawn between control and experimental samples.

3.3: Results

Fixed cells were examined under three different microscope conditions; bright field, fluorescence with inserted DAPI filter, and fluorescence with inserted rhodamine filter. Light microscopy reveals the basic cellular shape, gives an indication of pre-fixation viability of cells, and reveals some basic cellular structures (Figure 3.1a,d,g,j). Although most cultured cells had an oval shape, some cells displayed an elongated shape, or were clumped together with other cells. The pre-fixation viability could be assessed by the degree to which the cell membrane remained tightly pressed to the cell wall. Dead cells displayed extensive detachment of the membrane. Some of the basic structures visible within the cells with light microscopy are the nucleus, vacuoles, cytoplasm, and cell wall.

DAPI staining (Figure 3.1b,e,h,k) verified the location of the nucleus within the cell, indicated whether there was more than one cell present (based on the number of nuclei present) and sometimes revealed the mitotic stage of the cells.

Cultured tobacco cells showed a low level of autofluorescence in the rhodamine channel (Figure 3.1c), but this was not significant compared to the intensity of fluorescently labeled structures seen in the anti-histone immunolabeled positive control (Figure 3.1l). The positive control anti-histone antibody showed strong labeling of the nuclei, similar to the DAPI labeling (Figure 3.1k). The secondary antibody used in this experiment, Alexa⁵⁹⁴-tagged anti-rabbit antibody, did bind non-specifically to some internal cellular structures, such as the cell wall/membrane, and within the nucleus (Figure 3.1f), but the fluorescent signal was negligible in comparison to the positive control (Figure 3.1l). The pre-immune serum-stained cells showed a moderate amount of non-specific binding to cell membranes/walls and nuclei, as well as to some unidentified internal cellular structures (Figure 3.1i). However, pre-immune-labeled cells still showed a much lower fluorescence signal than the positive control (Figure 3.1l).



Controls (3 sec exposure except for anti-histone, 200 ms)

Figure 3.1: Immunolabeling Control Samples of Fixed Suspension Culture Wild Type Tobacco Cells

Figure 3.1 shows the light image, the DAPI stained image, and the rhodamine channel fluorescence of 4 different immunolabeling controls; untreated negative control, no primary with applied secondary Alexa⁵⁹⁴ anti-rabbit negative control, a rabbit pre-immune serum with secondary negative control, and anti-histone with secondary positive control.

As well as wild-type tobacco suspension cell culture, I had available a transgenic cell culture line in which SIPK is ectopically over-expressed. The SIPK transgene has been modified to include a FLAG epitope at the C-terminus of the SIPK protein. This cell culture line was included in my study because it was hypothesized that over-expression of SIPK might give a stronger SIPK subcellular localization signal. The advantage of having a FLAG-tag on the ectopic SIPK was that it would allow me to use anti-FLAG immunolabeling to visualize SIPK subcellular localization, as well as avoiding any potential non-specific binding an anti-SIPK antibody might have to similar MAPKs or other proteins. However, the OX:SIPK cultured cells displayed some physiological differences from WT (Appendix 3.0). OX:SIPK cultured cells were generally smaller than WT, had a somewhat higher level of native autofluorescence, and were predominantly spherical. These differences emphasize that the OX:SIPK cells cannot be directly compared to WT cells, but might still provide valuable information about general MAPK localization patterns as well as specific information about SIPK localization patterns in a SIPK over-expressing system.

Both WT and OX:SIPK cultured cells were immunolabeled with three different antibodies (aside from controls): anti-ERK, anti-*p*ERK and anti-FLAG. Anti-ERK antibody was used to show general MAPK distribution patterns within WT and OX:SIPK tobacco cells. Anti-*p*ERK antibody provides specificity, since it is a monoclonal antibody directed at the phosphorylated TEY sequence of 42-48 kDa MAPKs, which in tobacco are SIPK and WIPK. Phosphorylated SIPK and WIPK localization patterns could then be compared to overall MAPK cellular distribution in WT and OX:SIPK tobacco cells. The third antibody, anti-FLAG, would provide information about SIPK's

localization patterns in OX:SIPK tobacco cells, and could be compared to anti-ERK and anti-pERK immunolabeled OX:SIPK cells.

Each of these antibodies showed some discrete localization pattern that differed from the non-specific binding pattern associated with the pre-immune serum negative control in cultured cells. For every treatment group, approximately 100 cells were observed, and observed trends recorded. Images presented here from each treatment group represent typical patterns.

Untreated cultured cells probed with anti-ERK primary antibody (Figure 3.2 Cii) showed predominantly cytoplasmic localization of the signal. Although a few untreated cells did show some nuclear accumulation of label, the majority of cells displayed an even distribution of the label throughout the cytoplasm, extending from the nucleus through the cell to the outer periphery of the cell.

By contrast, most harpin-treated cells probed with anti-ERK primary antibody (Figure 3.2 Ciii) displayed increased nuclear localization of the signal, and within this population a considerable number of cells displayed strong accumulation of label in a central region of the nucleus, believed to be the nucleolus. A minority of harpin-treated cells probed with anti-ERK displayed cytoplasmic localization of label with no real accumulation in the nucleus or nucleolus.

Confocal projections of both untreated and treated anti-ERK-probed cells yielded a pattern similar to the results found with fluorescence microscopy (Figure 3.2: 2b,c), but the confocal analysis revealed a cleaner picture of the presence and absence of label within the cell, and provided images of higher resolution than basic fluorescence microscopy.

It should be noted that some of the bright punctate spots seen in this figure are not indicative of large labeled structures, but are an artifact of projecting multiple layers of images that contain smaller bright spots. These large spots were not present in all confocal projections of cells.

Cells treated with megaspermin showed no noticeable differences from those treated with harpin when probed with anti-ERK (Figure 3.3). Megaspermin-treated samples echoed a nuclear localization in the majority of cells, with considerable nucleolar accumulation.

Anti-ERK immunolabeled OX-SIPK cultured cells closely resembled the WT labeled cultured cell localization patterns. The majority of untreated cells showed cytoplasmic localization of signal (Figure 3.4 Cii, 2a). Harpin-treated OX:SIPK cells showed nuclear localization of label (Figure 3.4 Ciii, 2b), but did not display the distinctive nucleolar accumulation seen in harpin and megaspermin-treated WT cells (Figure 3.2 Ciii, 2c). Few sampled cells displayed cytoplasmic localization in treated OX:SIPK cells.

Cells immunolabeled with the anti-*p*ERK primary antibody displayed a more spatially restricted distribution of label. There was a stronger nuclear accumulation of label in anti-*p*ERK probed WT cells than in anti-ERK probed WT cells, but overall the distribution of anti-*p*ERK label in the majority of untreated cells remained predominantly cytoplasmic. WT cells harpin-treated (Figure 3.5 Ciii) showed strong nuclear localization of the anti-*p*ERK signal, but with very distinct nucleolar localization. The great majority of harpin-treated cells showed strong visible nuclear localization of the antibody signal, with a strong nucleolar signal within the nucleus. Nucleolar localization was also observed in untreated cells, but at a very low frequency, and label accumulation did not

exhibit the sharp edged localization pattern seen in the harpin-treated cells (Figure 3.5 Cii).

The nucleolar localization of signal in harpin-treated WT cultured cells is again observed in the confocal images (Figure 3.5: 2c), and also revealed that within the nucleolus there is a central region that shows no label. Of the cells that were examined, smaller nucleoli showed no internal black spot, whereas larger nucleoli show a distinct unlabeled central region. Confocal images of WT cultured cells that had not been exposed to harpin showed strong cytoplasmic localization extending from the nucleus to the cell periphery (Figure 3.3: 2b).

WT cells treated with megaspermin and probed with anti-*p*ERK primary antibody appeared indistinguishable from harpin-treated cells in terms of *p*ERK subcellular localization (Figure 3.6).

OX-SIPK cells immunolabeled with the anti-*p*ERK primary antibody showed different localization patterns to those from WT anti-*p*ERK labeled cultured cells. Approximately half of untreated OX-SIPK cells sampled already exhibited nuclear localization of signal, with the remainder exhibiting cytoplasmic localization (Figure 3.7 Cii). These results were also reflected in confocal projection images (Figure 3.7: 2b).

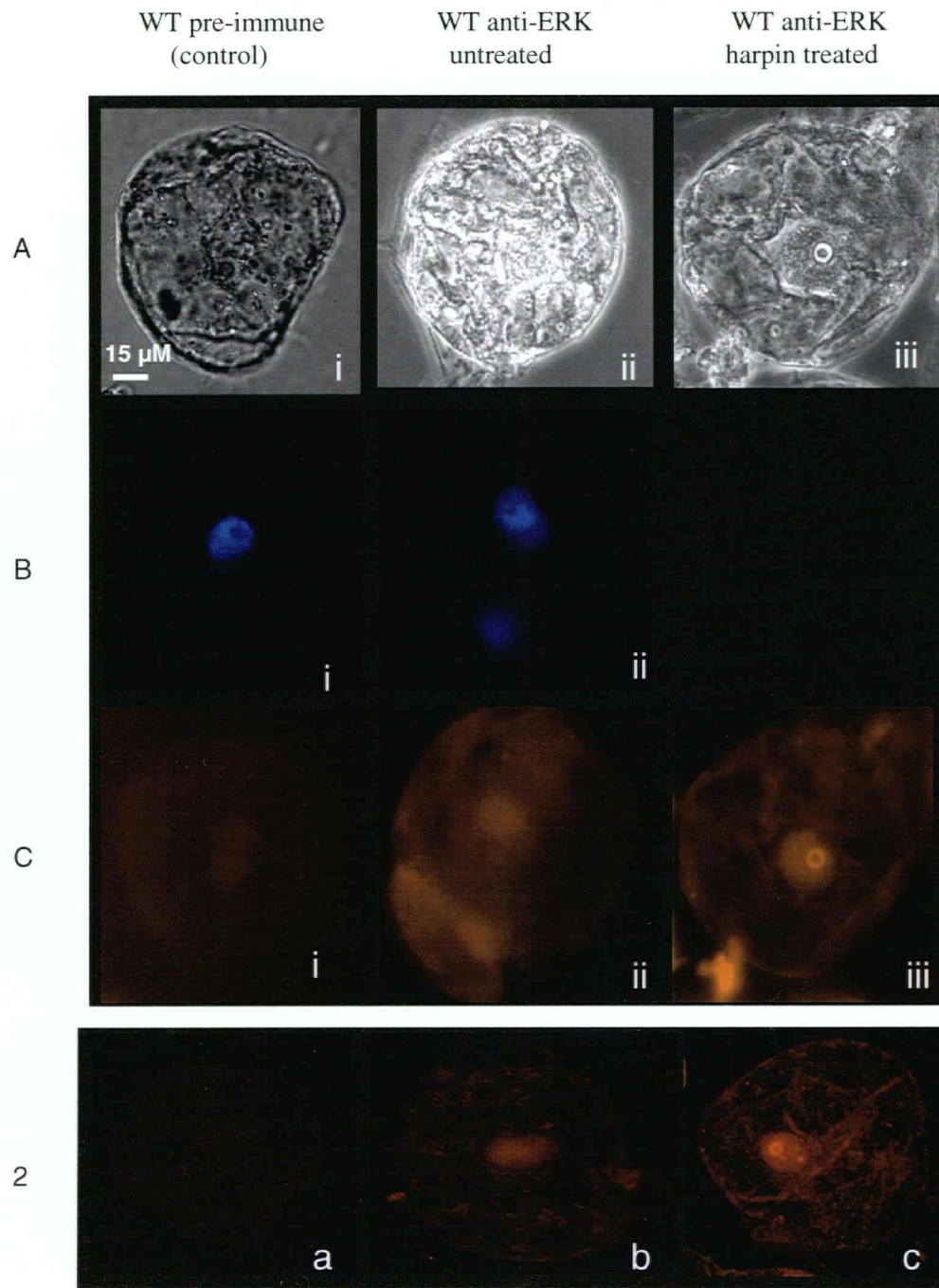
The majority of harpin-treated OX:SIPK cells probed with anti-*p*ERK displayed nuclear localization of signal, similar to WT immunolabeled cells, but only a few cells displayed prominent nucleolar localization (Figure 3.7 Ciii, Figure 3.7: 2c). Although nucleolar labeling in OX:SIPK cells was less pronounced than that observed in WT labeled cells, it was not totally absent.

The anti-FLAG polyclonal antibody from SIGMA was recommended by Brett Finlay's lab for immunolabeling purposes, based on their experience with both the monoclonal and polyclonal reagents. In their immunolabeling experiments, they had found less non-specific binding with the polyclonal form than with the monoclonal form. Western analysis of tobacco cell extracts with the polyclonal anti-FLAG antibody did show non-specific binding when concentrations of the antibody were high (data not shown). A dilution of 1:500 was used to achieve minimal non-specific binding during my immunolabeling experiments (Figure 3.8 Cii). As a result, signal intensities in anti-FLAG labeled cells appear lower than in anti-ERK and anti-*p*ERK probed cells. Non-specific binding of the anti-FLAG antibody in WT cells produced a diffuse signal throughout the cell, with higher amounts in the cell wall/membrane and the nucleus (Figure 3.8 Cii). OX:SIPK cells expressing the FLAG-tagged SIPK and not treated with an elicitor showed accumulation of label in both the cytoplasm and nucleus (Figure 3.8 Ciii). The signal within the cytoplasm appears to be associated with cytoplasmic strands extending toward the nucleus. In contrast to the anti-ERK and anti-*p*ERK, the nuclear signal appears to be largely excluded from the nucleolus. Among the 100 cells examined, the fluorescent signal was observed approximately half of the time to have a stronger cytoplasmic localization, and half of the time to display a stronger nuclear localization.

The harpin-treated OX:SIPK cells showed anti-FLAG immunolabeling signal patterns similar to those seen in untreated OX cells, but with slightly less cytoplasmic signal (Figure 3.7 C iv). The majority of the cells observed displayed higher nuclear localization, with a minority of the cells showing cytoplasmic localization (Figure 3.7). The label was diffusely localized throughout the nucleus. The confocal projection

images of harpin-treated OX-SIPK anti-FLAG immunolabeled cells (Figure 3.7: 2) reflect the fluorescent microscope image patterns, but have better resolution.

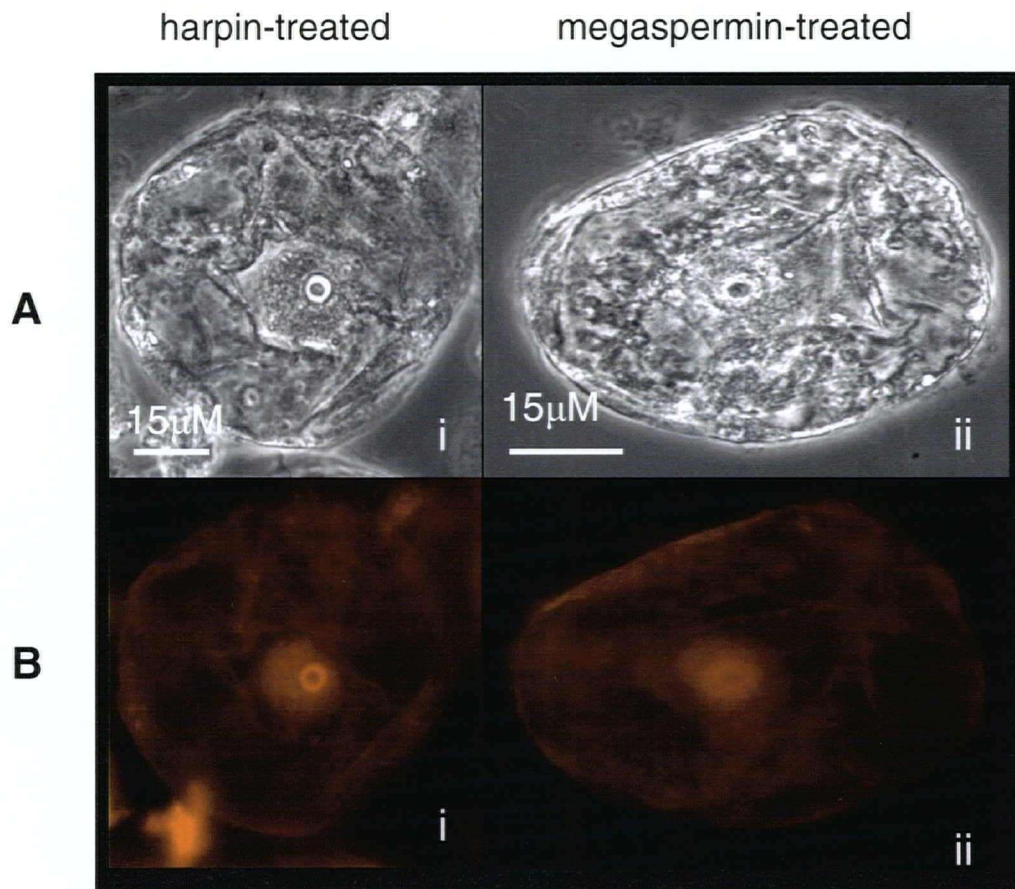
Localization patterns show higher immunolabeling signal in the anti-FLAG-treated OX cells (Figure 3.7: 2c,d) than in the anti-FLAG-treated WT control (Figure 3.7: 2b) or the untreated OX cells (Figure 3.7: 2a). Distinct punctate cytoplasmic labeling with general nuclear labeling is present in untreated OX cells (Figure 3.7: 2c), reflecting the patterns found with fluorescence microscopy. The treated OX-SIPK cells examined by confocal microscopy showed less cytoplasmic labeling and higher nuclear labeling (Figure 3.7: 2d), similar to results obtained from fluorescence microscopy.



A=LM, B=DAPI, C=Rhodamine (fluorescent) 3 sec exposure,
D=Rhodamine (fluorescent confocal projection)

Figure 3.2: Anti-ERK Immunolabeled Untreated and 30 min Harpin-Treated WT Tobacco Cells

Figure 3.2 shows the light (1i-iii), the fluorescence DAPI channel (2i-iii), and the fluorescence rhodamine channel images (3i-iii) and confocal projections (2a-c) from anti-ERK primary and Alexa⁵⁹⁴-tagged secondary immunolabeled WT tobacco cultured cells. Harpin treatment concentration was 40 μg/mL. Controls for this experiment were WT cells treated with rabbit pre-immune serum (column 1).

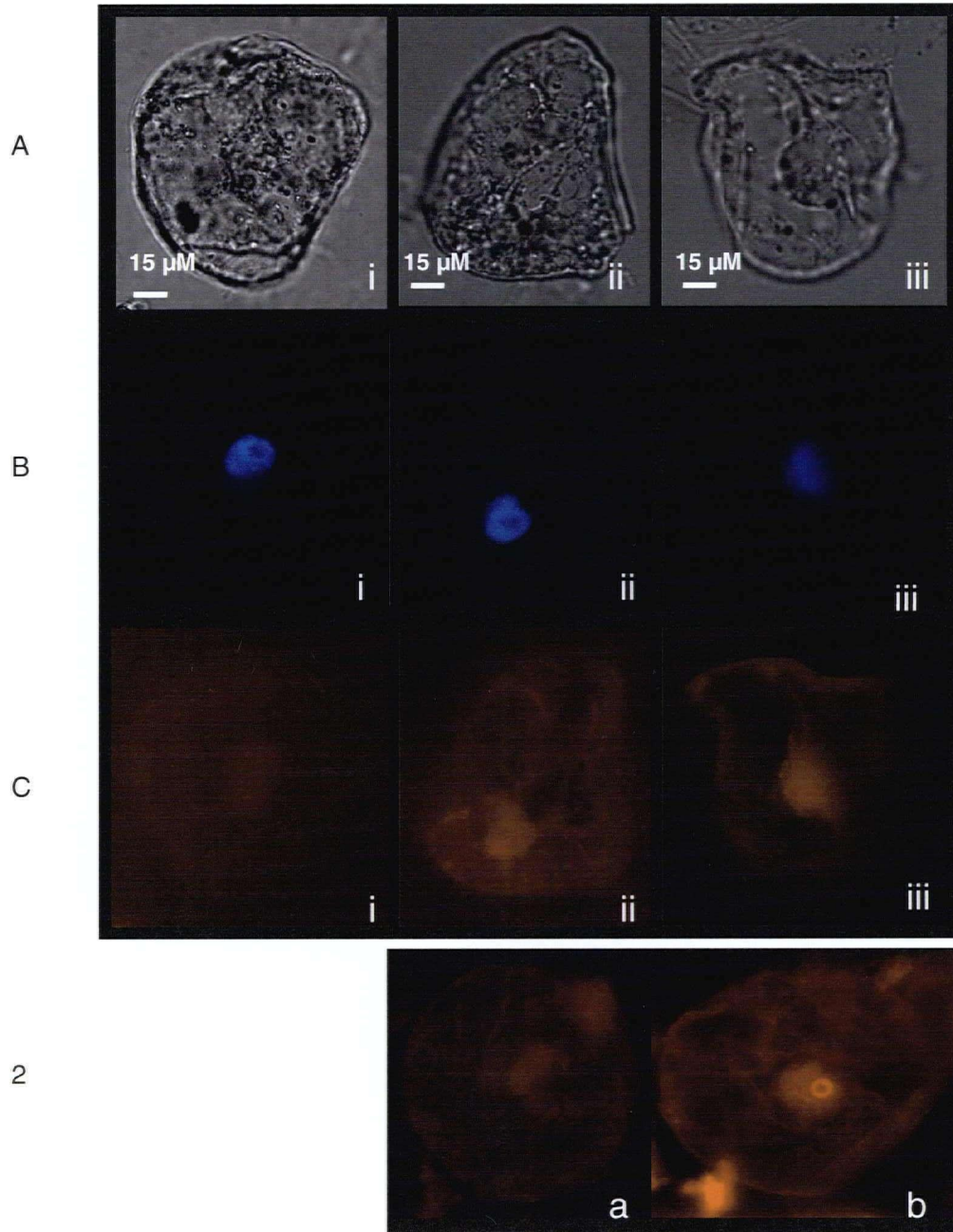


A=LM, B =Rhodamine (fluorescent), 2 sec exposure

Figure 3.3: Anti-ERK Comparison of Harpin and Megaspermin-Treated Cell Culture

Figure 3.3 shows the comparison of WT cells probed with anti-ERK treated with 40 μg/mL harpin or megaspermin for 30 min.

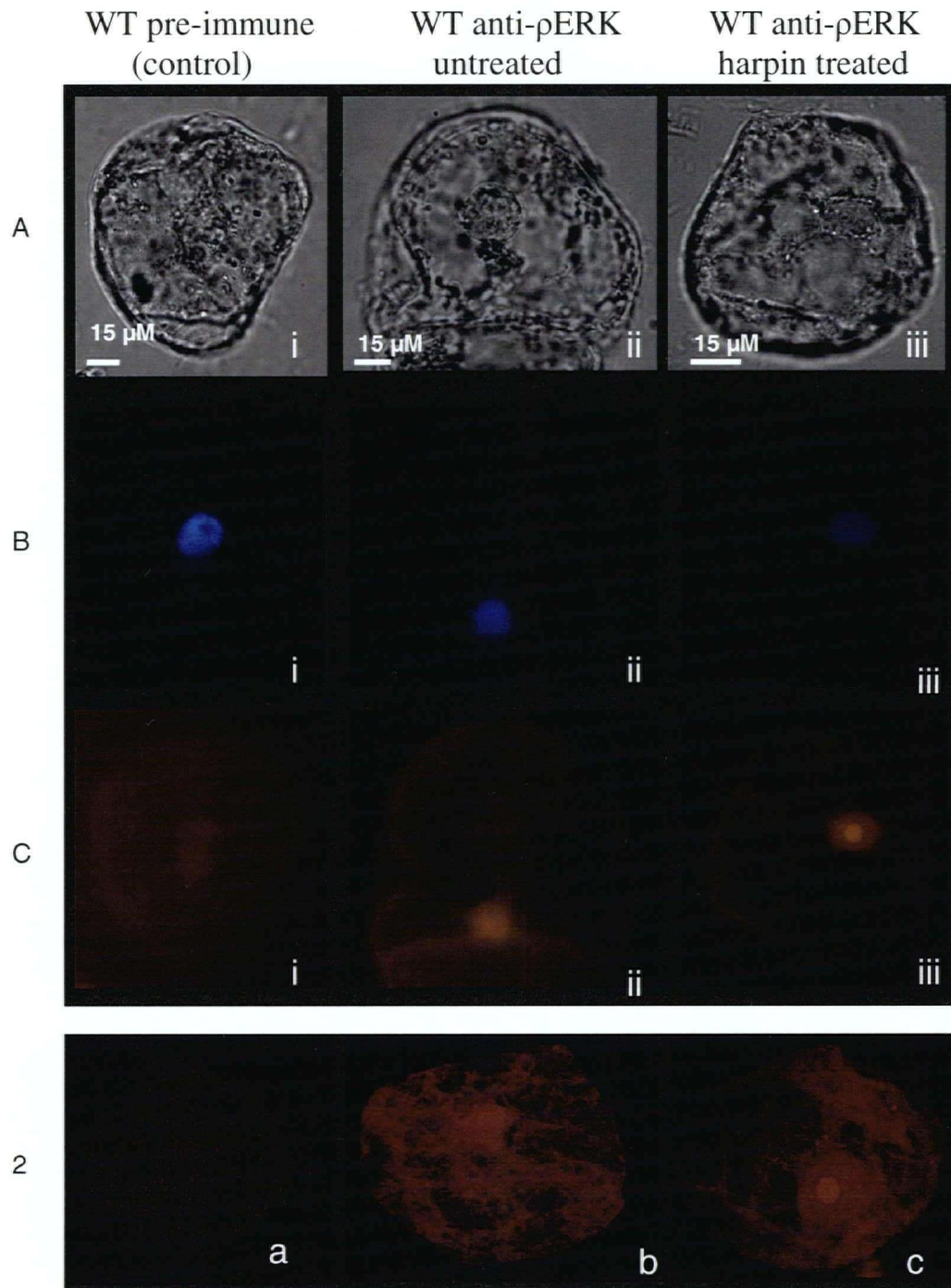
WT pre-immune (control) OX:SIPK anti-ERK untreated OX:SIPK anti-ERK harpin treated



A=LM, B=DAPI, C & D=Rhodamine (fluorescent), 2 sec exposure

Figure 3.4: Anti-ERK Immunolabeled Untreated and 30 min Harpin-Treated OX Tobacco Cells

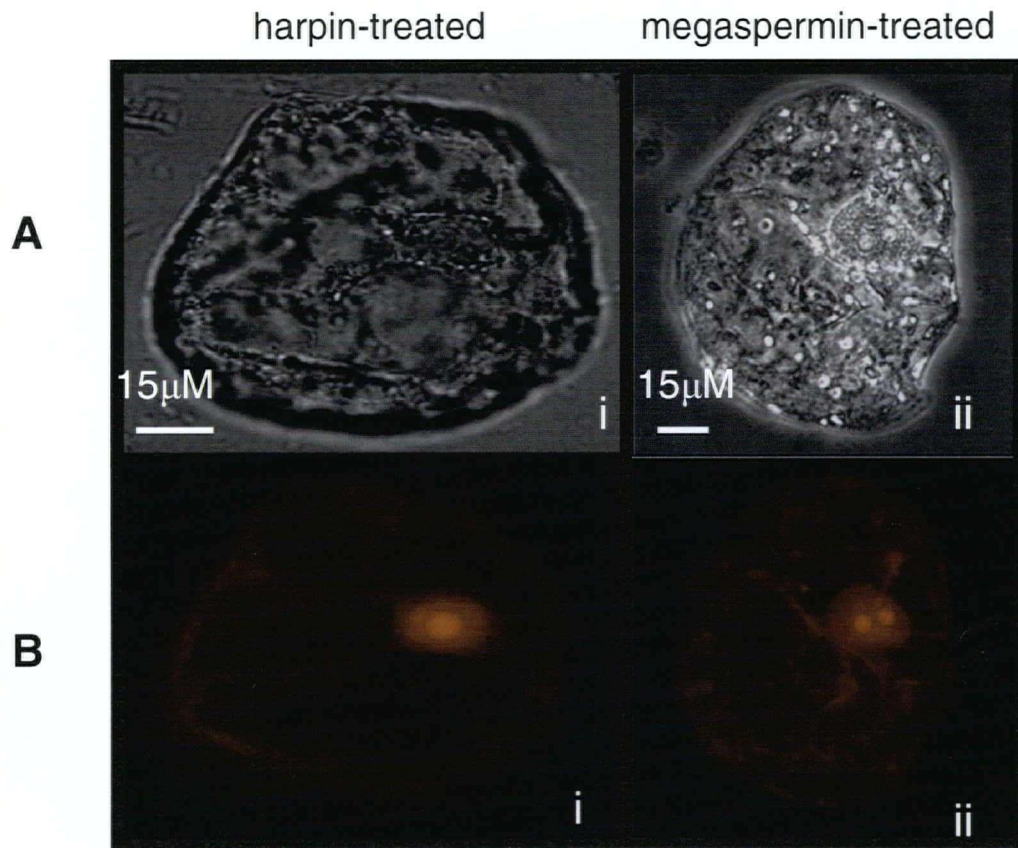
Figure 3.4 shows the light (1i-iii), the fluorescence DAPI channel (2i-iii), and the fluorescence rhodamine channel images (3i-iii) and confocal projections (2a-c) from anti-ERK primary and Alexa⁵⁹⁴-tagged secondary immunolabeled OX-SIPK tobacco cultured cells. Harpin concentration was 40 μg/mL. Controls for this experiment were cells treated with rabbit pre-immune serum (column 1).



A=LM, B=DAPI, C=Rhodamine (fluorescent) 3 sec exposure,
2a-c=Rhodamine (fluorescent confocal projection)

Figure 3.5: Anti- ρ ERK Immunolabeled Untreated and 30 min Harpin-Treated WT Tobacco Cells

Figure 3.5 shows the light (1i-iii), the fluorescence DAPI channel (2i-iii), and the fluorescence rhodamine channel images (3i-iii) and confocal projections (2a-c) from anti- ρ ERK primary and Alexa⁵⁹⁴-tagged secondary immunolabeled WT tobacco cultured cells. Harpin concentration was 40 μ g/mL. Controls for this experiment were cells treated with rabbit pre-immune serum (column 1).



A=LM, B =Rhodamine (fluorescent), 2 sec exposure

Figure 3.6: Anti-*p*ERK Immunolabeled Comparison of Harpin and Megaspermin-Treated Cultured cells

Figure 3.6 shows the comparison of 40 µg/mL harpin or megaspermin treated (30 min exposure) WT cells probed with anti-*p*ERK.

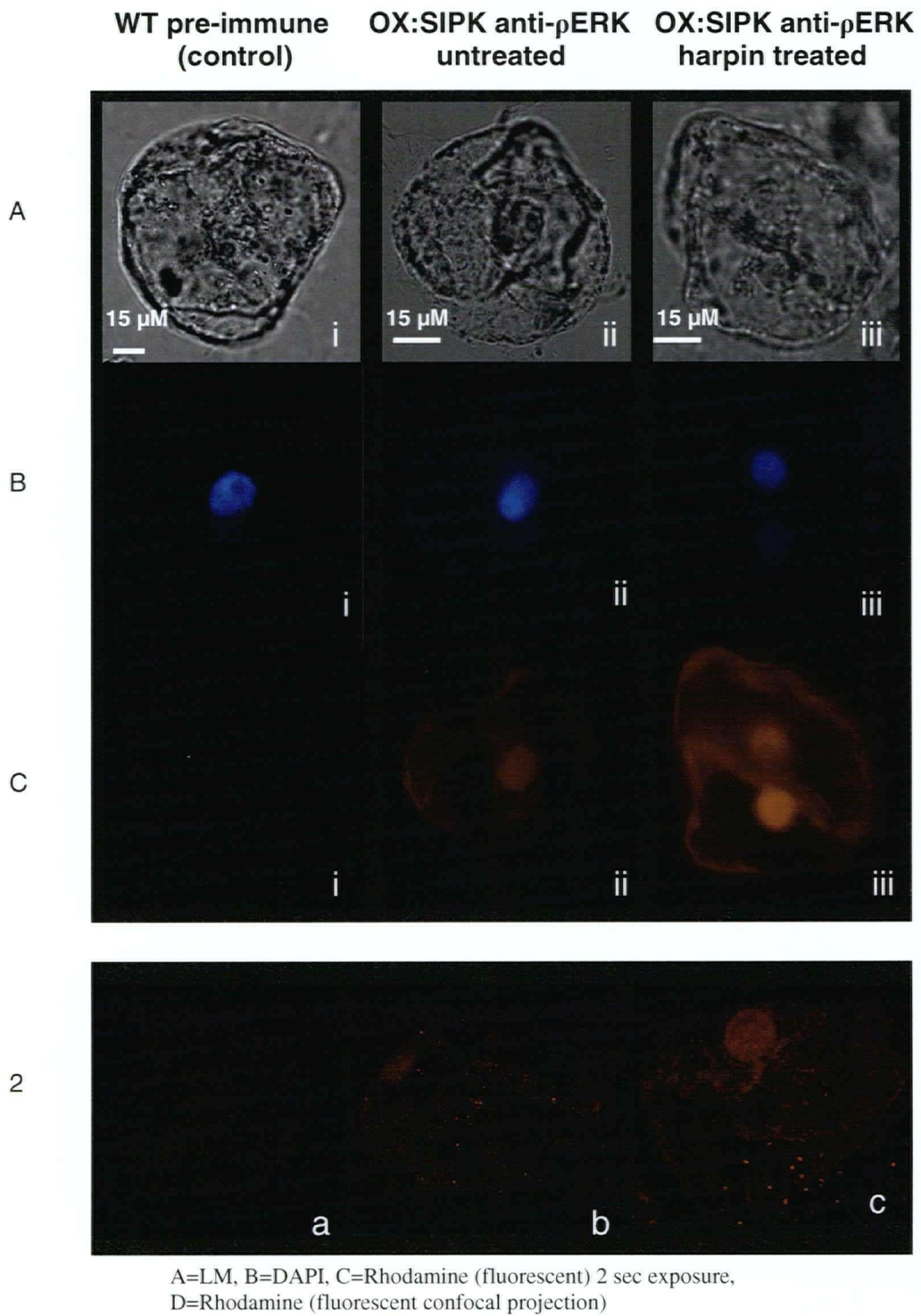
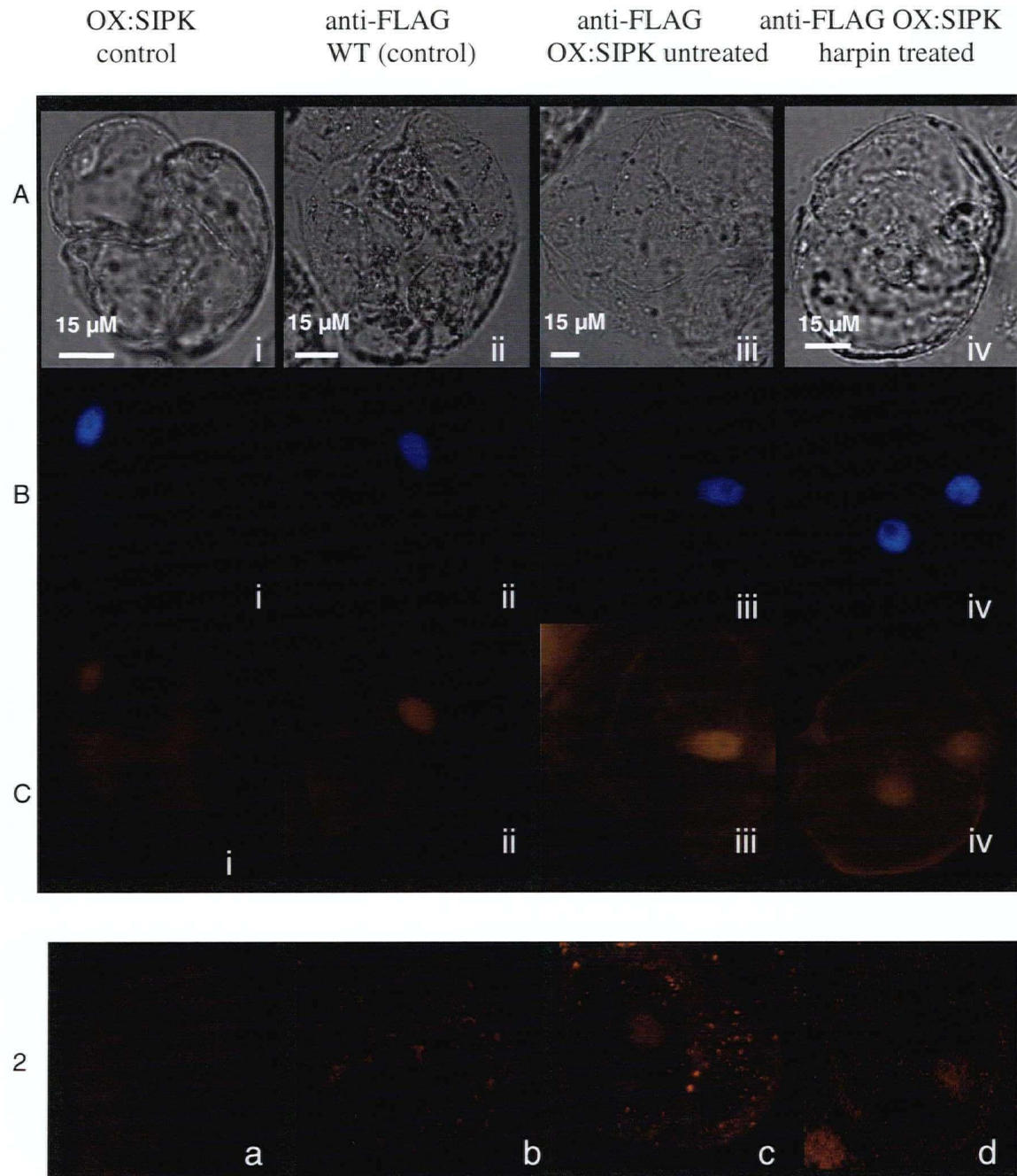


Figure 3.7: Anti- p ERK Immunolabeled Untreated and 30 min Harpin-Treated OX:SIPK Tobacco Cells

Figure 3.7 shows the light (1i-iii), the fluorescence DAPI channel (2i-iii), and the fluorescence rhodamine channel images (3i-iii) and confocal projections (2a-c) from anti- p ERK primary and Alexa⁵⁹⁴-tagged secondary immunolabeled OX-SIPK tobacco cultured cells. Harpin concentration was at 40 μ g/mL. Controls for this experiment were cells treated with rabbit pre-immune serum (column 1).



A=LM, B=DAPI, C=Rhodamine (fluorescent) 2 sec exposure,
D=Rhodamine (fluorescent confocal projection)

Figure 3.8: Anti-FLAG Immunolabeled WT, OX-SIPK, and 30 min Harpin-Treated OX-SIPK Tobacco Cells

Figure 3.8 shows the light (1i-iv), the fluorescence DAPI channel (2i-iv), and the fluorescence rhodamine channel images (3i-iv) and confocal projections (2a-d) from anti-FLAG primary and Alexa⁵⁹⁴-tagged secondary immunolabeled tobacco cultured cells. Controls for this experiment were untreated OX-SIPK cells (column 1), and WT cells immunolabeled with anti-FLAG (column 2) to show any non-specific binding of the FLAG antibody. Harpin treatment concentration was 40 μg/mL.

3.4: Discussion:

This study of subcellular localization of plant MAPKs in response to stress was carried out primarily in cultured cells as opposed to using whole plant material. Plant suspension cultures have been shown to reflect whole plant metabolism in many studies, including responses to fungal elicitors (Romeis et al., 1999). From the perspective of fluorescence microscopy, cell culture was a good experimental medium due to the lack of developed chloroplasts, and low autofluorescence. These characteristics, together with the relative uniformity of tobacco suspension cultured cells, and their ease of fixation and ease of digestion of the cell wall, made them a superior system for immunolabeling *in planta*.

The choice of paraformaldehyde as a fixative was based on its rapid rate of infiltration, its ability to penetrate cuticularized cell walls and coagulants within the fixative mixture, and the excellent preservation of cellular structure that it provides (O'Brien, 1981 pp4.22).

Fluorochrome-tagged immunolabeling was employed for these experiments because fluorescent compounds can be detected in very low concentrations, and MAPKs, especially phosphorylated MAPKs, are expected to be in low abundance within the cell. The Alexa⁵⁹⁴ secondary antibody was chosen based on fluorochrome stability, suitable emission wavelength, and the intensity of its fluorescence. The Alexa fluors are known to resist fading, and are not affected by pH variation within the cell. The Alexa⁵⁹⁴ fluor has emission that can be detected in the rhodamine channel (594 nm), which is convenient since Rhodamine and far red channels capture the least amount of autofluorescence from cultured tobacco cells. (data not shown). The Alexa⁵⁹⁴-labeled secondary antibody was found to yield a strong fluorescent signal in immunolabeled

tissue, as seen in the positive control anti-histone immunolabeled cell (Figure 3.11), and little to no non-specific binding when no primary antibody was applied (Figure 3.1f).

Labeling with the pre-immune serum is an important control that reveals any non-specific binding reactions. Preliminary experiments explored various measures to reduce non-specific binding, such as longer blocking solution treatments, shorter primary antibody incubation times, and decreased primary antibody concentrations. Based on these results, an optimized protocol was developed. Using this protocol, the pre-immune serum generated some diffuse non-specific binding throughout the cell (Figure 3.1i), although in comparison to the positive control this was minimal. From the low levels of non-specific binding observed on a western gel, it was hoped there would be little to no non-specific binding in whole cell immunolabeling as well. As it turned out, the levels of non-specific binding were higher than hoped, but were still considered acceptable for immunolabeling. When compared to the modest levels of staining subsequently observed in the anti-FLAG, anti-pERK, and anti-ERK labeled samples, this non-specific binding does appear more significant (Figures 3.2-3.6), but the patterns of non-specific binding of the pre-immune serum were always diffuse, rather than punctuate; i.e. they never showed a significant amount of accumulated label in one area. Pre-immune serum non-specific binding was therefore readily distinguishable from antibody labeled signal.

The choice of the anti-histone antibody as a positive control was based on the prediction that my protein of interest would show a higher nuclear localization upon treatment. The anti-histone antibody proved to give a clean and consistent nuclear localization pattern, and was a valuable resource for showing the effectiveness of the immunolabeling method (Figure 3.11).

Anti-ERK immunolabeling of cultured WT tobacco cells showed a significant amount of cytoplasmic labeling in untreated cells, with a high nuclear, and particularly nucleolar, accumulation of label (Figure 3.2). Pre-treatment of the cells with either harpin or megaspermin resulted in a shift in labeling intensity that could be interpreted as a re-localization of cytoplasmic SIPK/WIPK to the nucleus/nucleolus. This is consistent with numerous studies in other organisms showing that ERK and ERK homologues have a general cytoplasmic localization in untreated cells, and move at least partially to the nucleus upon induction with certain elicitors. Both harpin and megaspermin were shown to induce this change in localization pattern, as seen by probing with anti-ERK. It should be noted that the use of anti-ERK does not allow me to distinguish between SIPK and WIPK signals. However, it is known that the basal level of SIPK in untreated tobacco is ~10-fold higher than that of WIPK (Zhang and Klessig, 1998), which would imply that the majority of signal observed in these tobacco cells is associated with SIPK.

Since the activation of MAPKs by stress is known to be rapid (<10 min), it is reasonable to ask whether the infiltration rate for paraformaldehyde was faster than the ability of the cultured cells to detect the chemical stress. It was hypothesized that if this fixation was too slow, paraformaldehyde infiltration might trigger premature MAPK activation in untreated cells. To address this question, high pressure-frozen samples were compared to paraformaldehyde-treated samples. No obvious differences were found between dextran-fixed and paraformaldehyde-fixed samples, but the HPF sample sizes were too small for a thorough comparison (Appendix 5).

Anti-ERK was used to probe both WT and OX:SIPK-treated and untreated cultured cells. In an over-expressing system, it was believed there would be higher levels of

cellular SIPK, and thus more label present. The stable over-expression of both SIPK and WIPK in transgenic tobacco had been previously shown to not affect the activity of the kinases (Yang et al., 2001), but some physiological differences were noted in the OX-SIPK line. In cell culture, OX:SIPK cells were found to be smaller in size, sometimes half that of WT, and the culture consisted mainly of isodiametric cells, whereas cells in WT culture have multiple shapes and sizes ranging from round to oval, and from small (50 μ m diameter) to large size (100 μ m diameter) (Appendix 3). OX:SIPK plants were found to be slightly shorter overall when compared to similarly grown WT tobacco, and the overexpressing line had denser foliage and floral buds (unpublished data, Marcus Samuel). The OX:SIPK transgenic plants are also more sensitive to growth on high salt concentrations, or higher concentrations of some growth hormones. (unpublished data, Marcus Samuel). Since overexpression of SIPK thus has a number of observable pleiotropic consequences, it is perhaps not surprising to observe different ERK localization patterns in OX:SIPK cells as compared to WT cells. Higher levels of nuclear localized signal were observed in both treated and untreated OX:SIPK cells (Figure 3.4). Perhaps OX-SIPK cells are more sensitive to the stress associated with the handling of the cells, or with the fixation process, and thus displayed more of a constitutively active phenotype, even in untreated cells. In a recent study of parsley MAPK (PcMPK6) subcellular localization, Lee *et al.* found that 20% of cells in a deliberately stressed culture population did not show any different subcellular localization (2004). Their hypothesis was that a certain number of cells will typically remain unaffected by a given stress, a response pattern that may help maintain stability. In an analogous fashion, it is

also possible that in untreated over-expressing SIPK cultured cells there is a higher frequency of cells within the population that act stressed at all times.

There are several possible explanations for the differences in localization patterns observed between WT and OX:SIPK cells. First, overexpressing SIPK may cause a shift in MAPK signaling patterns that does not reflect native signaling patterns. An accumulation of SIPK within the cell could also cause competition for interaction with NtMEK2 in the cytoplasm, causing diminished activated WIPK signal. Overexpressing SIPK could also cause a variety of effects outside the MAPK signaling pathway that might affect the subcellular localization of the kinase. For example, over-expressed SIPK could be targeted for degradation. Higher levels of the kinase could trigger some cellular SIPK threshold level that activates processes that would not be active under native SIPK levels. Perhaps overexpressed SIPK draws in other interacting proteins in an inappropriate manner and thus confounds the signaling pathway.

Although anti-ERK antibodies have been shown to recognize both SIPK and WIPK in western gel analysis, this is not as specific an antibody as the anti-*p*ERK. The anti-*p*ERK antibody recognizes only those proteins that are doubly phosphorylated on the -TXY- motif. The two proteins recognized by anti-*p*ERK antibodies in stressed tobacco tissue were previously determined to be SIPK (46 kDa) and WIPK (44 kDa).

Untreated wild type cells probed with anti-*p*ERK antibodies showed a general cytoplasmic localization of signal, with higher concentration in the nucleus. Phosphorylation of MAPKs does indicate activation of the MAPKs. Since anti-*p*ERK only recognizes the activated form of SIPK and WIPK, one might not expect much label to be present in non-induced cells. From western gel analysis SIPK and WIPK are

known to have increased activation in response to stress, but there is still a relatively low basal level of activated MAPKs present in non-induced cells. This basal level of activated MAPKs is what is observed in untreated anti-*p*ERK-probed WT cultured cells. These activated MAPKs might have functions outside of stress signaling, or may be responding to a different stress than the applied one. Activated MAPKs are known to show a nuclear localization trend in response to a variety of inducers. Higher basal levels of nuclear localized anti-*p*ERK in non-induced WT cells (as compared to anti-ERK probed cells) reflect the localization of active MAPKs in untreated cells.

Non-induced OX:SIPK cells, much like the non-induced WT cells when probed with anti-*p*ERK, had a higher basal level of nuclear label accumulation as well. There were more cells displaying higher nuclear accumulation of label in OX:SIPK cells than in WT cells. In OX:SIPK cells, the higher nuclear accumulation of anti-*p*ERK label in untreated cells could reflect increased levels of SIPK signaling that may (or may not) be involved in stress signaling. The higher nuclear label localization does suggest that OX:SIPK cells are either more sensitive to handling than the WT cells, or that there are higher levels of signaling activity constitutively underway in untreated OX:SIPK cells, or both.

Both harpin and megaspermin-treated WT and OX:SIPK cultured cells probed with anti-*p*ERK showed particularly strong signal localization patterns in the interior of the nucleus. The distinct round body within the nucleus, which is presumably the nucleolus, showed a higher level of label accumulation than was seen with any other antibody treatment, including anti-*p*ERK-probed OX:SIPK cells.

The nucleolar accumulation of SIPK/WIPK appears to be a novel immunolabeling result. Cell fractionation of human nuclei, and protein analysis of the subcellular

fractions, found ERK to indeed be present in the cytoplasm and nucleus, but to be distinctly absent from the nucleolus (Scherl et al., 2002). It should be noted, however, that these tests were performed on non-induced cells.

It is possible that nucleolar accumulation of SIPK/WIPK might be uniquely associated with tobacco cell culture systems. In an attempt to answer this question, whole roots from tobacco seedlings were fixed, immunolabeled and analyzed by immunolabeling for comparison to results from cultured cells (Appendix 4). Although results were not very good due to extremely low resolution and lack of full penetration of fixative, antibodies, and washes through this thick tissue, some conclusions could still be drawn. A higher nuclear accumulation of label was still observed in treated cells, and within the nuclei some distinct spots appeared brighter than other parts of the nucleus. However, the sharp-edged, extremely distinct nucleolar accumulation pattern seen in cultured cells was not observed in tobacco seedling roots.

The major function of the nucleolus is thought to be the assembly of ribosomes. However, it is also involved in various other tasks such as signal recognition particle assembly, cell cycle regulation, control of aging, modification of small nuclear RNA's and modification of telomerase functions (Olson, 2004). Recent studies have found that the pattern of proteins identified in fractions from the nucleolus do not map well onto the presumed functions of the nucleolus. After finding high sustained levels of p53 in the nucleolus of human cells following treatment with 11 different stress-related treatments, Rubbi and Miller proposed that the nucleolus may act as a major cellular stress sensor that helps regulate p53 activity (2003). Elevated p53 levels can inhibit mammalian cell growth and lead to cell death (Olson, 2004). It is unknown what the stress signal

perceived by the nucleolus might be. It is also unknown how the cell distinguishes between stresses and decides whether to repair the damage, or to trigger cell death.

There are many functions SIPK/WIPK could have in the nucleolus. Some functions might include roles in the cell death process, or regulation of transcription factors. WIPK activity, either alone or with SIPK has been proposed to be involved in induction of cell death in cultured tobacco cells by fungal elicitor treatments (Zhang et al., 2000), so the presence of either MAPK in the nucleus, or nucleolus, following induction with harpin and/or megaspermin could be related to controlling the commitment to the cell death process. SIPK/WIPK might therefore have roles in plants that resemble the roles of mammalian p38 rather than the roles played by ERK.

MAPK involvement in activation regulation of transcription factors has also been extensively documented. In humans, ERK has been shown to phosphorylate transcription factors such as p62^{TCF}/elk-1. A recent microarray study of tobacco cell culture treated with harpin or megaspermin showed that expression of a range of transcription factors was significantly affected by elicitation, including members of the WRKY, SCARECROW, TINY, LIM, bHLH, SWI1, and IIE families (unpublished data, Hardy Hall). The close plant homologues of SIPK and WIPK in arabidopsis, AtMPK6 and AtMPK3, have been found to interact with the transcription factors WRKY22 and WRKY29 (Jonak et al., 2002) adding further support to the idea of a possible SIPK/WIPK:WRKY interaction.

A different nuclear labelling pattern was seen in treated OX:SIPK cells than in WT cells probed with anti-pERK. There was significantly less nucleolar label in harpin-treated OX:SIPK cells than in WT cells. As with the anti-ERK-labelled OX:SIPK cells,

some of these differences may reflect constitutive (pleiotropic) differences in physiology and biochemistry between these genotypes. One possible explanation is that the strong nucleolar signal might be specifically indicative of WIPK accumulation, since in an overexpressing SIPK line, WIPK is underexpressed, and the nucleolar signal would be reduced.

The commercially available anti-*p*ERK antibodies are raised against a synthetic phospho-peptide based on the rat ERK1/2 sequence, and since ERK homologues have differing degrees of sequence similarity, these antibodies might have a higher affinity for one kinase over another. Such a binding preference could affect the immunohistochemical results and give “unbalanced” MAPK localization patterns in wild type cells. This, together with shifts in the relative abundance of SIPK and WIPK, could offer an additional explanation for some of the localization differences between WT and OX anti-*p*ERK immunolabeled cells. One way to test this possibility would be to immunolabel transgenic cultured cells derived from a SIPK deficient genotype. SIPK elimination has been shown to lead to prolonged hyper-activation of WIPK in stressed cells, a pattern which would perhaps give a clear signal of WIPK localization. Unfortunately, the RNAi-SIPK transgenic tobacco lines available to me were not found to be a good candidate for such an experiment due to drastic physiological differences compared to WT (Appendix 3). The RNAi-SIPK cultured cells contained high levels of unidentified phenolics that produced strong autofluorescence. Large members of round grape-like structures accumulated in the cells, and the culture had a mixed composition of isodiametric and elongated cells.

By comparing the anti-ERK and anti-*p*ERK localization results, I was able to draw preliminary conclusions, but it was not clear that all nuclear-localized SIPK/WIPK represents the phosphorylated forms of these MAPKs. Phosphorylation of MAPKs does induce conformational changes that increases their catalytic activity, but phosphorylation does not dictate ERK's ability to enter the nucleus. As previously reported in humans by use of an ERK:GFP fusion protein, ERK:GFP accumulated in the nucleus regardless of the phosphorylation state (Matsubayashi et al., 2001). My results do, however, suggest that there are higher levels of cytoplasmic unphosphorylated SIPK/WIPK when comparing non-induced levels of both anti-ERK and anti-*p*ERK probed cells. There are higher phosphorylated SIPK/WIPK basal levels within the nucleus in anti-*p*ERK probed cells than in anti-ERK probed cells. Double-labelling using anti-ERK and anti-*p*ERK could have been tested, but would have been difficult as both were rabbit antibodies.

Although this study indicated that subcellular localization patterns observed in OX-SIPK and WT cells were not identical, there were many similar localization trends observed. Nuclear signal accumulation in harpin-treated cultured cells was observed in all genotypes, and with all three tested antibodies, anti-FLAG, anti-*p*ERK, and anti-ERK. The most notable differences between the OX-SIPK and WT lines were the higher percentage of nuclear localized signal in untreated cells in the overexpressing line, and the lack of strong nucleolar localization signal in harpin-treated OX:SIPK samples.

The specificity of the anti-FLAG antibody was important to this immunolabeling study, since it tracked just SIPK's localization. However, non-specific binding in WT cells with anti-FLAG was higher than non-specific binding from the pre-immune serum in WT cells, indicating that the anti-FLAG polyclonal antibody from Sigma was not ideal for cultured

cells. With anti-FLAG antibody concentrations set lower than the other two experimental probes (1:500 dilution vs 1:200 dilution) the observed fluorescent signal was lower, and the overall signal/noise ratio was more significant.

Despite noise difficulties, untreated cells showed a general cytoplasmic distribution, with an increase in nuclear accumulation upon treatment with harpin, similar to the results observed with anti-ERK and anti-*p*ERK probed cells. There was very little nucleolar accumulation of the FLAG epitope, which was effectively absent from the nucleolus. Based on the results from anti-FLAG-probed cells, the localization of basal SIPK in OX:SIPK-cultured cells appears to generally be throughout the cell. Upon treatment with harpin, enhanced nuclear accumulation of SIPK is observed in OX:SIPK cells.

The results obtained with anti-FLAG-probed OX:SIPK-treated and untreated cells mirror those from the anti-ERK-probed treated and untreated cells. It is therefore possible to draw the conclusion that the majority of the signal observed in anti-ERK-probed OX:SIPK cells is likely to be SIPK. Since anti-FLAG-probed OX:SIPK cells did not show nucleolar accumulation of label, it appears SIPK does not accumulate significantly in the nucleolus in these cells. From these results, it can be hypothesized that SIPK does not significantly accumulate in the nucleolus in WT cultured cells. To address this question, SIPK-specific antibodies could be used on fixed WT cultured cells, or SIPK:GFP fusion proteins could be tracked through live cell imaging.

By putting together the information that anti-*p*ERK antibody recognizes SIPK and WIPK in tobacco cells, and that anti-*p*ERK probed harpin/megaspermin-treated cells show a strong nucleolar accumulation, one can deduce that one, or both, of the MAPKs

have a function in the nucleolus following elicitation. Since my data suggests that it is probably not SIPK localizing to the nucleolus, there is a good hypothesis generated that WIPK specifically has a nucleolar function.

MAPKs, once activated, must find their target. To allow it to function in the regulation of multiple pathways, MAPK must have the ability to recognize a number of substrates. All MAPKs recognize similar phospho-acceptor sites of target proteins, (serine and threonine followed by a proline residue). Gene expression in eukaryotes is ultimately controlled at the transcriptional level by transcription factors. Many different stimuli that affect gene expression also lead to MAPK activation indicating that transcription factor function is highly dependent on phosphorylation and dephosphorylation cycles that are catalyzed by protein kinases and protein phosphatases (Hunter and Karin, 1992). A likely model for activated MAPKs is that they modify transcription factors by activation or deactivation through phosphorylation, and thus cause changes in transcription of target genes. The results of my experiment support the hypothesis that the tobacco MAPKs SIPK and WIPK are predominantly cytoplasmic, although basal levels can be found in almost all other regions of the cell in non-induced cells. Upon activation, SIPK, and most likely WIPK, move in part to the nucleus. It is hypothesized through deductive reasoning based on immunolabeling results that WIPK concentrates in the nucleolus. This shift in MAPK localization may be part of the dynamic by which they exert a regulatory role over transcription factors involved in pathogen regulation and cell death processes.

Quantification of results using imaging software to compare the intensities of label found in various parts of the cell may have better characterized shifts in subcellular distribution and complimented observed localization trends.

Whole cell immunolabeling in tobacco cultured cells is an effective means of determining subcellular localization, and the specific methods used to immunolabel tobacco cultured cells were shown to be robust. Both negative and positive controls (Figure 2.1) showed expected results, and the experimental antibodies revealed discrete information about MAPK cellular distribution in untreated and harpin-treated cultured tobacco cells.

Immunolabeling Troubleshooting

The three main technical problems that arose in this study were autofluorescence from contaminants and from the tissue itself, non-specific binding of antibodies, and low abundance of immunolabeling signal within the tissue. These problems can be further discussed for insight on improvement of the methods.

Autofluorescence: Immunolabeling using fluorescent probes often presents difficulty with artifactual fluorescence from natural sources within the tissue. Each tissue set offers its own difficulties, and it is important to minimize their effect, by choosing appropriate fixatives, fluorescent probes, filters, tissue types, and chemical treatments designed to minimize autofluorescence.

Glycine (1mM) can be used to bind free aldehydes (Eystathioy et al., 2002) and reduce autofluorescence. Autofluorescence from the cell wall was seen in my material, but was minimized by digestion of the cell wall and treating with glycine. This autofluorescence was most likely due to secondary structures within the cell wall. In plant tissues, some of

the most well known natural autofluorescent chemicals are chlorophyll, carotenoids, lignin, tannins, and phenolics (O'Brien, 1981)pp 2.27). Plant chloroplasts are another major source of autofluorescence within the plant. Chloroplasts occur predominantly in leaves, in the cortex of stems, and generally in tissues exposed to light. They are involved in photosynthesis, synthesis of lipids, nitrate reduction, and the temporary build up of starch (Cutter, 1978). Plant mesophyll cells contain 30-500 chloroplasts (Cutter, 1978). Chloroplasts emit red autofluorescence which can often be separated from other fluorescence during fluorescence microscopy by using appropriate filter sets (Kohler et al., 1997), but leaf and stem tissue is not the preferred tissue for immunolabeling due to the levels of chlorophyll and lignin/phenolic autofluorescence present.

Non-specific binding: A second problem that arose in this study was non-specific binding. Although antibodies are supposed to recognize only one substrate, and are often purified multiple times to ensure purity, there is often non-specific binding to the experimental tissue. This problem can be accentuated by using too high a concentration of antibody. Treating your sample with appropriate blocking solutions can help reduce non-specific binding, and optimization of antibody concentrations can aid in improving substrate specificity.

Weak Signal: A third problem present in this study was the low abundance of immunolabeling signal within the tissue. Some explanations for the low signal could be a low abundance of native SIPK and WIPK, a low abundance of the phosphorylated form of the MAPKs, a low level of exposed epitopes within the fixed tissue or a lowered specificity of the antibody for the protein in its fixed form. Low levels of SIPK and WIPK are observed by western gel analysis where there appears to be a moderate to low

level of the phosphorylated protein in the non-induced, and higher amounts present in the harpin induced state. The low levels of phosphorylated MAPKs found in my experiments were consistent with the fluorescent immunolabeling and TEM data reported by Coronado *et al.* (2002) using the same antibody on tobacco. They found very low levels of the phosphorylated protein in the cytoplasm and nucleus, but were unable to demonstrate increased nuclear localization in mature pollen (Coronado *et al.*, 2002). The levels of protein may appear higher in these experiments as whole cell immunolabeling was employed, whereas the Coronado group used thin sections of material.

CHAPTER 4: General Discussion

Protein kinases, and in particular MAPKs, have an essential role in eukaryotic stress signaling pathways, as they control signaling of defense mechanisms including transcription factor activation and systemic responses. MAPKs also function as negative regulators or desensitizers of defense responses and cell death pathways (Asai et al., 2002); (Romeis, 2001).

There are numerous reports of induced MAPK activity in tobacco tissues by both biotic and abiotic stresses. The most frequently studied tobacco MAPKs are SIPK and WIPK. These two kinases respond to a range of stimuli, but in particular, they are known to respond to treatment with harpin and megaspermin (Appendix Two).

The objective of this study was to determine the subcellular localization of the plant MAPKs SIPK and WIPK in response to pathogen attack by harpin and megaspermin. Although ERK subcellular localization has been well studied in mammalian systems, ERK plant homologues have been studied to a lesser degree. The apparent involvement of the tobacco ERK homologues SIPK and WIPK in stress signaling, and probable involvement in cell death makes their study exceedingly important in both agricultural, and biomedical circles.

Tobacco was chosen as the biological system for these experiments due to its extensive use and study of in our laboratory, and due to its ease of transformation, and its availability in plant and cell culture form. Observation of living cells and tissues is an important tool for understanding the dynamic aspects of plant structure and function. It is equally as important as the study of embedded or sectioned material. This study used both methods to look at MAPK subcellular localization patterns. A GFP:SIPK fusion

construct was created for study *in planta*, and the antibodies anti-ERK, anti-pERK and anti-FLAG were used to probe MAPKs in paraformaldehyde fixed cultured cells.

The SIPK:GFP construct design and assembly was shown to yield functional GFP in yeast and SIPK *in planta*, but due to time constraints the construct was never studied in stable transgenic lines. In stable lines, SIPK's translation, localization, change of location in response to stimuli, and duration of localizations could have been studied using live cell imaging. The fusion construct is, however, an excellent tool for future MAPK research.

The immunolabeling studies of fixed tobacco cultured cells allowed for the imaging of MAPK subcellular localization in untreated, harpin-treated, and megaspermin-treated cells. With all three antibodies used to probe the cells, it was revealed that there was a general cytoplasmic localization of MAPK within the cell, and a higher localization of label in nuclei of harpin and megaspermin-treated cells.

There were variations of label distribution between cells probed with anti-ERK, anti-pERK, and anti-FLAG, and between WT and over-expressing SIPK (OX:SIPK)-treated cultured cells. Differences between antibody treatment groups reflected both the antibodies themselves and the subcellular localization of their respective targets. The use of anti-ERK, which is known to recognize SIPK and WIPK in all activation states, provided information about the general distribution of MAPKs in tobacco in untreated, harpin-treated, and megaspermin-treated cultured cells. The majority of non-induced cells revealed a cytoplasmic localization, and upon induction, there was a shift in localization to the nucleus. In WT cells, there was also nucleolar localization of label observed. This trend was not observed in transgenic OX:SIPK cultured cells.

The use of anti-*p*ERK, which is known to be specific to the phosphorylated forms of SIPK and WIPK, revealed subcellular localization patterns of activated MAPKs within untreated and treated cultured cells. Although the majority of untreated cells revealed a general cytoplasmic localization of label, there was a higher basal level of nuclear localized MAPK in anti-*p*ERK-treated cultured cells. As with the anti-ERK probed harpin and megaspermin-treated cells, there was a strong re-localization of label to the nucleus, and more specifically to the nucleolus in anti-*p*ERK-treated wt cultured cells. Treated OX:SIPK cultured cells did show a high nuclear accumulation of label, but did not show the nucleolar accumulation observed in WT cells.

Anti-FLAG was used to probe FLAG-tagged OX:SIPK transgenic cultured cells. The OX:SIPK cultured cells were a valuable tool for tracking SIPK's subcellular localization apart from that of WIPK. In OX:SIPK cultured tobacco cells, SIPK was found to have a general cytoplasmic localization, with higher nuclear accumulation of label in harpin-treated cells. There was not a strong nucleolar accumulation observed in harpin-treated OX:SIPK anti-FLAG probed cells.

MAPK relocation is believed to coincide with a function in the new location. SIPK/WIPK's probable role in the nucleus and nucleolus, discussed in greater detail in Chapter 3, is most likely to phosphorylate transcription factors involved in stress perception and response elicitation. Some tools that could be used to identify the downstream targets of SIPK and WIPK include phospho-protein profiles in various transgenic genotypes of SIPK and WIPK, and using proteomic tools such as ICAT, 2D gel electrophoresis combined with mass spectrometry and microarray profiling. Preliminary microarray profiling of harpin and megaspermin-treated cultured cells has

revealed many putative interactors with MAPKs, many of which are transcription factors (unpublished data, Hardy Hall). Activation of these transcription factors upon elicitation with harpin or megaspermin could coincide with my subcellular localization results.

The MAPK localization differences observed between OX:SIPK and WT cells are strongly believed to be secondary effects from over-expressing SIPK under the 35S promoter in cultured cells. It was hoped that a line over-expressing SIPK would merely magnify the observable SIPK signal, but after examination of immunolabeling results, it was apparent that there are many other factors involved that change native MAPK localization patterns in the over-expressing line. These possible factors, discussed in Chapter 3, either diminish, or eliminate a strong nucleolar signal in OX:SIPK-cultured cells that was otherwise observed under the same conditions of WT-cultured cells. My hypothesis from deductive reasoning is that the observed nucleolar signal stems from WIPK re-localization, and that overexpression of SIPK either suppresses WIPK, or competes with WIPK, thus altering WIPK's subcellular re-localization under elicited stress with either harpin or megaspermin.

In light of the different immunolabeling patterns seen in OX:SIPK cultured cells when compared to WT, it is possible that the transgenic SIPK:GFP might have behaved in a similar fashion to OX:SIPK immunolabeled cells, giving a false impression of tobacco MAPK subcellular localization patterns. The 35S induced constructs produce un-natural amounts of the protein in regions where it might not otherwise be expressed. For a better look at native SIPK subcellular localization the upstream promoter of SIPK would need to be identified, amplified, and used in a binary vector to control SIPK's expression.

Although cultured cell immunolabelling experiments were not fully mirrored in seedling roots, there was an observed increase in nuclear label in harpin and megaspermin-treated seedling roots. It is possible that many of the observed localization patterns were specific to cultured cells and do not reflect the localization patterns within intact tissue. Despite the observed differences in tissue type, cell type, and differences between the antibodies used to probe these cells, all MAPK immunolabeling results revealed a general nuclear accumulation of label upon elicitation with harpin or megaspermin

To effect intracellular changes MAPKs can be activated/deactivated, can activate/deactivate other proteins, and can re-locate within the cell. I have shown activated MAPK concentrates in part to the nucleus upon treatment with harpin or megaspermin. MAPKs in eukaryotic cells control gene expression through activation of downstream transcription factors, and therefore links extracellular stimuli with appropriate patterns of gene expression. These mechanisms are essential to stress perception, and reaction.

APPENDIX 1:

A: Media Recipe for Micro-propagation of Tobacco

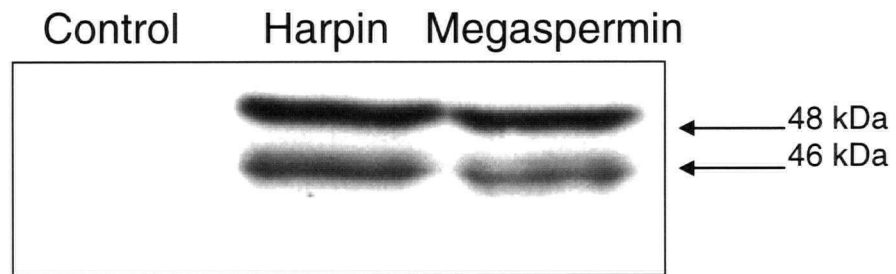
	SIM (1L)	RIM (1L)
MS salts*	4.3 g	4.3 g
Vitamin mix (below)	1.0 mL	1.0 mL
Glycine	0.200 g	0.200 g
Sucrose	30.0 g	30.0 g
Agar	3.0 g	3.0 g
Phytigel	1.1 g	1.1 g
NAA (1 mg/mL)	100 μ L	-
BA (1 mg/mL)	2 mL	-
pH (w/ 1 N NaOH)	5.6	5.6
Hygromycin	0.250 g	0.250 g
Carbenicillin	0.500 g	0.500 g
Cefotaxime	0.250 g	0.250 g

MS salts*: Murashige & Skoog salt mixture (Murashige and Skoog, 1962) (Invitrogen)

B: Vitamin Mix (1000 X)

Chemical	For 1 L of Stock
Myo-Inositol	100.0 g
Thiamine-HCl	100.0 g
Nicotinic acid	500.0 g
Pyridoxine-HCl	500.0 g

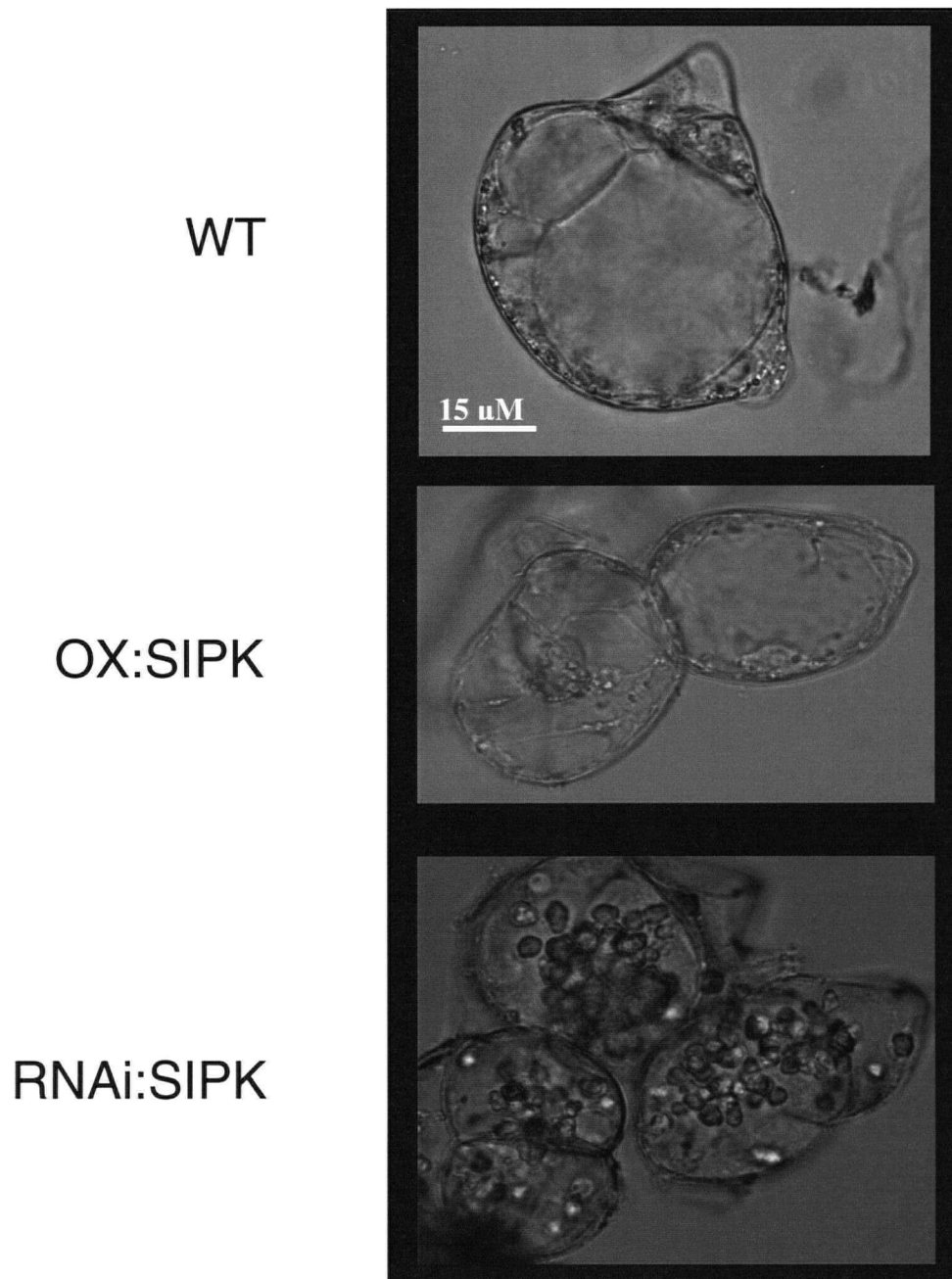
APPENDIX 2



Western Analysis of ERK1/2 from Tobacco Cultured cells treated with 40 µg/ml harpin

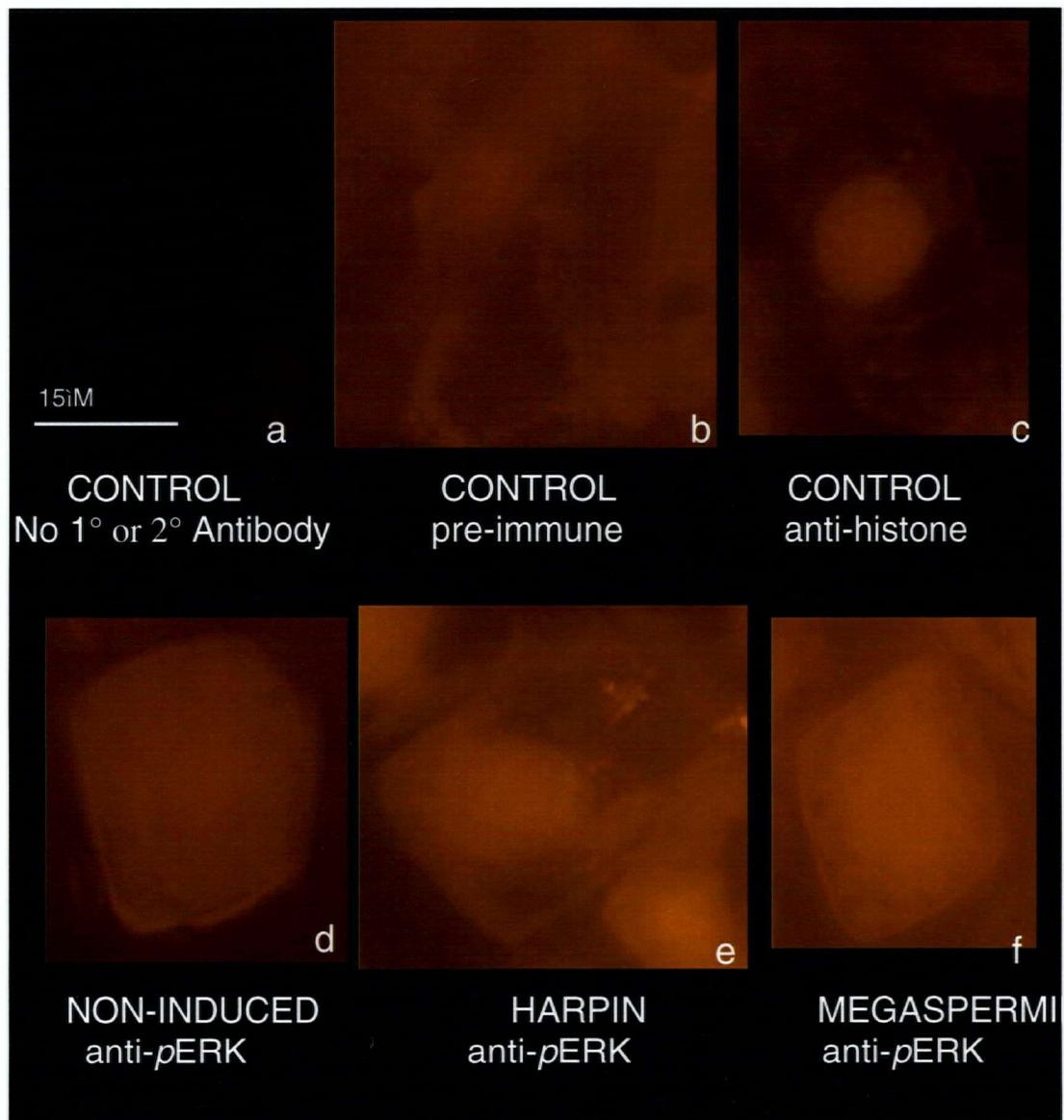
Appendix 1.0: western analysis of 3 day old WT cultured cells at 30 min after eliciting with 40 µg/ml harpin and megaspermin-treated with 1:1000 anti-*p*ERK overnight followed by treatment with 1:5000 anti-rabbit alkaline phosphatase for 2 h. The film was exposed for 15 min before developing. Work done by Hardy Hall.

APPENDIX 3



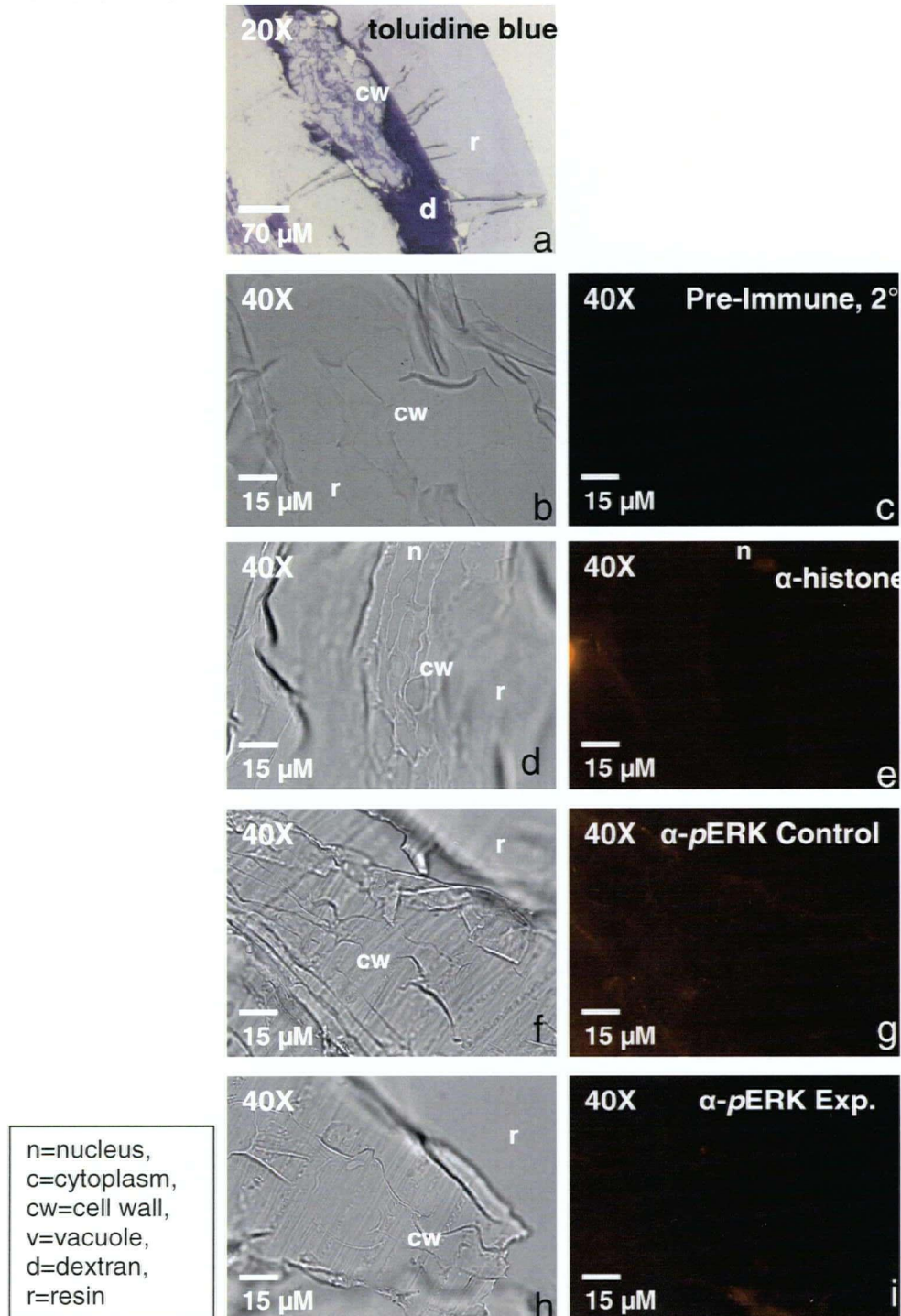
Appendix 3 shows the light microscope images of 3 different populations of cultured tobacco cells; *Xanthi* WT, overexpressing SIPK, and RNAi knock-out SIPK lines. These non-fixed cells were subcultured at 4 days, and grown in MS with hormones and shaken on a gyratory shaker in the dark. Transgenics were grown in media containing 50 mg/L kanamycin.

APPENDIX 4



Appendix 4 shows the results of immunolabelling 2 week old tobacco seedling root tips fixed with paraformaldehyde and probed with anti-pERK (1:200). Controls are the no primary or secondary application (a) shows natural autofluorescence of roots. Application of a pre-immune serum (1:200) with secondary Alexa⁵⁹⁴ conjugated anti-rabbit IgG (1:500) (b) shows non-specific binding within root tissue. Application of anti-histone (1:500) positive control with secondary Alexa⁵⁹⁴-conjugated anti-mouse IgG (1:500) (c) shows immunolabelling of cellular histone. Anti-pERK (1:200) with secondary Alexa⁵⁹⁴-conjugated anti-rabbit IgG (1:500) show the subcellular location of cellular MAPKs SIPK and WIPK. Harpin (40 µg/mL) and megaspermin elicited (40 µg/mL) samples were treated for 20 min. Samples were viewed by fluorescence microscopy and images captured at a 3 second exposure.

APPENDIX 5



Appendix 5 shows toluidine blue stained (a), light and fluorescent images (b-i) of immunolabelled high pressure frozen two week old tobacco seedling roots embedded in LR white resin and sectioned (1 µM). A rabbit pre-immune serum (1:200) shows non-specific binding of the antibody(c). Anti-histone (1:500) positive control indicates cellular histone location. Anti-pERK labeled samples show the location of the MAPKs SIPK and WIPK. Alexa⁵⁹⁴-conjugated IgG (1:200) was used as a secondary antibody. Images were captured on a fluorescence microscope equipped with a digital camera, and exposure times were set at 3 seconds for fluorescence, and 100 ms for light images.

REFERENCES:

- Asai T, Tena G, Plotnikova J, Willmann MR, Chiu WL, Gomez-Gomez L, Boller T, Ausubel FM, Sheen J (2002) MAP kinase signalling cascade in Arabidopsis innate immunity. *Nature* **415**: 977-983
- Baillieul F, de Ruffray P, Kauffmann S (2003) Molecular cloning and biological activity of alpha-, beta-, and gamma-megaspermin, three elicitors secreted by *Phytophthora megasperma* H20. *Plant Physiol* **131**: 155-166
- Barr RK, Bogoyevitch MA (2001) The c-Jun N-terminal protein kinase family of mitogen-activated protein kinases (JNK MAPKs). *Int J Biochem Cell Biol* **33**: 1047-1063
- Bogre L, Ligterink W, Meskiene I, Barker PJ, Heberle-Bors E, Huskisson NS, Hirt H (1997) Wounding Induces the Rapid and Transient Activation of a Specific MAP Kinase Pathway. *Plant Cell* **9**: 75-83
- Brandizzi F, Fricker M, Hawes C (2002) A greener world: the revolution in plant bioimaging. *Nat Rev Mol Cell Biol* **3**: 520-530
- Brandizzi F, Irons SL, Johansen J, Kotzer A, Neumann U (2004) GFP is the way to glow: bioimaging of the plant endomembrane system. *J Microsc* **214**: 138-158
- Braun DM, Walker JC (1996) Plant transmembrane receptors: new pieces in the signaling puzzle. *Trends Biochem Sci* **21**: 70-73
- Breitbart RE, Andreadis A, Nadal-Ginard B (1987) Alternative splicing: a ubiquitous mechanism for the generation of multiple protein isoforms from single genes. *Annu Rev Biochem* **56**: 467-495
- Canagarajah BJ, Khokhlatchev A, Cobb MH, Goldsmith EJ (1997) Activation mechanism of the MAP kinase ERK2 by dual phosphorylation. *Cell* **90**: 859-869
- Cardinale F, Meskiene I, Ouaked F, Hirt H (2002) Convergence and divergence of stress-induced mitogen-activated protein kinase signaling pathways at the level of two distinct mitogen-activated protein kinase kinases. *Plant Cell* **14**: 703-711
- Cazale AC, Droillard MJ, Wilson C, Heberle-Bors E, Barbier-Brygoo H, Lauriere C (1999) MAP kinase activation by hypoosmotic stress of tobacco cell suspensions: towards the oxidative burst response? *Plant J* **19**: 297-307
- Choi KY, Satterberg B, Lyons DM, Elion EA (1994) Ste5 tethers multiple protein kinases in the MAP kinase cascade required for mating in *S. cerevisiae*. *Cell* **78**: 499-512
- Coronado MJ, Gonzalez-Melendi P, Segui JM, Ramirez C, Barany I, Testillano PS, Risueno MC (2002) MAPKs entry into the nucleus at specific interchromatin domains in plant differentiation and proliferation processes. *J Struct Biol* **140**: 200-213
- Cutter EG (1978) *Plant Anatomy Part I: Cells and Tissues*. Clowes and Sons Ltd., London
- Dangl JL, Dietrich RA, Richberg MH (1996) Death Don't Have No Mercy: Cell Death Programs in Plant-Microbe Interactions. *Plant Cell* **8**: 1793-1807
- Davis RJ (1999) Signal transduction by the c-Jun N-terminal kinase. *Biochem Soc Symp* **64**: 1-12
- Davis SJ, Vierstra RD (1998) Soluble, highly fluorescent variants of green fluorescent protein (GFP) for use in higher plants. *Plant Mol Biol* **36**: 521-528

- Desikan R, Hancock JT, Ichimura K, Shinozaki K, Neill SJ** (2001) Harpin induces activation of the Arabidopsis mitogen-activated protein kinases AtMPK4 and AtMPK6. *Plant Physiol* **126**: 1579-1587
- Droillard MJ, Thibivilliers S, Cazale AC, Barbier-Brygoo H, Lauriere C** (2000) Protein kinases induced by osmotic stresses and elicitor molecules in tobacco cell suspensions: two crossroad MAP kinases and one osmoregulation-specific protein kinase. *FEBS Lett* **474**: 217-222
- Eckardt NA** (2002) Alternative splicing and the control of flowering time. *Plant Cell* **14**: 743-747
- Eystathioy T, Chan EK, Tenenbaum SA, Keene JD, Griffith K, Fritzler MJ** (2002) A phosphorylated cytoplasmic autoantigen, GW182, associates with a unique population of human mRNAs within novel cytoplasmic speckles. *Mol Biol Cell* **13**: 1338-1351
- Fukuda M, Gotoh Y, Nishida E** (1997) Interaction of MAP kinase with MAP kinase kinase: its possible role in the control of nucleocytoplasmic transport of MAP kinase. *Embo J* **16**: 1901-1908
- Gartner A, Nasmyth K, Ammerer G** (1992) Signal transduction in *Saccharomyces cerevisiae* requires tyrosine and threonine phosphorylation of FUS3 and KSS1. *Genes Dev* **6**: 1280-1292
- Giancotti FG, Ruoslahti E** (1999) Integrin signaling. *Science* **285**: 1028-1032
- Gonzalez FA, Raden DL, Davis RJ** (1991) Identification of substrate recognition determinants for human ERK1 and ERK2 protein kinases. *J Biol Chem* **266**: 22159-22163
- Hammond-Kosack KE, Jones JD** (1996) Resistance gene-dependent plant defense responses. *Plant Cell* **8**: 1773-1791
- Hanks SK, Quinn AM, Hunter T** (1988) The protein kinase family: conserved features and deduced phylogeny of the catalytic domains. *Science* **241**: 42-52
- Heim R, Prasher DC, Tsien RY** (1994) Wavelength mutations and posttranslational autooxidation of green fluorescent protein. *Proc Natl Acad Sci U S A* **91**: 12501-12504
- Horgan AM, Stork PJ** (2003) Examining the mechanism of Erk nuclear translocation using green fluorescent protein. *Exp Cell Res* **285**: 208-220
- Hoyos ME, Zhang S** (2000) Calcium-independent activation of salicylic acid-induced protein kinase and a 40-kilodalton protein kinase by hyperosmotic stress. *Plant Physiol* **122**: 1355-1363
- Hunter T, Karin M** (1992) The regulation of transcription by phosphorylation. *Cell* **70**: 375-387
- Impey S, Obrietan K, Wong ST, Poser S, Yano S, Wayman G, Deloulme JC, Chan G, Storm DR** (1998) Cross talk between ERK and PKA is required for Ca²⁺ stimulation of CREB-dependent transcription and ERK nuclear translocation. *Neuron* **21**: 869-883
- Jonak C, Kiegerl S, Ligterink W, Barker PJ, Huskisson NS, Hirt H** (1996) Stress signaling in plants: a mitogen-activated protein kinase pathway is activated by cold and drought. *Proc Natl Acad Sci U S A* **93**: 11274-11279
- Jonak C, Okresz L, Bogre L, Hirt H** (2002) Complexity, cross talk and integration of plant MAP kinase signalling. *Curr Opin Plant Biol* **5**: 415-424

- Kan Z, Rouchka EC, Gish WR, States DJ** (2001) Gene structure prediction and alternative splicing analysis using genomically aligned ESTs. *Genome Res* **11**: 889-900
- Kiegerl S, Cardinale F, Siligan C, Gross A, Baudouin E, Liwosz A, Eklof S, Till S, Bogre L, Hirt H, Meskiene I** (2000) SIMKK, a mitogen-activated protein kinase (MAPK) kinase, is a specific activator of the salt stress-induced MAPK, SIMK. *Plant Cell* **12**: 2247-2258
- Kim JY, Yuan Z, Jackson D** (2003) Developmental regulation and significance of KNOX protein trafficking in Arabidopsis. *Development* **130**: 4351-4362
- Klessig DF, Durner J, Noad R, Navarre DA, Wendehenne D, Kumar D, Zhou JM, Shah J, Zhang S, Kachroo P, Trifa Y, Pontier D, Lam E, Silva H** (2000) Nitric oxide and salicylic acid signaling in plant defense. *Proc Natl Acad Sci U S A* **97**: 8849-8855
- Kohler RH, Zipfel WR, Webb WW, Hanson MR** (1997) The green fluorescent protein as a marker to visualize plant mitochondria in vivo. *Plant J* **11**: 613-621
- Kovtun Y, Chiu WL, Tena G, Sheen J** (2000) Functional analysis of oxidative stress-activated mitogen-activated protein kinase cascade in plants. *Proc Natl Acad Sci U S A* **97**: 2940-2945
- Kultz D** (1998) Phylogenetic and functional classification of mitogen- and stress-activated protein kinases. *J Mol Evol* **46**: 571-588
- Lazar G, Goodman HM** (2000) The Arabidopsis splicing factor SR1 is regulated by alternative splicing. *Plant Mol Biol* **42**: 571-581
- Lee J, Klessig DF, Nurnberger T** (2001) A harpin binding site in tobacco plasma membranes mediates activation of the pathogenesis-related gene HIN1 independent of extracellular calcium but dependent on mitogen-activated protein kinase activity. *Plant Cell* **13**: 1079-1093
- Lee J, Rudd JJ, Macioszek VK, Scheel D** (2004) Dynamic changes in the localization of MAP kinase cascade components controlling pathogenesis-related (PR) gene expression during innate immunity in parsley. *J Biol Chem*
- Lenormand P, Sardet C, Pages G, L'Allemain G, Brunet A, Pouyssegur J** (1993) Growth factors induce nuclear translocation of MAP kinases (p42mapk and p44mapk) but not of their activator MAP kinase kinase (p45mapkk) in fibroblasts. *J Cell Biol* **122**: 1079-1088
- Leppa S, Bohmann D** (1999) Diverse functions of JNK signaling and c-Jun in stress response and apoptosis. *Oncogene* **18**: 6158-6162
- Lewis TS, Shapiro PS, Ahn NG** (1998) Signal transduction through MAP kinase cascades. *Adv Cancer Res* **74**: 49-139
- Ligterink W, Kroj T, zur Nieden U, Hirt H, Scheel D** (1997) Receptor-mediated activation of a MAP kinase in pathogen defense of plants. *Science* **276**: 2054-2057
- Liu Y, Zhang S, Klessig DF** (2000) Molecular cloning and characterization of a tobacco MAP kinase kinase that interacts with SIPK. *Mol Plant Microbe Interact* **13**: 118-124
- Manning G, Whyte DB, Martinez R, Hunter T, Sudarsanam S** (2002) The protein kinase complement of the human genome. *Science* **298**: 1912-1934

- Marshall CJ** (1995) Specificity of receptor tyrosine kinase signaling: transient versus sustained extracellular signal-regulated kinase activation. *Cell* **80**: 179-185
- Matsubayashi Y, Fukuda M, Nishida E** (2001) Evidence for existence of a nuclear pore complex-mediated, cytosol-independent pathway of nuclear translocation of ERK MAP kinase in permeabilized cells. *J Biol Chem* **276**: 41755-41760
- Meyer P, Saedler H** (1996) Homology-Dependent Gene Silencing in Plants. *Annu Rev Plant Physiol Plant Mol Biol* **47**: 23-48
- Miles GP, Samuel, M.A. and Ellis, B.E.** (2002) Suramin inhibits oxidant-induced MAPK signalling in plants. *Plant Cell Environment* **25**: 521-527
- Mitogen-activated protein kinase cascades in plants: a new nomenclature. (2002) *Trends Plant Sci* **7**: 301-308
- Mizoguchi T, Ichimura K, Shinozaki K** (1997) Environmental stress response in plants: the role of mitogen-activated protein kinases. *Trends Biotechnol* **15**: 15-19
- Munnik T, Ligterink W, Meskiene I, Calderini O, Beyerly J, Musgrave A, Hirt H** (1999) Distinct osmo-sensing protein kinase pathways are involved in signalling moderate and severe hyper-osmotic stress. *Plant J* **20**: 381-388
- Nuhse TS, Peck SC, Hirt H, Boller T** (2000) Microbial elicitors induce activation and dual phosphorylation of the Arabidopsis thaliana MAPK 6. *J Biol Chem* **275**: 7521-7526
- O'Brien TP, McCully, M.E.** (1981) *The Study of Plant Structure Principles and Selected Methods*. Bradford House Pty, Ltd., South Melbourne, Australia
- Olson MO** (2004) Sensing cellular stress: another new function for the nucleolus? *Sci STKE* **2004**: pe10
- Pal-Bhadra M, Bhadra U, Birchler JA** (1997) Cosuppression in Drosophila: gene silencing of Alcohol dehydrogenase by white-Adh transgenes is Polycomb dependent. *Cell* **90**: 479-490
- Porter AC, Vaillancourt RR** (1998) Tyrosine kinase receptor-activated signal transduction pathways which lead to oncogenesis. *Oncogene* **17**: 1343-1352
- Rane SG** (1999) Ion channels as physiological effectors for growth factor receptor and Ras/ERK signaling pathways. *Adv Second Messenger Phosphoprotein Res* **33**: 107-127
- Romeis T** (2001) Protein kinases in the plant defence response. *Curr Opin Plant Biol* **4**: 407-414
- Romeis T, Piedras P, Zhang S, Klessig DF, Hirt H, Jones JD** (1999) Rapid Avr9- and Cf-9 -dependent activation of MAP kinases in tobacco cell cultures and leaves: convergence of resistance gene, elicitor, wound, and salicylate responses. *Plant Cell* **11**: 273-287
- Ryals J, Uknes S, Ward E** (1994) Systemic Acquired Resistance. *Plant Physiol* **104**: 1109-1112
- Samaj J, Ovecka M, Hlavacka A, Lecourieux F, Meskiene I, Lichtscheidl I, Lenart P, Salaj J, Volkmann D, Bogre L, Baluska F, Hirt H** (2002) Involvement of the mitogen-activated protein kinase SIMK in regulation of root hair tip growth. *Embo J* **21**: 3296-3306
- Scherl A, Coute Y, Deon C, Calle A, Kindbeiter K, Sanchez JC, Greco A, Hochstrasser D, Diaz JJ** (2002) Functional proteomic analysis of human nucleolus. *Mol Biol Cell* **13**: 4100-4109

- Seo S, Okamoto M, Seto H, Ishizuka K, Sano H, Ohashi Y** (1995) Tobacco MAP kinase: a possible mediator in wound signal transduction pathways. *Science* **270**: 1988-1992
- Seth A, Alvarez E, Gupta S, Davis RJ** (1991) A phosphorylation site located in the NH₂-terminal domain of c-Myc increases transactivation of gene expression. *J Biol Chem* **266**: 23521-23524
- Shapiro PS, Vaisberg E, Hunt AJ, Tolwinski NS, Whalen AM, McIntosh JR, Ahn NG** (1998) Activation of the MKK/ERK pathway during somatic cell mitosis: direct interactions of active ERK with kinetochores and regulation of the mitotic 3F3/2 phosphoantigen. *J Cell Biol* **142**: 1533-1545
- Sheahan MB, Rose RJ, McCurdy DW** (2004) Organelle inheritance in plant cell division: the actin cytoskeleton is required for unbiased inheritance of chloroplasts, mitochondria and endoplasmic reticulum in dividing protoplasts. *Plant J* **37**: 379-390
- Suzuki K, Shinshi H** (1995) Transient Activation and Tyrosine Phosphorylation of a Protein Kinase in Tobacco Cells Treated with a Fungal Elicitor. *Plant Cell* **7**: 639-647
- Tanoue T, Maeda R, Adachi M, Nishida E** (2001) Identification of a docking groove on ERK and p38 MAP kinases that regulates the specificity of docking interactions. *Embo J* **20**: 466-479
- Tena G, Asai T, Chiu WL, Sheen J** (2001) Plant mitogen-activated protein kinase signaling cascades. *Curr Opin Plant Biol* **4**: 392-400
- Tian GW, Mohanty A, Chary SN, Li S, Paap B, Drakakaki G, Kopec CD, Li J, Ehrhardt D, Jackson D, Rhee SY, Raikhel NV, Citovsky V** (2004) High-Throughput Fluorescent Tagging of Full-Length Arabidopsis Gene Products in Planta. *Plant Physiol*
- Tibbles LA, Woodgett JR** (1999) The stress-activated protein kinase pathways. *Cell Mol Life Sci* **55**: 1230-1254
- van Drogen F, Peter M** (2001) MAP kinase dynamics in yeast. *Biol Cell* **93**: 63-70
- van Drogen F, Peter M** (2004) Revealing protein dynamics by photobleaching techniques. *Methods Mol Biol* **284**: 287-306
- Volmat V, Pouyssegur J** (2001) Spatiotemporal regulation of the p42/p44 MAPK pathway. *Biol Cell* **93**: 71-79
- von Arnim AG, Deng XW, Stacey MG** (1998) Cloning vectors for the expression of green fluorescent protein fusion proteins in transgenic plants. *Gene* **221**: 35-43
- Weld R, Heinemann J, Eady C** (2001) Transient GFP expression in *Nicotiana glauca* suspension cells: the role of gene silencing, cell death and T-DNA loss. *Plant Mol Biol* **45**: 377-385
- Wilsbacher JL, Goldsmith EJ, Cobb MH** (1999) Phosphorylation of MAP kinases by MAP/ERK involves multiple regions of MAP kinases. *J Biol Chem* **274**: 16988-16994
- Xing J, Kornhauser JM, Xia Z, Thiele EA, Greenberg ME** (1998) Nerve growth factor activates extracellular signal-regulated kinase and p38 mitogen-activated protein kinase pathways to stimulate CREB serine 133 phosphorylation. *Mol Cell Biol* **18**: 1946-1955

- Yang KY, Liu Y, Zhang S** (2001) Activation of a mitogen-activated protein kinase pathway is involved in disease resistance in tobacco. *Proc Natl Acad Sci U S A* **98**: 741-746
- Yuasa T, Ichimura K, Mizoguchi T, Shinozaki K** (2001) Oxidative stress activates ATMPK6, an Arabidopsis homologue of MAP kinase. *Plant Cell Physiol* **42**: 1012-1016
- Zhang J, Zhang F, Ebert D, Cobb MH, Goldsmith EJ** (1995) Activity of the MAP kinase ERK2 is controlled by a flexible surface loop. *Structure* **3**: 299-307
- Zhang S, Klessig DF** (1997) Salicylic acid activates a 48-kD MAP kinase in tobacco. *Plant Cell* **9**: 809-824
- Zhang S, Klessig DF** (1998) Resistance gene N-mediated de novo synthesis and activation of a tobacco mitogen-activated protein kinase by tobacco mosaic virus infection. *Proc Natl Acad Sci U S A* **95**: 7433-7438
- Zhang S, Klessig DF** (1998) The tobacco wounding-activated mitogen-activated protein kinase is encoded by SIPK. *Proc Natl Acad Sci U S A* **95**: 7225-7230
- Zhang S, Klessig DF** (2000) Pathogen-induced MAP kinases in tobacco. *Results Probl Cell Differ* **27**: 65-84
- Zhang S, Klessig DF** (2001) MAPK cascades in plant defense signaling. *Trends Plant Sci* **6**: 520-527
- Zhang S, Liu Y, Klessig DF** (2000) Multiple levels of tobacco WIPK activation during the induction of cell death by fungal elicitors. *Plant J* **23**: 339-347
- Zhu JH, Kulich SM, Oury TD, Chu CT** (2002) Cytoplasmic aggregates of phosphorylated extracellular signal-regulated protein kinases in Lewy body diseases. *Am J Pathol* **161**: 2087-2098